Theoretical and experimental study of integrated membrane / distillation processes for industrial applications

Paulo Perez



TR diss
4881

Stellingen behorende bij het proefschrift van P. Perez

Theoretische en experimentele studie naar geïntegreerde membraan / destillatieprocessen voor industriële toepassingen

1. Keramische membranen hebben duidelijk grotere fluxen dan polymere membranen voor de meeste toepassingen (Hoofdstukken 4, 5 en 6 van deze dissertatie). Niettemin moeten twee belangrijke kwesties opgelost worden voordat keramische membranen wijdverbreid commerciële toepassing kunnen vinden: prijs en stabiliteit.
2. Concentratiepolarisatie hangt niet af van voedingsconcentratie en selectiviteit, zoals wordt geloofd (Hoofdstukken 3 en 7 van deze dissertatie). In plaats daarvan wordt concentratiepolarisatie direct beïnvloed door het stroom regime en de membraanpermeance (die direct gerelateerd is aan de flux).
3. Pervaporatie en damppermeatie zijn gelijksoortige processen op micro- en macroschaal en de beslissing om de ene dan wel de andere te gebruiken hangt vooral af van de productspecificaties en de locatiecondities.
4. Damppermeatie vereist minder oppervlak dan pervaporatie wanneer de zwaarste component het product is. Evenzo vereist pervaporatie minder oppervlak dan damppermeatie wanneer de vluchtigste component het product is (Hoofdstuk 7 van *deze dissertatie*).
5. De industrie is sceptisch over membraantechnologie omdat, tot nu toe, de opschalingsprocedure het onopgeloste probleem blijft.
6. Het gevolg van stelling nummer vijf is dat de industrie opschalingskennis zou moeten ontwikkelen, hetgeen een groot risico met zich meebrengt en dat is niet in het belang van de meeste industrieën.
7. Als onderzoekers meer aandacht willen voor hun bevindingen, zouden ze moeten beginnen hun experimenten bij minder ideale condities uit te voeren.
8. Er is een duidelijke relatie tussen persoonlijke ontwikkeling en bescheidenheid.
9. Nederland is waarschijnlijk het enige land waar een "onbepaaldetijd" verblijfsvergunning slechts 5 jaar geldig is.
10. Een muur bouwen betekent dat er geen wil is om een probleem op te lossen.

Deze stellingen worden opponeerbaar en verdedigbaar geacht en zijn als zodanig goedgekeurd door de promotoren, Prof. dr. ir. P.J. Jansens en Prof. Dr. –Ing. A. Górak.

TR diss
4881

Propositions accompanying the PhD thesis of P. Perez

Theoretical and experimental study of integrated membrane / distillation processes for industrial applications

1. Ceramic membranes have definitively larger fluxes than polymer membranes for most applications (Chapters 4, 5 and 6 of this thesis). However there are two important issues to solve before ceramic membranes can be widely commercially applied: price and stability.
2. Concentration polarization does not depend on feed concentration and selectivity as wrongly believed (Chapters 3 and 7 of this thesis). Instead concentration polarization is affected directly by the flow regime and membrane permeance (which is directly related to flux).
3. Pervaporation and vapor permeation are similar processes at micro and macro scales and the decision whether to use one or the other depends more on product specifications and site conditions (Chapter 7 of this thesis).
4. Vapor permeation requires less area than pervaporation when the heaviest component is the product. Similarly, pervaporation requires less area than vapor permeation when the most volatile component is the product (Chapters 7 of this thesis).
5. Industry is skeptical of membrane technology because the scale-up procedures remain the unsolved problem up to now.
6. The consequence of proposition number five is that industry should develop the up-scaling know-how of membrane technology, which is very risky and out of interest of most industries.
7. If researchers want more attention to their findings they should start performing their experiments in less "ideal" conditions.
8. There is a clear relation between personal development and modesty.
9. Netherlands is probably the only country where a "permanent" residence permit is valid only for 5 years.
10. Building a wall means that there is no will to solve a problem.

These propositions are considered opposable and defendable and as such have been approved by the supervisors, Prof. dr. ir. P.J. Jansens and Prof. Dr.-Ing. A. Górak

Theoretical and experimental study of integrated membrane / distillation processes for industrial applications

Paulo Pérez

TR diss
4881

Theoretical and experimental study of integrated membrane / distillation processes for industrial applications

Proefschrift

ter verkrijging van de graad van doctor

aan de Technische Universiteit Delft,

op gezag van de Rector Magnificus prof. dr. ir. J.T. Fokkema,

voorzitter van het College voor Promoties,

in het openbaar te verdedigen op maandag 22 januari 2007 om 13:00 uur

door

Paulo César PÉREZ García

Ingeniero Químico

geboren te Azcapotzalco, México

Dit proefschrift is goedgekeurd door de promotor(en):

Prof. dr. ir. P.J. Jansens

Prof. Dr.-Ing. A. Górak

Toegevoegd promotor:

Dr. Ž. Olujić

Samenstelling promotiecommissie:

Rector Magnificus	Voorzitter
Prof. dr. ir. P. J. Jansens	Technische Universiteit Delft, promotor
Prof. Dr.-Ing. A. Górak	Universiteit Dortmund, promotor
Dr. Ž. Olujić	Technische Universiteit Delft, toegevoegd promotor
Prof. dr. ir. J. de Graauw	Technische Universiteit Delft
Prof. dr. ir. J. C. Jansen	Universiteit Stellenbosch (Zuid Afrika)
Prof. dr. M. Wesseling	Universiteit Twente
Dr. H. A. Kooijman	Shell Global Solutions

This thesis has been possible thanks to the financial support of: EET projects EETK 20046 and EETK20061 and the Marie Curie Fellowship HPMT-CT-2001-00408.

ISBN 90-8559-274-7

Copyrights ©2007 by P. Perez

No part of the material protected by this copyright notice may be reproduced or utilized in any form or by any means, electronic or mechanical, including photocopying, recording or by any information storage and retrieval system, without written permission from the author.

Printed in The Netherlands

Summary

In industrial practice the separation of an azeotropic mixture usually involves adding a third component to the distillation process to break the azeotrope. The major disadvantages of this so-called azeotropic and extractive distillation are the relatively high capital and high energy costs and the possibility of product contamination. If we consider that it is estimated that about 5% of the total energy consumption in Canada and the USA can be attributed to separation processes, we can see the need for new separation methods that require less energy.

Pressure Swing Adsorption (PSA) is another process employed for separation of azeotropes. In a PSA process the mixture is led through a bed where one of the components is preferably adsorbed. When the bed is saturated it needs to be regenerated, therefore multiple beds are necessary making the construction and operation more complicated. However, the energy requirement of PSA is lower than for azeotropic distillation.

A rather new alternative for breaking azeotropes and a fine example of process intensification is coupling membranes with distillation. First steps in this direction were made using well-established polymer membranes, which however proved to be prone to swelling and thermal decomposition at elevated temperatures. High performance membranes are required for successful commercial implementation. In addition to large flux and selectivity, membrane stability at higher temperatures in harsh chemical environment is quite important. Considering the fact that permeation at higher temperature gives larger fluxes, resulting in smaller membrane

areas, inorganic porous membranes could find a wider application in practical separation and purification processes. However conditions that are beneficial for membranes can result in a disadvantage for the distillation side. Membrane separation at elevated temperatures may require distillation to be operated at an increased pressure, which increases both the number of stages and the energy requirement. Advantages and disadvantages should be balanced appropriately to arrive at an optimized integrated process.

In this thesis, the above mentioned features are addressed (Chapter 1). The study focuses on the industrial implementation of ceramic membranes. For this purpose simulations (Chapter 3), lab scale (Chapter 4, 6 and 7) and pilot experiments (Chapter 5) are carried out with different systems.

Chapter 1 gives an overview of the state of the art of membrane processes that are well suited for integration in a distillation process: pervaporation and vapor permeation. This chapter also provides the theoretical background and addresses the potential problems and possible solutions for their commercial implementation.

Chapter 2 emphasizes the importance of an effort to develop alternative separation technologies. It also defines the framework of the specific projects that were covered during the present thesis. Finally it gives the objective and outline of the thesis. The main objective was to find out which combination of ceramic membrane and distillation conditions is technically feasible and economically attractive.

Basic features of the simulation tool developed for the design of shell and tube modules for vapor permeation are explained in Chapter 3. The predictive model describes a ceramic membrane module using the resistance-in-series model that accounts for concentration polarization and support layer contributions. Using ethanol dehydration by means of vapor permeation as base case, a parametric study was carried out to demonstrate the effects associated with changes in operating conditions such as feed flow rate, feed pressure, module feed side, membrane perm

selectivity and tube diameter. High feed pressure and temperature increases the driving force and thus the flux, despite a counteracting effect of increased concentration polarization. From the outcome of these simulations, basic rules to qualitatively predict the performances of vapor permeation modules are suggested.

Chapter 4 describes the vapor permeation lab-scale experiments performed to identify the most suitable membrane for industrial implementation. Two single tube, multilayer ceramic membrane tubes were tested with the water / ethanol mixture. One of them displayed high flux and low selectivity; the other showed lower flux but high selectivity. For each membrane the characteristic membrane parameters were extracted from the experimental results and using the subroutine described in Chapter 3. An integrated membrane distillation process was then simulated to identify the membrane that is more convenient to use for industrial applications. From the simulation results it appears that working with high flux / low selectivity membranes at high column pressure and membrane feed concentration well below the azeotropic composition appears to be the most promising operating condition for the hybrid process.

Chapter 5 rounds up the study of ethanol dehydration making an evaluation of a combined distillation / membrane process based on a pilot-scale set-up equipped with a commercial 7-tube ceramic membrane module for which the permeance and selectivity were measured. The module was tested in a "long duration" experiment and the performance when changing feed concentration and superheating was studied. The membrane performance in the base case (3 bar, 91 % wt ethanol in feed and superheating of 1.5 °C) was a flux of 5.1 kg/h m^2 and selectivity of 5.5. Simulations of the combined process demonstrate that in a process with these membranes the utility requirement of the column is comparable to the requirement of an azeotropic distillation process with three columns. The reason for the high energy consumption was the disappointing low selectivity of the membrane module. However there is still an advantage for the membrane process because it is a "green process" since it doesn't introduce any entrainer, therefore avoids

product contamination and at the same time saves the purchase of entrainer.

Chapter 6 deals with the pervaporative dehydration of the mixture isopropanol (IPA) / water / acetone, which appears during the production of acetone from isopropanol. This study was performed in a joint effort with the group of Prof. Górak at the University of Dortmund. Compared with the available literature, ternary pervaporation experiments showed rather large fluxes at atmospheric pressure (0.5 to 3 kg/h m^2) for different water concentrations (5 to 20 % wt) in the range of 60 to 75 °C. From the characterization experiments model parameters were retrieved and used to simulate the performance of a pervaporation module coupled to a distillation column. The purpose of this flow scheme is to separate pure acetone as overhead and almost pure IPA (95 % wt) at the bottom of the column, while water can be retrieved from a side stream as permeate. A parametric study showed the best conditions for the combined process regarding reboiler heat duty, side stream flow and the position of the feed and retentate streams. The membrane feed should be taken from the middle of the stripping section and the retentate should preferably be recycled to the bottom tray. Compared to the classic two column process an energy saving of about 40% can be reached. Rough economic calculations showed that the hybrid separation process is competitive against the current two column process. However the major hurdle for use of the membrane assisted distillation process is still the high cost of ceramic membranes (In this work estimated at 2000 euros per m^2).

Finally pervaporation (PV) and vapor permeation (VP) through ceramic membranes were compared experimentally at lab-scale and with computer simulations (Chapter 7). This study was carried out with a single tube ceramic module and the system methanol / methyl-tert-buthyl ether (MTBE). At saturation conditions up to 155 °C pure methanol fluxes through a methylated silica membrane appeared to be equal for both pervaporation and vapor permeation. Also the separation of mixtures containing 18 % wt methanol in the liquid feed (PV) and 21.1 to 24.8 % wt in the vapor feed (VP) resulted in comparable methanol fluxes at equal driving force. From

simulations it appeared that at comparable Reynolds numbers the concentration polarization is for pervaporation only a few percent higher than for vapor permeation. The choice of pervaporation or vapor permeation has be made on basis other aspects such as the amount heat required to evaporate the feed for vapor permeation or the heat required for interstage heating in pervaporation. The influence on further separation units also has to be taken into account.

Samenvatting

In de industriële praktijk impliceert de scheiding van een azeotropic mengsel doorgaans het toevoegen van een derde component aan de destillatie om de azeotroop te breken. De belangrijkste nadelen van deze zogenaamde azeotropische en extractieve destillatie zijn de relatief hoge kapitaal- en energiekosten en de mogelijkheid van productvervuiling. Als men in overweging neemt dat ongeveer 5% van het totale energieverbruik in Canada en de V.S. toegeschreven kan worden aan scheidingsprocessen, is duidelijk dat er behoefte is aan nieuwe methoden die minder energie kosten.

Pressure swing adsorption (PSA) is een ander proces dat wordt aangewend voor de scheiding van azeotropen. In een PSA proces wordt het mengsel door een bed geleid waarin één van de componenten preferent wordt geadsorbeerd. Wanneer het bed verzadigd is, moet het worden geregenereerd, waardoor er meerdere bedden nodig zijn en de constructie en de operatie gecompliceerder worden. Nochtans is het energieverbruik bij PSA is lager dan bij azeotropische destillatie.

Een nieuw alternatief voor het breken van azeotropen en een goed voorbeeld van procesintensificatie is het koppelen van membranen en destillatie. Eerste stappen in deze richting zijn gemaakt met gebruikmaking van bekende polymeermembranen, die echter geneigd bleken om te zwellen en thermisch te ontleden bij hoge temperaturen. Hoogwaardiger membranen zijn nodig voor een succesvolle commerciële implementatie. Naast een grote flux en een grote selectiviteit

is de stabiliteit van het membraan bij hogere temperaturen in aggressieve chemische media belangrijk. In overweging nemend dat permeatie bij hogere temperaturen grotere fluxen geeft en dus kleinere membraanoppervlakken, zouden anorganische poreuze membranen breder toepassing moeten kunnen vinden in scheidings- en zuiveringsprocessen. Echter, condities die voordelig zijn voor membranen kunnen problematisch zijn voor de destillatie. Een membraanscheiding bij een hogere temperatuur kan betekenen dat de destillatie bij een hogere druk bedreven moet worden, waardoor het aantal benodigde schotels en het energieverbruik toenemen. De voor- en nadelen moeten nauwgezet tegen elkaar worden afgewogen om tot een geoptimaliseerd geïntegreerd proces te komen.

In deze dissertatie worden de bovengenoemde kwesties behandeld (hoofdstuk 1). Het onderzoek concentreert zich op de industriële implementatie van keramische membranen. Hiertoe zijn simulaties (hoofdstuk 3) uitgevoerd, experimenten op laboratoriumschaal (hoofdstukken 4, 6 en 7) en pilot-schaal proeven (hoofdstuk 5) met verschillende systemen.

Hoofdstuk 1 geeft een overzicht van de modernste membraanprocessen die geschikt zijn voor integratie in een destillatieproces: pervaporatie en damppermeatie. Dit hoofdstuk behandelt ook de theoretische achtergrond en de mogelijke problemen en oplossingen voor commerciële implementatie.

Hoofdstuk 2 benadrukt het belang van het ontwikkelen van alternatieve scheidingstechnologieën. Het definieert ook het kader van de projecten die tijdens dit onderzoek uitgevoerd zijn. Tenslotte behandelt het de doelstelling en de opbouw van de dissertatie. Het belangrijkste doel was uit te vinden welke combinatie van keramisch membraan en destillatiecondities technisch mogelijk en economisch aantrekkelijk is.

De kenmerken van het simulatiemodel, ontwikkeld voor het ontwerp van pijpenbundel ("shell-and-tube") modules voor damppermeatie, worden in hoofdstuk 3 toegelicht. Het voorspellende model beschrijft een keramisch-membraanmodule met gebruik van een weerstanden-in-serie

model. Concentratiepolarisatie en steunlaagcontributies worden hierin in rekening gebracht. Ethanoldehydratie door damppermeatie werd gebruikt als basissysteem en een parametrische studie werd gedaan om de effecten te demonstreren die geassocieerd worden met veranderingen in bedrijfscondities, zoals voedingsstroomsnelheid, voedingsdruk, voedingszijde van de module, membraanpermselectiviteit en buisdiameter. Een hoge voedingsdruk en een hoge voedingstemperatuur vergroten de drijvende kracht en zodoende de flux, ondanks een tegenwerkend effect van de toegenomen concentratiepolarisatie. Op basis van de uitkomsten van de simulaties zijn basisregels opgesteld voor een kwalitatieve voorspelling van de prestaties van damppermeatiemodules.

Hoofdstuk 4 beschrijft de laboratorium-schaal experimenten die uitgevoerd zijn om het membraan te identificeren dat het meest geschikt is voor industriële implementatie. Twee enkelbuis meerlaags keramische membraanbuizen zijn getest met een water/ethanol mengsel. Eén ervan vertoonde een hoge flux en een lage selectiviteit, terwijl de andere een lage flux en hoge selectiviteit had. Voor elk membraan werden de karakteristieke membraanparameters uit de experimentele resultaten afgeleid en ingevoerd in de subroutine beschreven in hoofdstuk 3. Vervolgens werd een geïntegreerd destillatie / membraan proces gesimuleerd om het membraan te identificeren dat het meest geschikt is voor industriële toepassing. Uit de simulatieresultaten komt naar voren dat het werken met een hoge flux / lage selectiviteit membraan, bij hoge kolomdruk en een membraanvoedingsconcentratie ver beneden de azeotropische samenstelling, de meest veelbelovende manier van werken is voor het hybride proces.

Hoofdstuk 5 rondt de studie van ethanoldehydratie af met een evaluatie van een gecombineerd destillatie / membraanproces op een pilot-plant opstelling met een commerciële keramisch-membraanmodule met zeven buizen. De module werd getest in een langlopend experiment en de prestatie werd bestudeerd bij veranderende voedingsconcentratie en oververhitting. De membraanprestatie in het basissysteem (3 bar, 91 % wt ethanol in de voeding en een oververhitting

van 1.5 °C) was een flux van 5.1 kg/uur/m^2 en een selectiviteit van 5.5. Simulaties van een gecombineerde proces met deze membranen laten zien dat het "utility" verbruik vergelijkbaar is met dat van een azeotropisch destillatieproces met drie kolommen. De reden van het hoge energieverbruik was de teleurstellend lage selectiviteit van de membraanmodules. Toch is er nog immer een voordeel voor het membraanproces, aangezien het een "groen proces" is. Er wordt geen hulpstof geïntroduceerd waardoor het product niet wordt vervuild en bovendien wordt er op grondstoffen bespaard.

Hoofdstuk 6 behandelt de pervaporatie dehydratie van het mengsel isopropanol (IPA) / water / aceton, een mengsel dat bij de productie van aceton uit isopropanol ontstaat. Dit onderzoek werd uitgevoerd in samenwerking met de groep van Prof. Górak aan de Universiteit Dortmund. Vergeleken met de literatuur vertoonden ternaire pervaporatie experimenten vrij grote fluxen bij atmosferische druk (0.5 tot 3 kg/uur/m^2) voor verschillende waterconcentraties (5 tot 20 % wt) in een bereik van 60 tot 75 °C. Uit de karakteriseringsexperimenten zijn modelparameters afgeleid en gebruikt om de prestatie te meten van een pervaporatiemodule gekoppeld aan een destillatiekolom. Het doel van het model was het afscheiden van zuiver aceton over de top en vrijwel zuiver IPA (95 % wt) uit de onderzijde van de kolom. Water kan worden afgevangen uit een zijstroom, als permeaat. Een parametrisch onderzoek leverde de optimale condities voor het gecombineerde proces qua reboiler warmte, grootte van de zijstroom en de locatie van de voedings- en retentaatstromen. De membraanvoeding moet afgetapt worden uit het midden van de stripsectie en de het retentaat moet bij voorkeur worden teruggevoerd naar de onderste schotel. Vergeleken met het conventionele tweekoloms proces kan er zo een energiebesparing van circa 40% worden gerealiseerd. Een globale economische analyse toonde aan dat het hybride scheidingsproces concurrerend is ten opzichte van het tweekoloms proces. Nochtans is de hoge kost van keramische membranen (in dit werk geschat op 2000 euro per m^2) nog steeds de grootste drempel voor de membraan / destillatie processen.

Ten slotte zijn pervaporatie (PV) en damppermeatie (VP) door keramische membranen met elkaar vergeleken door middel van laboratoriumschaal experimenten en met behulp van computersimulaties (hoofdstuk 7). Dit onderzoek werd uitgevoerd met een enkelbuis keramische module en het systeem methanol / methyl-tert-butylether (MTBE). Als verzadigingscondities bleken de fluxen van zuiver methanol door een gemethyleerd silicamembraan tot 155 °C gelijk te zijn voor PV en VP. Ook de scheidingen van mengsels van 18 % wt methanol in de vloeistofvoeding (PV) en 21.1 tot 24.8 % wt in de dampvoeding (VP) resulteerden in vergelijkbare methanolfluxen bij gelijke drijvende kracht. Uit simulaties bleek dat bij vergelijkbare Reynoldsgetallen de concentratiepolarisatie voor pervaporatie slechts enkele procenten hoger was dan voor damppermeatie. De keuze voor pervaporatie of damppermeatie dient dan ook gemaakt te worden op basis van andere aspecten, zoals de hoeveelheid warmte die nodig is om de voeding te verdampen bij damppermeatie of de warmte die nodig is voor de tussentraps opwarming bij pervaporatie. De invloed op andere scheidingseenheden moet ook in de overweging worden meegenomen.

Table of Contents

1 Introduction **1**
1.1 Membrane technology in the chemical industry 2
1.1.1 Membrane classification 3
1.1.2 The development path of membrane technology 4
1.2 Pervaporation and Vapor Permeation 5
1.2.1 *Pervaporation* 6
1.2.2 Vapor Permeation 7
1.2.3 Common challenges 9
1.3 Overview 12

2 Project framework and outlook **15**
2.1 The EET project 16
2.2 Framework definition 17
2.3 *Objective and outline of the thesis* 19

3 Modeling and simulation of inorganic shell and tube membranes for vapor permeation **21**
3.1 Introduction 22
3.2 Model Description 23
3.2.1 Membrane mass transfer 24
3.2.2 Shell and tube module 27
3.3 Simulation inputs 28
3.4 Results and Discussion 28
3.5 Membrane Performance Rating 34
3.6 Conclusions 37

4 Vapor permeation with single tube ceramic membranes. Preliminary study of integrated process for ethanol dehydration **39**
4.1 Introduction . . . 40
4.1.1 Polymer materials . . . 41
4.1.2 Ceramic materials . . . 44
4.2 Model Description . . . 47
4.2.1 Thermodynamics . . . 48
4.2.2 Working Equations . . . 48
4.3 Experimental part . . . 50
4.3.1 Set-up and procedure . . . 50
4.3.2 Membrane characteristics and experimental conditions . . . 51
4.4 Results and discussion . . . 52
4.5 Model Validation . . . 55
4.6 Process Simulation . . . 56
4.7 Conclusions . . . 60

5 Vapor permeation with multitube ceramic modules. Pilot-scale study of integrated process for ethanol dehydration **63**
5.1 Introduction . . . 64
5.2 Industrial dehydration processes . . . 64
5.2.1 Distillation-based processes . . . 65
5.2.2 Adsorption-based processes . . . 66
5.2.3 Membrane-based processes . . . 67
5.2.4 Future direction in the ethanol industry . . . 68
5.3 Model Description . . . 69
5.4 Experimental part . . . 70
5.4.1 Set-up and procedure . . . 70
5.4.2 Membrane characteristics and experimental conditions . . . 72
5.5 Results and discussion . . . 74
5.5.1 Base case experiments . . . 74
5.5.2 Long-run test . . . 74
5.5.3 Effect of superheating . . . 76
5.5.4 Effect of feed composition . . . 77
5.6 Process Simulation . . . 79

5.6.1 Model parameters . . . 79
5.6.2 Process conditions . . . 81
5.6.3 Simulation results . . . 82
5.6.4 Cost calculation . . . 83
5.6.5 Comparison of results . . . 86
5.7 Conclusions . . . 90

6 Combined distillation / pervaporation process for the improvement of acetone production **91**
6.1 Introduction . . . 92
6.1.1 Isopropanol dehydrogenation process . . . 92
6.1.2 Review of dehydration of acetone or IPA with membranes . . . 95
6.2 Model Description . . . 98
6.2.1 Thermodynamics . . . 98
6.2.2 Model Approach . . . 101
6.3 Experimental part . . . 103
6.3.1 Membrane set-up . . . 103
6.3.2 Distillation set-up . . . 103
6.4 Results and Discussion . . . 104
6.4.1 Pervaporation Results . . . 104
6.4.2 Distillation Results . . . 108
6.5 Process Simulation . . . 109
6.5.1 Process Specifications . . . 109
6.5.2 Simulations with ideal modules . . . 112
6.5.3 Simulations with real modules . . . 117
6.6 Economic evaluation . . . 117
6.7 Conclusions . . . 123

7 Experimental and module-scale comparison of pervaporation and vapor permeation **125**
7.1 Introduction . . . 126
7.1.1 MTBE process . . . 126
7.1.2 Comparison pervaporation / vapor permeation in literature . . . 127
7.2 Model description . . . 129

7.2.1 Driving force 129
7.3 Experimental section 132
7.3.1 Set-up and procedure 132
7.3.2 Membranes and conditions 132
7.4 Results and discussion 133
7.4.1 PV and PV for pure methanol 133
7.4.2 PV and VP for the mixture methanol / MTBE 134
7.5 Simulation study 136
7.5.1 Conditions and specifications 136
7.5.2 Simulation cases 137
7.5.3 Simulation results 138
7.5.4 Operational aspects 140
7.6 Conclusions 142
Appendix 1 143
Appendix 2 148
Bibliography 154
List of Symbols 171
Acknowledgements 176
List of publications 179
Curriculum Vitae 181

List of Figures

1.1 Water condensation temperature at sub-atmospheric pressure 10

3.1 Concentration polarization resistance as function of Re-number and pressure . . 30
3.2 Polarization resistance as function of Reynolds number and tube diameter for modules with feed in the tubes (solid lines) and on the shell side (dashed lines) 30
3.3 Contribution of boundary, support and selective layer to total permeation resistance as function of diameter, pressure, feed flow and module feed side. 31
3.4 Retentate pressure drop as a function of Reynolds and tube diameter for modules with feed in the tubes (solid lines) and on the shell side (dashed lines) 32
3.5 Retentate pressure drop as function of Reynolds and feed pressure 32
3.6 Permeate and retentate pressure drop for modules with feed in the tubes (dashed lines) and on the shell side (solid lines). Circles represent retentate pressure drop, triangles represent permeate pressure drop 33

4.1 Experimental and simulated ethanol / water VLE data 48
4.2 TNO experimental set-up for single tube experiments 51
4.3 Experimental performance of M1 and M2 53
4.4 Water flux against partial pressure difference for M1 and M2 54
4.5 Ethanol flux against partial pressure difference for M1 and M2 54
4.6 Experimental and calculated fluxes with parameters from Table 4.3 56
4.7 Flow scheme for process simulation 57
4.8 Membrane area as function of (column) feed pressure and top composition . . . 59
4.9 Column reboiler heat duty required for different pressures 59
4.10 Membrane area required for different operating pressure 60

5.1 TU Delft distillation / membrane pilot-scale set-up used during experiments . . 71

5.2 Photo of the 7-tube membrane module used for experiments 73
5.3 Membrane module used in pilot plant experiments (measures are in mm) 73
5.4 Variation of flux during the long-run test 76
5.5 Variation of flux with superheating temperature (line is only an eyeguide) . . . 77
5.6 Flux as function of partial pressure for two different superheating (sh) temperatures 78
5.7 Variation of flux as function of ethanol (membrane) feed concentration for two different superheating (sh) temperatures 79
5.8 Experimental against calculated fluxes with parameters in Table 5.3 80
5.9 Flow scheme for process simulation 81
5.10 Total flux and Reynolds profile along membrane modules 82
5.11 Water depletion and driving force profile along membrane modules 83
5.12 Contribution of the most important equipment (including installation) to the total investment cost (1.7 Meuro) 84
5.13 Distribution of the annual production cost (1.2 Meuro) for the combined distillation / membrane process 85
5.14 Utility requirements for the previous [128] and current studies 86
5.15 Total investment for the previous [128] and current studies 88
5.16 Annual cost for the previous [128] and current studies 89

6.1 Acetone production process via isopropanol dehydrogenation 94
6.2 Vapor - liquid equilibrium for the system IPA / water at atmospheric pressure . 99
6.3 Ternary diagram for the system acetone / IPA / water 99
6.4 Ternary vapor - liquid equilibrium diagram as function of temperature at atmospheric pressure (generated by Chemsep v6) 100
6.5 Photo of set-up and membrane module used for experiments at Uni. Dortmund 104
6.6 Continuos distillation set-up used for experiments (image from Uni.Dortmund) 105
6.7 Membrane performance during experiments with IPA / water mixture 106
6.8 Membrane performance during experiments with ternary mixture 107
6.9 Experimental against calculated fluxes with parameters from Table 6.2 108
6.10 Mass balance and flows during distillation experiments 109
6.11 Experimental and simulated column profiles 110
6.12 Flow scheme for process simulation 110
6.13 Change in column composition profile as function of installed membrane area . 113
6.14 Change in column composition profile with different configurations 114

6.15 Membrane area as function of Φ ratio and reboiler duty for ideal modules . . . 116
6.16 Membrane flux and water composition profile for configuration III.c 118
6.17 Utility requirements for the studied configurations and 2-column process 120
6.18 Membrane area required for the studied configurations 121
6.19 Investment cost for the studied configurations (including installation) 121
6.20 Annual costs calculated for the studied configurations 122

7.1 Pure methanol experiments as function of temperature for pervaporation and vapor permeation 134
7.2 Pervaporation fluxes for methanol and MTBE as function of temperature for binary mixture (experimental series III, IV and V) 135
7.3 Pervaporation and vapor permeation fluxes for methanol and MTBE as function of temperature (a) or fugacity difference (b) for binary mixture using membrane M4 135
7.4 Increase of polarization resistance as function of methanol permeance for PV and VP 141

List of Tables

3.1 Base case data and values used in the parametric study 29
3.2 Variation of polarization as functrion of permeance and perm-selectivity 35
3.3 Module performance indicator 36
3.4 Example inputs and results 36

4.1 Fluxes gathered from literature review for the system ethanol / water 47
4.2 Membrane tube characteristics 52
4.3 Membrane parameters determined from experiments 53
4.4 Process simulation input 57
4.5 Feed pressure and composition for process simulation 58

5.1 Initial pervaporation performance of the module (measured by producer) 72
5.2 Base case conditions for pilot-scale set-up 75
5.3 Membrane parameters determined from experiments 80
5.4 Process simulation input 81
5.5 Data used for economic evaluation 84
5.6 Results from preliminary study for ethanol dehydration with membranes [128] . 87

6.1 Fluxes gathered from literature review for the system acetone / water or IPA / water 97
6.2 Membrane parameters determined from experiments 107
6.3 Description of simulation cases 111
6.4 Simulation results with the lowest membrane area (2 MW) 115
6.5 Simulation results for ideal modules 116
6.6 Simulation results for real modules 118
6.7 Data used for economic evaluation 119

7.1 Membrane tube characteristics 132

7.2 Experimental conditions 133
7.3 Membrane parameters determined from experiments 136
7.4 Description of simulation cases 138
7.5 Simulation results 139
A1-1 Simplification of Maxwell-Stefan equation 149

Chapter 1

Introduction

Every year millions tons of solvents are dehydrated worldwide, most of them form azeotropes with water. There is then a large worldwide market for efficient solvent dehydration systems. The first step in the production of organic solvents is the synthesis, after which the solvent must be separated from the reaction mixture. Water is frequently present in industrial mixtures. Normally this separation is carried out by distillation. The usual technique for the separations of mixtures containing azeotropes by distillation involves the separation in (at least) two distillation columns.

One of the methods uses distillation at high pressure in the first column, almost reaching azeotropic composition. The distillation in the second column is carried out at low pressure where the azeotropic point is at a different concentration and the solvent can be distilled without problems. Obviously this method only works when the azeotrope varies with pressure. The disadvantage of this method is the energy requirement because the specification in the first column is very close to the azeotrope, as a consequence high reflux and reboiler duty are needed.

Other distillation method to separate azeotropic mixtures uses the addition of a third component (entrainer) to the mixture. This component forms an (heterogeneous) azeotrope with lower

boiling point than the previous azeotropic mixture. Cyclohexane is used as entrainer in most of the alcohol dehydration plants.

Alternative dehydration methods include Pressure Swing Adsorption and membrane technology. In Pressure Swing Adsorption (PSA) water selectively adsorbs on mesoporous material at a certain (high) pressure. Water is later released by decreasing the pressure in the vessel. It has been demonstrated that the combination of distillation and PSA can be cheaper than azeotropic distillation [55, 118].

Early attempts using membrane technology in combination with distillation for solvent dehydration are reported in literature [2, 113, 112, 137]. This particular combination uses less energy and cooling water. Further, membrane technology doesn't make use of any extra chemicals that can be toxic for health and environment. From estimations seems that the reduction in energy costs as a result of implementation of membrane technology for solvent production can be around 1.2 PJ/y only in the Netherlands, this is equivalent to the reduction of 70,000 ton CO_2, 600,000 ton cooling water and 270 ton cyclohexane per year [129]. There are further savings if membrane technology would be applied for the recuperation and reuse of solvents.

1.1 Membrane technology in the chemical industry

Membrane technology has gained a huge importance in the last 30 years, competing with long established technologies in fields as drinking water production, food processing, bio-chemical and medical applications. In the future membranes can give a special contribution to green chemistry, not only reducing energy consumption, recovering valuable products and minimizing environmental problems, but also in the field of alternative energy as they are one of the fundamental parts within fuel cells.

1.1.1 Membrane classification

Different methods of membrane preparation have been published in several reviews [126, 74, 49, 7]. As the objective of the present work is not related to membrane preparation or characterization, these subjects won't be further detailed, and just a brief introduction will be given.

Membranes can be classified, according to their morphology, as dense (polymers and metals), porous (most of them are inorganic) and composite (mixtures of different materials). According to their support structure they can be divided in symmetric and asymmetric. Symmetric membranes are made completely of one material while for asymmetric membranes different layers are used.

The development of membranes for pervaporation and vapor permeation was highly influenced by the development of desalination and gas separation membranes and the theoretical knowledge of their structure and transport. There are basically two different types of membranes used for pervaporation and vapor permeation: hydrophilic and organophilic membranes. The first permeates preferentially water or some small alcohol molecules from other organics, while the organophilic membranes permeate preferentially non-polar compounds.

Polymeric materials used for hydrophilic membranes include polyvinyl alcohol (PVA), polyamides, natural polymers like chitosan or cellulose acetate (CA) or alginates. Instead, most of the organophilic membranes are made from polydimethylsiloxane (PDMS) or polymethyl-octyl-siloxane (POMS). Zeolite NaA is extremely hydrophilic and the crystal pore is only accessible for water molecules, in consequence they present large selectivity and flux. However, the more hydrophilic the zeolite is, the more sensible to acid conditions. Amorphous silica is also used for membrane applications and as the surface contains hydroxyl groups, the separation layer is highly hydrophilic too. The advantage of this material is that it is stable against acid conditions. Modifying the surface with different functional groups, zeolite and silica membranes can be used

as organophilic membranes to separate small from big organic molecules.

1.1.2 The development path of membrane technology

Each successful application for membranes is the result of a whole series of technical (first) and commercial (second) activities. Typically the development occurs as follows:

1. Identification of a potential application: Is the separation of one of the components in the process the limiting factor for the whole process? Is membrane technology a candidate for such separation/recovery?

2. Membrane material selection: Does a material exist with the combination of flux and selectivity desired for this application? Is the material resistant to chemicals, temperature and pressures present in the application?

3. Membrane form: How can the selected material take the form suited for the application? Is that a film, a tube or a hollow fiber?

4. Membrane module geometry: Membrane tubes, fibers of sheets should be accommodated into a module that combines the most membrane area required in the least volume without affect the performance of the module due to hindering in driving force or hydrodynamic problems.

5. Sealing: Is the sealing material suitable to withstand process conditions?

6. Module manufacture: Can the membrane module be manufactured in a cost effective manner?

7. Membrane characterization: Can the membrane/module perform as predicted? Are the results reproducible for different modules?

8. Process design: Can the membrane be incorporated into a flowsheet to optimize the combined process? Can start-up and shut-down simulated and predict the best-operation measures?

9. Membrane system: Can the membrane be packaged into a "plug-and-play" system that will operate with any peripheral equipment? Can the membrane system be upscaled by just adding more of the membrane modules? Are the systems compact and or mobile?

10. First applications: Where will be tested commercially by the first time? Which scale would be acceptable for the operation?

11. Cost and performance: Can the membrane system beat the current technology?

12. Marketing and sales: After successful industrial application it is needed to let know to the chemical industry and attract attention to the new technology in order to get more potential customers and applications.

All these steps are relevant and the failure of any of them may cause the failure of membranes for the intended application.

1.2 Pervaporation and Vapor Permeation

Pervaporation (PV) and Vapor Permeation (VP) are very closely related membrane separation processes. In both cases the mass transport through the membrane is a gradient in chemical potential that can be better understood as a gradient in activities of the sorbed components. The separation is governed by the physico-chemical affinity between the membrane material and the components to separate. The main difference between the processes is the phase and the thermodynamic condition of the feed side mixture.

1.2.1 Pervaporation

Applications History

In 1917 P.A. Kober published a paper in which he described his observations that "a liquid in a collodion bag, which was suspended in the air, evaporated, although the bag was tightly closed" [94]. Later considerable effort was devoted during the fifties to produce effective membranes in order to produce pervaporation as an industrial separation process. The materials used in that time were natural and synthetic rubbers, cellulose esters and several polyolefines. However, none of these early membranes could be applied industrially due to an insufficient flux and selectivity. In 1982 the first pervaporation membrane was brought into the market by the German GFT [14, 9, 13]. The removal of water from industrial solvents was the first application for this system. In 1983 the first ethanol dehydration plant started operations in Brazil, with a capacity of 1200 liters per day of pure ethanol. Following the example of Brazil, other plants used pervaporation for the same purpose [113]. With the experience gained with the ethanol plants, an ester dehydration plant started operations in 1988. Soon after other azeotrope-forming solvents followed. The first plant that used a membrane reactor for the production of diester started operations in 1994 [90]. With help of pervaporation water was continuously removed from the reaction mixture shifting the reaction equilibrium towards the wanted product. Removal from VOC's from aqueous streams using pervaporation with organophilic membranes has been tested [31, 12, 15, 127], but not yet found industrial application. Other potential applications for pervaporation include difficult organic / organic separations like aromatic from aliphatic, olefins from paraffins, fractionation of isomers, the separation of aroma components from natural products and many more. The first pilot-plant separating methanol from trimethylborate (TMB) started operations in 1997 [143]. As the selectivity and stability of current membrane increases as well as the discovery and applications of new membrane materials, there is still a lot of potential

for the use of pervaporation in commercial applications.

Pervaporation characteristics

A detailed explanation of pervaporation principles is not intended. An excellent review of the theory behind pervaporation and the industrial practices can be found in [49, 90, 85, 106].

Pervaporation employs liquid as feed, the liquid should be rather at high temperature since the driving force depends on it. As the liquid feed mixture flows over the membrane, the most permeable component is removed and its concentration lowered in the feed side. The heat of evaporation is given by the liquid, thus a drop in concentration and temperature occurs between the entrance and the exit of the module. On the permeate side, the pressure is kept low by vacuum pumps, and the permeated vapors are condensed at a sufficient low temperature.

In pervaporation, the driving force of the components is fixed by their own characteristics, namely their composition and the system temperature, whereas the total pressure is of no influence, as long as the liquid mixture can be regarded as incompressible. Only by increasing the temperature of the liquid mixture the partial vapor pressure can be increased for a given feed mixture.

1.2.2 Vapor Permeation

Applications History

Though pervaporation is already known for decades, the research and application of vapor permeation is quite recent. It is clear the number of publications and applications regarding pervaporation is outrageous comparing those about vapor permeation. However, vapor permeation appears as more convenient alternative for some particular applications. The choice of applying pervaporation or vapor permeation depends mainly on specific site conditions, for instance,

vapor permeation is preferred when the feed is already available as vapor, or when there are dissolved or undissolved solids present in the original feed, or when the additional heat consumption (to evaporate the liquid feed) is not an issue. The major advantage of vapor permeation over pervaporation is that no temperature drop of the retentate occurs, thus intermediate heat exchangers are not needed and that concentration polarization is less pronounced. Today vapor permeation processes are used in the dehydration of some organic solvents [33, 41], in the removal of methanol from other organic components [25, 81] or in the removal of VOC's from process streams and some other applications [112, 143, 19].

Vapor Permeation characteristics

A detailed explanation of vapor permeation principles is not intended. An excellent review of the theory behind vapor permeation and the industrial practices can be found in [49, 90, 85, 106].

Vapor permeation differs from pervaporation because the liquid feed to be separated is already evaporated. In this way vapor is directly in contact with the membrane surface. As the feed is already a vapor, no phase change occurs across the membrane and no temperature polarization is observed. However, concentration polarization still occurs. Although the diffusion coefficient is much higher for a vapor than for a liquid, concentration polarization effects may still be observed when membranes with large fluxes are used.

In vapor permeation the driving force of the components is fixed by their composition and the system pressure. Temperature plays a secondary role and depending on the membrane material it may have a positive or a negative influence on membrane flux [121].

1.2.3 Common challenges

The commercial success of pervaporation has not been as researchers and process developers expected in the early eighties. To avoid further discredit of VP and PV the recognition and solution of several operational adversities should be cleared up. The most common practical difficulties and future challenges are discussed in what follows.

Permeate side conditions

The driving force for mass transport through the membrane is applied and maintained by reducing the partial vapor pressure at the permeate side. It is obvious that the lower the pressure, the lower the concentration of the most permeable component that can be reached on the feed side, but having a very low permeate pressure has actually more disadvantages than advantages. First of all because when the permeate pressure is too low, so it is the condensation temperature. For example, if the permeate component is water, Figure 1.1 shows the condensation temperature of water at pressures below atmospheric. Chilled water is required for condensation temperatures below 25 °C, while for temperatures below 10 °C refrigeration machines are required. Both of the above mentioned solutions are expensive and use a lot of energy. When the required condensation temperature drops below the value of -20 °C, recompression in a large vacuum pump and condensation at sub-atmospheric pressure (e.g. 0.1 bar) offers a better alternative.

The permeate side is especially sensitive to pressure losses. Since permeate pressure determines the condensation temperature in the permeate side, there has to be an unobstructed flow from the membrane module to the condenser because even a pressure drop of a couple of millibars will have severe effect on the performance of the system.

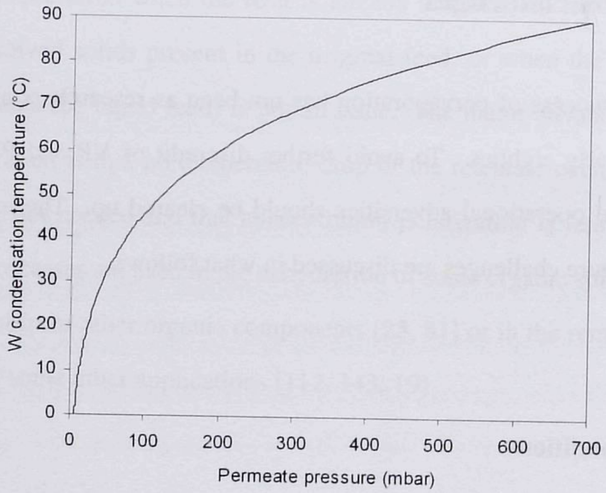


Figure 1.1: Water condensation temperature at sub-atmospheric pressure

Module Design

Initially, the design of pervaporation and vapor permeation modules has been practically copied from the modules used for water treatment. Though, the specific requirements of pervaporation and vapor permeation demand significant modifications to those modules.

In the last few years the poor design of PV and VP modules has been recognized and several studies about modeling and design of membrane modules and hybrid processes have been published [107, 77, 76, 148, 157, 67, 125, 10, 139]. Recently Computational Fluid Dynamics (CFD) has been used thoroughly in all fields of engineering and membrane technology has not been the exception [150, 144, 124, 73, 62, 80, 72, 39]. Nevertheless, CFD has not given breakthrough guidelines towards better and / or more efficient membrane modules, mainly because the reported studies struggle with the dilemma of what to improve and simulate, the fluid dynamics or the mass transfer performance.

The problems to tackle in module design are slightly different for pervaporation and vapor permeation. The main difficulties in module design are discussed in what follows.

Pressure drop at the feed side has to be reduced to a minimum for vapor permeation, otherwise the module would no longer operate at constant pressure, decreasing the components driving force and also the vapor could reach the region of superheating. For pervaporation the pressure losses are not so important, but placing several modules in series will eventually reach the vapor pressure limit.

Pressure drop at the permeate side is even more important for PV and VP, especially when low final concentrations of one of the components has to be reached. Therefore any pressure losses, even in the range of a few millibar, have to be avoided at the permeate side by means of smart module design.

The chemical and mechanical compatibility of all of the components of the module towards the mixtures to separate and the process conditions is of vital importance. This is not limited to membrane material, but also includes gaskets, spacers, potting material and, if used, glues. Their lifetime will determine the good performance of a membrane module.

Membrane characteristics

Membrane selectivity has to be determined according with the product specifications together with the process conditions. Selectivity has to be high when the feed concentration of the component to remove is also high, especially to avoid the loss of the main product (most of the times the less-permeating component). But when very low concentrations have to be reached, high selectivity is no longer desirable. Membranes with low selectivity will allow the permeation of some molecules of the most retained component and this will decrease the partial pressure of the most permeable component, increasing thus the driving force. It might be possible to use membranes with two different selectivities in the same separation process.

Pre-requisite for successful implementation of membranes is the long term stability and high flux. Driving force increases with higher temperature and pressure at the feed, thereby increasing the membrane flux and decreasing the required membrane area. In this respect ceramic materials suit better in harsh conditions, where polymer membranes may degrade or suffer from swelling within short time [120]. Blending and cross-linking polymer materials can resolve this problem to a certain extent; however due to their better chemical, mechanical and thermal stability, ceramic membranes offer a better perspective for industrial applications. In spite of the higher stability of ceramic materials, water interacts a lot with silica and the decrease of flux within time is frequently seen for silica membranes [25, 121, 39, 147, 6], due to adsorption and reaction with silanol groups on the silica surface, causing a densification of the silica [39]. The consequence is the decrease in both permeability and selectivity. Furthermore, there might be reactions of the alcohol with the supporting alumina layers [24] spoiling at all levels the performance of the membrane. Further research has to focus on the improve of membrane materials, obtaining materials with stable performance from 3 to 5 years at process conditions.

1.3 Overview

The present thesis gives a clear and objective perspective of the opportunities and challenges of membrane technology. Looking at literature it seems that the breakthrough of pervaporation and vapor permeation technology will be in dehydration applications. However to make solvent dehydration with membranes more attractive, some key issues should be improved seriously: material stability, constant performance, membrane and module durability and finally lower price. From a previous PhD thesis at our group [33] it appears that the permeability and thermal stability of polymer membranes is not suitable for bulk commercial applications. On the other hand ceramic membranes have a better permeability and their stability allows them

to withstand high temperatures and pressures, which favors driving force. Another study [128] showed that an optimized distillation / vapor permeation process with ceramic membranes uses only 36% of the energy used by the azeotropic distillation process and less energy than with any other membrane material, which seems a very attractive option for commercialization. It is clear that although membranes seem to be a perfect solution for several tough separations some intrinsic separation and practical problems are still unresolved:

Although the fact that membranes don't follow vapor - liquid equilibrium and therefore are not limited by azeotropic mixtures, they are limited by the component driving force and when dealing with deep purification of one of the components the driving force becomes so small that 50% of the membrane area (or more) will be used for the removal of traces.

Retentate pressure is important to increase driving force, but if the system is coupled with distillation, the separation will be more difficult. Another problem is that permeate pressure is a very important variable, especially in the case of high purity. At the same time there are several practical problems when using deep vacuum, condensers under vacuum and, eventually, permeate sweep installations. Both problems might be solved placing intermediate compressors (after the distillation column and before the permeate condenser, respectively) to have the advantage of increased pressure only where convenient. Nevertheless compressors are expensive, consume a lot of energy and are very sensitive during operation. All these problems have to be tackled during design and operation of the complete process.

Each of the above mentioned problems bring an opportunity for research and development of new materials, methods and processes with the final objective of making membrane technology more reliable, easier and cheaper.

Chapter 2

Project framework and outlook

In 2001 the European Commission adopted an action plan to reduce the dependency on (imported) oil and to achieve commitments related to the Kyoto protocol. This action plan [130] consists of two proposals: The first proposal concerns a directive requiring an increasing proportion of biofuel sold in the member states and announcing, for a second phase, the obligation to blend a certain percentage of biofuels into all gasoline and diesel. The second proposal creates a European-wide framework allowing member states to apply differential tax rates in favor of biofuels.

The outlook in the coming 20 to 30 years in Europe is that oil production is expected to decline and as consumption will increase this will result in increasing dependency on imports. The Kyoto protocol commits the European Union to an 8% reduction of greenhouse gas emissions by 2010 [130]. Biofuels would reduce greenhouse gas emissions. The production of bio-ethanol based on agricultural crops will also produce employment and development in rural areas, as well as investments.

2.1 The EET project

Every year millions tons of solvents are dehydrated worldwide. The world production of ethanol was estimated in more than 32 million tons per year in 2005, from which the largest part (90%) is bio-ethanol (from biomass) [152]. There are around 90 industrial solvents that form azeotropes with water. There is then a large worldwide market for efficient solvent dehydration systems and membrane technology seems to have several advantages over the existing dehydration methods.

Few years ago, a joint initiative of the Dutch Ministries of Economic Affairs, Education, Culture and Sciences and that of Housing, Spatial Planning and Environment, promoted several national Economy, Ecology and Technology projects (so-called EET projects) to bring the necessary technology to industry and reduce energy use and generation of pollutants. The development of clean and low-energy separation processes is very important to limit carbon dioxide (CO_2) emissions and to improve the energy efficiency, especially, in the chemical industry. Improving the efficiency of current processes will be reflected, among others, in the reduction of the use of cooling water, chemical entrainers and fuel for the production of energy or heat.

The present thesis was performed in the frame of two EET projects (EETK 20046 and EETK 20061), which promote the integration of the available knowledge in membrane technology to arrive to more efficient processes for the dehydration of solvents. One objective is to improve the current distillation processes by integrating distillation and membranes, in this way the use of entrainers will be diminished. Another of the objectives is to decrease the dehydration costs and energy savings by means of better and cheaper membrane modules. It is expected to develop membranes "fit to purpose", i.e., membranes meeting specific requirements related to permeability, selectivity, temperature application range and compatibility with the process conditions. Also the production of membranes and module design should meet special requirements. Membrane and module design should account the adverse effects of the decrease in driving force, pressure

and eventually temperature drop. Finally it is intended to demonstrate if the use of membrane technology can be applied without the use of expensive cooling machines.

2.2 Framework definition

The first part of this thesis was developed for the Economy, Ecology and Technology national project EETK 20046. Ethanol is nowadays regarded as the most attractive fuel in the mid- and long-term, with an enormous potential of sustainable production and CO_2 reduction. In the last decade oil price has increased from a yearly average of 18 (in 1997) to around 60 (in 2006) USD per barrel (equivalent to 0.085 and 0.285 euro per liter, respectively). This has brought a debate on how our society will maintain their fuel demand when the oil reserves in the surface scarce drastically or finish up. Scientist point towards renewable and sustainable energy sources and ethanol seem to fulfill all requirements to substitute gasoline to fuel our motors. The challenge is that only pure ethanol ($\geq$ 99.9 % wt) can be used as motor fuel and at the moment a lot of energy is used during the purification of ethanol with the so-called azeotropic distillation process, which uses several distillation columns to break the azeotrope with water. An alternative process makes use of simple distillation in combination with vapor permeation, i.e. sending directly the overhead vapor from the column to a membrane unit. If vapor permeation satisfies the requirements regarding permeability, selectivity and membrane stability, it could provide a cheaper alternative for the current processes. There are several references about the opportunities of membranes in chemical industry [103, 113, 79, 146, 70, 57] but until now, only few membrane processes has been successfully commercialized [70, 57, 137, 147, 83, 122]. From a preliminary study [128] appears that the permeability and thermal stability of polymer membranes does not suit their bulk commercial application. On the other hand ceramic membranes have a better permeability and their stability allows them to withstand high temperatures and pressures, which

favors intermembrane driving force. In the same study it is demonstrated that an optimized distillation / vapor permeation process uses only 36 % of the energy used by the azeotropic distillation process, which poses a very attractive option for commercialization.

The second part of this thesis was possible with the kind cooperation of Prof. Andrzej Górak and his Chair of Fluid Separation Processes (TVT) at Dortmund University and the Marie Curie office (HPMT-CT-2001-00408). We have worked together to investigate the feasibility of the combination of distillation with pervaporation for the separation of water from the reactor effluent in the acetone production process. Acetone is one of the most used solvents in industry and in the current production process the reactor effluent is a mixture of acetone, isopropanol and water which is separated with several distillation columns obtaining pure acetone as overhead product and recovering azeotropic isopropanol in a second column that is sent back to the reactor. Making use of pervaporation membranes this process can be retrofited by withdrawing a liquid side stream from the column and returning the retentate back. This makes possible to obtain pure acetone at the top, high purity isopropanol in the bottom and almost pure water as permeate in one column only. This eliminates the need of a second column for the recovery of isopropanol.This process also uses less energy because less water is sent back to the reactor, where it must be evaporated and further separated, saving in both ways considerable amount of money and energy.

The last part of this thesis was also in the frame an EET project (EETK20061) with the same objectives mentioned in section 2.1. In this case the main work was developed by F.T. de Bruijn [25], studying the molecular phenomena that occurs during the permeation of methanol from methyl-tert-butyl-ether with methylated silica membranes. He focused on understanding the contribution of the several membrane layers to mass transfer resistance, the adsorption behavior and the relation of pore size distribution and the separation performance on this kind of membranes, in both pervaporation and vapor permeation. Since the beginning we saw a lot of

synergy between both projects, because the observations and conclusions at molecular level can help to design a better module, with the final objective of improve the overall performance of the whole process. We also have tried to answer the (obvious) question *"which one is more convenient: pervaporation or vapor permeation?"*, but the answer is not easy. We have tackled this problem from a new perspective, comparing them at the same chemical potentials, rather than the approaches studied earlier [91, 89, 34]. The present study has been implemented in different scales: at molecular level and modular scale. With this we have tried to give a general quantitative answer but, in spite of our effort, it seems that only particular answers can be given, depending on the process conditions and product specifications.

2.3 Objective and outline of the thesis

The present work concerns about the application of membrane based separations, more specifically pervaporation and vapor permeation, for the dehydration of organic solvents. The membrane properties, module design and process configuration are detailed studied to identify when the combination of distillation with membranes is technically feasible and economically attractive. The current study focuses in particular on ceramic membranes because they offer a better thermal, chemical and mechanical stability than polymeric membranes and, above all, larger fluxes. The combined processes are compared with the state-of-the-art technology, revealing their true potential to compete with the current commercial processes. Three promising applications are closely investigated

1. Dehydration of bio-ethanol with vapor permeation (discussed in Chapters 4 and 5),
2. Purification of acetone with pervaporation (discussed in Chapter 6), and
3. Purification of methyl-tert-butyl-ether with both vapor permeation and pervaporation (dis-

cussed in Chapter 7)

On each of the above mentioned cases the overall process performance is enhanced with hybrid distillation / membrane systems. The present thesis place several unknowns and specific challenges to membrane technology that must be answered in the best technical and (most of all) economical way.

Chapter 3

Modeling and simulation of inorganic shell and tube membranes for vapor permeation

[1] *Basic features of a simulation tool developed to enable tailor made design of shell and tube modules for vapor permeation are demonstrated. The predictive model describes a ceramic membrane module using the resistance-in-series model that accounts for concentration polarization and support layer contributions. Using ethanol dehydration as base case, a parametric study is carried out to demonstrate the effects associated with changes in variables such as feed flow rate, feed pressure, module feed side, membrane perm-selectivity and tube diameter. From the outcome of these simulations, basic rules to qualitative predict the performances of vapor permeation modules are suggested.*

[1] **This chapter has been published in:** *Chemical Engineering and Processing* 45 (2006) p. 973-979

3.1 Introduction

Separations of azeotropic mixtures, such as alcohol / water and recovery of solvents, are typical examples of bulk chemical processes where combining membranes with distillation has proved to be technically and economically attractive alternative for processes that just rely in distillation [112, 84, 41, 81, 79]. As in some of these processes a saturated mixture at near azeotropic composition leaves the top of the column, an evident choice is to apply vapor permeation instead of pervaporation. Though vapor permeation requires the supply of a certain degree of superheating to the membrane feed to avoid the possibility of condensation in the membrane tubes [112, 19].

Ethanol dehydration is a typical industrial application where pervaporation combined with distillation is an already established technology [84, 57, 90]. Vapor permeation is more suitable than pervaporation for alcohol dehydration, because the vapor leaving the top of the column can be the feed stream for the membrane unit. Membranes with high flux are a better option for this purpose, since the permeate stream can be recycled back to the distillation column to recover the permeated ethanol. Unfortunately, in all applications, a decline in flux has been observed with time [5, 16, 102]. Currently, the stability of the high flux performance is a main concern of the ceramic membrane manufacturers. Namely, a prerequisite for successful implementation of membranes in bulk chemicals separation is achieving a rather high and stable flux.

For the configuration in which the membrane is coupled directly in the distillate stream, the membrane feed pressure is the same as in the top of the column, therefore the driving force for mass transport through the membrane can only be altered by column pressure and/or superheating temperature. This may well imply operation at pressures and temperatures well above that utilized with well established polymeric membranes [54]. Such a trend led to increased interest for development of suitable inorganic membranes. Unfortunately, the manufacture of ceramic membranes is intrinsically more expensive and complicated than for polymers, which is

an additional argument for pushing toward a flux as high as possible.

However, concerning the design/rating of vapor or liquid mass transfer equipment there is always a strong relation between the hydrodynamics imposed by geometry and the mass transfer performance of the contacting device. In other words, a designer should be able to minimize intrinsic membrane limitations and find the operation at the most favorable conditions. Regarding the associated complexities this is not an easy task, which nevertheless could be easier if a reliable design tool would be available.

The current chapter introduces the model that will be used throughout the thesis. A summary with the relation between the detailed mass transfer approach (Maxwell-Stefan equation) and the present approach is given in the Appendix 1 at the end of this thesis. The modifications to the model for applying it for pervaporation are given in Chapter 6.

This study introduces a model that includes the relation between design, operating variables and the performance of a vapor permeation module. Using the dehydration of ethanol as base case, a parametric study is carried out to determine the effects associated with the changes in some variables and the mass transfer resistances. From the outcome of these simulations, basic rules to improve the performance of vapor permeation modules are suggested and the validity of the rules is demonstrated by some examples.

3.2 Model Description

The present model is comprised of a membrane mass transfer model and a shell and tube module model. The first accounts for the mass transported from the feed to the permeate side in a differential of length and the second includes the geometry and hydraulic conditions and integrates lengthwise the complete module. In the present model, the pressure drop is calculated using established engineering models [101]. The assumptions of the model are: a) steady state, b) binary

system, c) isothermal operation and d) no back-mixing effects considered. The latter is justified by the fact that the values of Bodestein number encountered in this study were well above those implying a significant role of back-mixing [107].

3.2.1 Membrane mass transfer

Regarding the mass transfer resistance, an inorganic membrane may be defined as a permselective barrier or interface between two phases [85], with a very thin (selective) layer which determines the separation. A thicker (support) layer is necessary to give mechanical strength because the thickness of the selective layer is in the nanometer range. The top (selective) layer must be a defect free surface, since a few defects can reduce significantly the selectivity without having much influence on the flux. A recent study [27] has indicated that the support layer could have a significant effect for membranes with high flux. Another resistance to mass transfer is that associated with the feed side boundary layer caused by the change in composition of the most permeable component. Each of individual resistances is described in greater detail in what follows.

Selective Layer

The transport properties of the different components through the membrane are described by the permeance Q_i, which is defined as the transport flux per unit driving force. Usually it is determined in laboratory scale membrane characterization experiments with pressure, temperature and feed composition varied over the range of interest. The corresponding mass transfer resistance can be expressed as

$$\frac{1}{k_m} = \frac{1}{Q_i RT} \tag{3.1}$$

where R is the gas constant and T is the absolute temperature.

The temperature dependence of the permeance is usually described using an Arrhenius type equation. However, in this chapter, a constant experimental value for the permeance is used.

Support Layer

The support layer must have an open porous network to minimize the mass transfer resistance. For porous membranes, the resistance can be governed by different mechanisms depending on the size of the molecules and other support characteristics. The well known Knudsen number, Kn, which relates the membrane pore diameter with the mean free path of the molecule, determines the type of transport mechanism through the pores. For the support layer of the membrane considered in this study the calculated Kn is between 10 and 100, asserting the validity of the Knudsen regime in this layer. Knudsen diffusivity is defined as

$$\mathbb{D}_{Kn} = \frac{d_p}{3}\sqrt{\frac{8RT}{\pi MW}} \tag{3.2}$$

where d_p is the mean pore diameter of the support layer and MW is the molecular weight of the permeation species. The corresponding mass transfer resistance can be expressed as

$$\frac{1}{k_{sl}} = \frac{\delta}{\mathbb{D}_{Kn}} \tag{3.3}$$

where δ is the thickness of the support layer.

Boundary Layer

During membrane operation the component to be separated permeates at higher rate than the other components in the feed, which implies a certain degree of depletion in the immediate vicinity of the selective layer. This phenomenon known as concentration polarization affects the

membrane flux adversely, because it causes a significant reduction in the driving force. In fact this is a typical mass transfer resistance which can be described using appropriate expressions for the mass transfer coefficient, k_{bl} :

$$Sh = \frac{k_{bl} \cdot d_h}{\mathbb{D}_{ab}} = C_1 Re^{C_2} Sc^{C_3} \left(\frac{d_h}{l}\right)^{C_4} \tag{3.4}$$

where d_h is the (hydraulic) diameter, $\mathbb{D}_{ab}$ is the diffusion coefficient and C_i are constants of the Sherwood correlation that depend on the hydraulic conditions. The values of the constants C_1, C_2, C_3 and C_4 are 1.62, 0.33, 0.33 and 0.33 for laminar flow (Re < 2100) and 0.04, 0.75, 0.33 and 0 for turbulent flow [85], respectively.

Overall mass transfer resistance

According to resistance-in-series approach, the overall mass transfer resistance can be defined as

$$\frac{1}{k_{ov}} = \frac{1}{k_m} + \frac{1}{k_{bl}} + \frac{1}{k_{sl}} \tag{3.5}$$

where the subindices *m*, *bl* and *sl* stand for the membrane, boundary layer and the support layer, respectively.

An overall permeance, Q_{ov}, can be defined in analogy to Equation 3.1

$$\frac{1}{Q_{ov}} = \frac{1}{Q_m} + \frac{1}{Q_{bl}} + \frac{1}{Q_{sl}} \tag{3.6}$$

this overall permeance is used in the flux equation

$$J_i = Q_{ov}\, \Delta f_i \tag{3.7}$$

where J_i is the molar flux, Q_{ov} the overall membrane permeance and Δf_i the driving force for membrane transport. Equation 3.7 is discussed in detail in the Appendix 1.

Since resistance of the selective layer is assumed constant, and that of support layer appears to be practically constant at the conditions studied, the boundary layer resistance is the only one which can be influenced significantly by design/operating conditions. As a consequence, the results of the parametric study will indicate clearly to which extent the boundary layer resistance affects overall membrane performance as well as the relative distribution of resistances.

3.2.2 Shell and tube module

For the case of binary permeation where the feed and selective layer are inside the tubes, the differential total and component mass balances in the feed side can be written as

$$-dL = dV \tag{3.8}$$

$$-d(Ly_i)_{feed} = d(Vy_i)_{permeate} \tag{3.9}$$

$$\frac{d(Ly_i)_{feed}}{dz} = N_t \cdot \pi \cdot d_h \cdot Q_{ov} \left\{(P \cdot y_i)_{feed} - (P \cdot y_i)_{perm}\right\} \tag{3.10}$$

where V and L are the local molar flow rates, d_h is the (hydraulic) diameter, N_t is the number of membrane tubes, Q_{ov} is the overall membrane permeance and y_i is the local mol fraction of component i in the feed and permeate side. For countercurrent flow, the left side terms of equations 3.8 and 3.9 appear with a positive sign.

Pressure drop is described with the standard flow expression for a fluid flowing through a smooth pipe

$$\frac{dP}{dz} = f \frac{l}{d_h} \frac{\rho u^2}{2} \tag{3.11}$$

where f is the friction factor, l is the tube length, ρ is the fluid density and u is the fluid velocity.

The permeate flux is obtained by solving numerically the differential equations above. For co-current operation the integration proceeds straightforward because feed flows and compositions entering the module are known. The Runge-Kutta method has been adopted to integrate numerically the working equations. In the case of counter-current operation the solution is iterative and the subroutine starts with co-current calculations to get initial values for the permeate stream. The Regula-Falsi method is used to estimate the next permeate condition and this procedure is repeated until the calculated and the actual feed values match each other.

3.3 Simulation inputs

In the following analysis a stand alone membrane module is considered and the membrane selective layer always faces the feed stream. In order to assess the performance of the membrane module at different conditions, a base case is selected. Table 3.1 gives the data of the base case and the values used to determine the effects associated with changes in variables. Only the variables given in the figures are varied. Any other variable was kept constant.

3.4 Results and Discussion

Figure 3.1 indicates the contribution of concentration polarization to overall mass transfer resistance as a function of the feed side Reynolds number and the operating pressure. It is clear that concentration polarization increases when decreasing Re-number and/or increasing operating pressure. High pressure is beneficial for flux, because it enhances the driving force; however, this positive effect is partly counteracted by the increase in concentration polarization. The

Table 3.1: Base case data and values used in the parametric study

Variable	Base case	Range studied	Remarks
Feed flow (kg/h)	50	25 and 100	–
Feed pressure (bar)	3	1.5 and 6	–
Feed temperature	3°C superheating	none	to avoid condensation
Feed composition (% wt Et)	80	none	–
Permeate pressure (bar)	0.2	none	allow CW condensation
Tube length (m)	0.5	0.25 and 1	–
Inner diameter (m)	0.010	0.005 and 0.001	–
Outer diameter (m)	0.013	0.007 and 0.002	for 10, 5 and 1 mm
Number of tubes	19	53 and 80	for 10, 5 and 1 mm
Shell diameter (m)	0.1	none	tubes Δ 1.5·d_{out}
Water permeance (kg/h ·m^2· bar)	11.08	15.5 and 22.0	α_i = 25, 50 and 100, respectively
Module feed	tube side	shell side	–

reason for this is that vapor diffusivity decreases with pressure. There is a strong decrease in diffusivity in the range of pressures between 1 and 3 bar, that is why the polarization resistance is so high at 6 bar and low Re-numbers.

Figure 3.2 indicates that concentration polarization depends strongly on the tube diameter and the location of selective layer. Clearly, larger diameter tubes are much more prone to concentration polarization effect than the small diameter ones. Modules fed in the shell side (dashed lines) exhibit more pronounced polarization resistance than the ones with feed inside the tubes (solid lines). The reason for this is because under the same conditions the (hydraulic) diameter is larger, leading to a decrease in the value of mass transfer coefficient.

Concentration polarization can be affected by carefully choosing the flow conditions on the feed side. For a module working properly, the main mass transfer resistance should be located in the selective layer. Figure 3.3 shows the relative contribution to membrane resistance when tube diameter, feed pressure, flow rate and module feed side are varied. It is clear that concen-

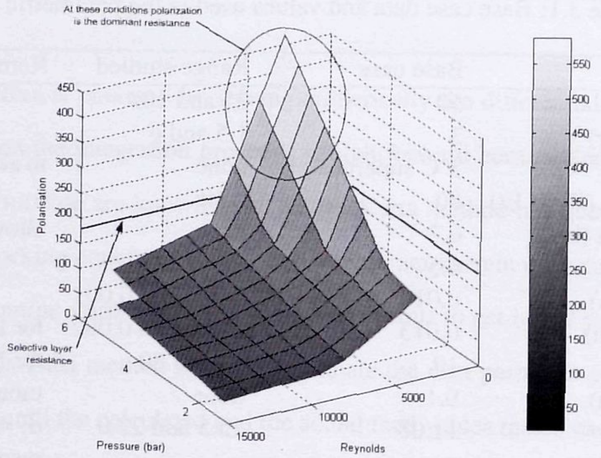


Figure 3.1: Concentration polarization resistance as function of Re-number and pressure

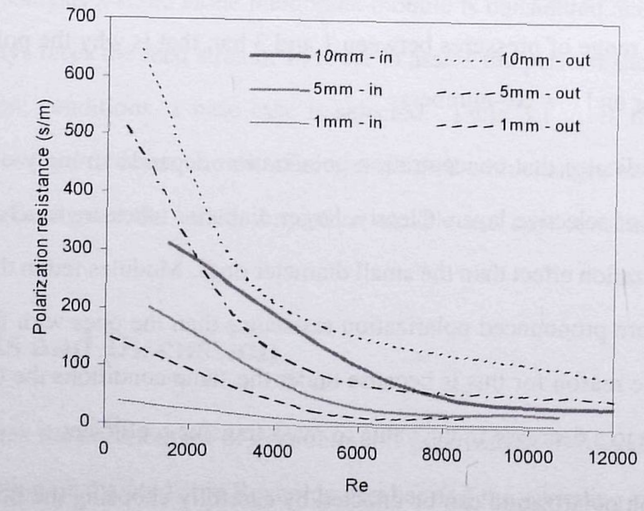


Figure 3.2: Polarization resistance as function of Reynolds number and tube diameter for modules with feed in the tubes (solid lines) and on the shell side (dashed lines)

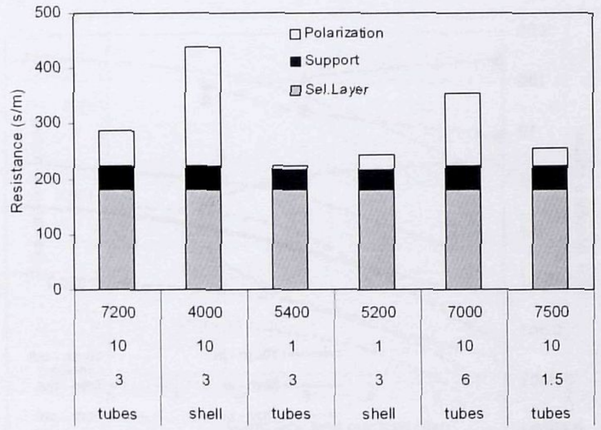


Figure 3.3: Contribution of boundary, support and selective layer to total permeation resistance as function of diameter, pressure, feed flow and module feed side.

tration polarization is practically negligible with small diameter tubes, however, the operation at given Re-numbers could be accompanied by an unacceptable pressure drop. Accordingly, inducing large flows on the feed side is the remedy against concentration polarization effect, which practically means operation at highest allowable feed velocity, keeping pressure drop within reasonable limits. In other words, the knowledge of the pressure drop on both sides and its relation to other variables is very important for successful design and layout of membrane modules.

Retentate side pressure drop is shown in Figure 3.4 as a function of Reynolds number with the tube diameter as a parameter, for a module with the feed inside tubes (solid lines) and on the shell side (dashed lines). As expected, the pressure drop increases with the Re-number and the pressure drop of smallest diameter tube is the largest in both cases. However, the pressure drop for modules with feed inside the tube is roughly two orders of magnitude larger than the modules with feed on the shell side.

In Figure 3.5 the pressure drop is expressed as a function of Re-number and operating pres-

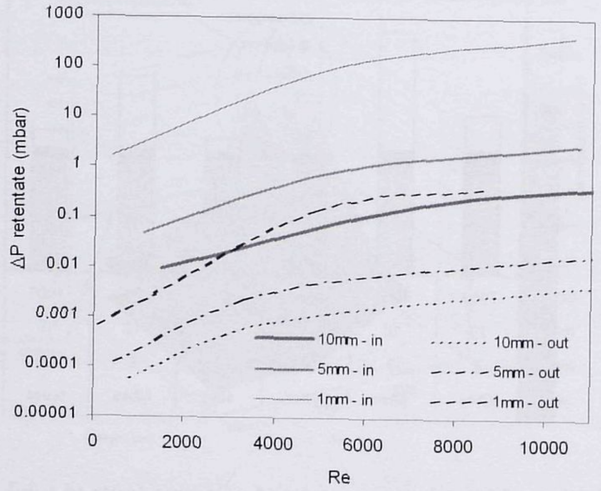


Figure 3.4: Retentate pressure drop as a function of Reynolds and tube diameter for modules with feed in the tubes (solid lines) and on the shell side (dashed lines)

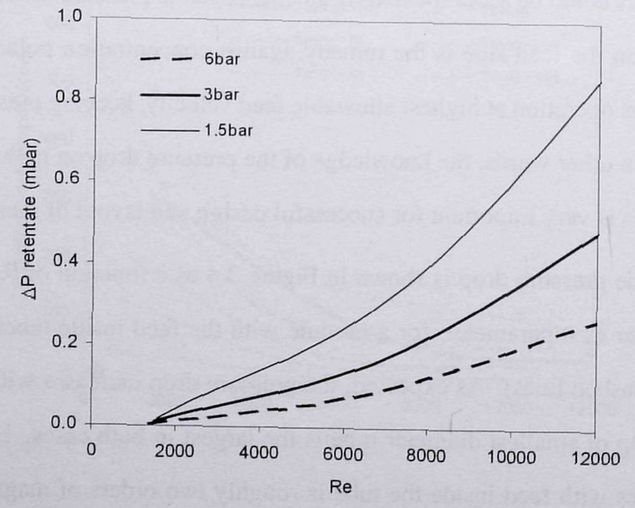


Figure 3.5: Retentate pressure drop as function of Reynolds and feed pressure

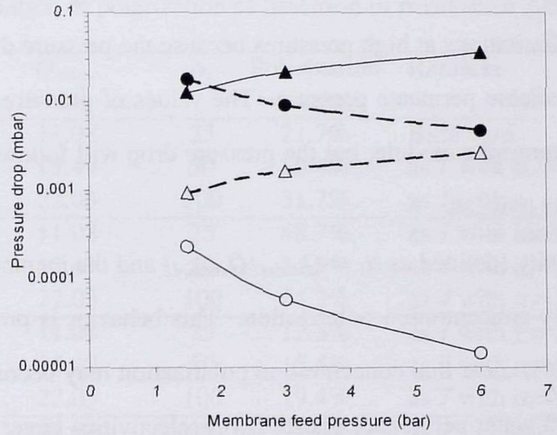


Figure 3.6: Permeate and retentate pressure drop for modules with feed in the tubes (dashed lines) and on the shell side (solid lines). Circles represent retentate pressure drop, triangles represent permeate pressure drop

sure. The retentate side pressure drop decreases when increasing operating pressure. This effect is produced by the decrease in volumetric flow (and therefore velocity in the tubes) due to the increase in pressure in the feed side.

Figure 3.6 shows a comparison between the retentate and permeate pressure drop at different feed pressures for two modules, one with the feed inside tubes (dashed lines), another on the shell side (solid lines). Obviously the pressure drop inside tubes (filled symbols) is much larger than on the shell side (open symbols). However, it is interesting to observe that the tendency of the pressure drop is the same for permeate (triangles) and retentate (circles) streams, regardless the feed side. The permeate pressure drop trend is opposite to the one observed at the retentate side. The reason for this lies in the fact that with an increase in feed side pressure the membrane flux increases. As a result the pressure drop lines for a module with feed inside the tubes tend to come together, while the opposite trend is seen for modules with the feed on the shell side.

This behavior brings up an important operational aspect, meaning that modules with feed on the shell side may have limitations at high pressures because the pressure drop at the permeate side can approach the available permeate pressure. The values of pressure drop in Figuire 3.6 are simulations for a 10mm tube module, but the pressure drop will follow the trend of Figure 3.4 when tube diameter is reduced.

The perm-selectivity (defined as $\alpha_i = Q_{water}/Q_{ethanol}$) and the membrane permeance doesn't seem to affect greatly concentration polarization. This behavior is presented in Table 3.2 for various conditions. It is clear that concentration polarization may become a problem for membranes with very high water permeance and/or perm-selectivities larger than 100. On the other hand, the relation of perm-selectivity with pressure drop is more pronounced on the permeate side, because the changes in flux affect more permeate than retentate flow rate. Summarizing, the effect of perm-selectivity on concentration polarization and pressure drop is rather small for the range studied in these simulations (α between 25 and 100), but it could become influential, especially for small diameter tubes and/or high-flux membranes.

Finally, tube length affects directly pressure drop in both sides, but the effect of length in concentration polarization is negligible regardless the diameter, feed flow rate and pressure (results not shown).

3.5 Membrane Performance Rating

The results of the simulations carried out in this study can be summarized in form of a qualitative membrane performance indicator (Table 3.3), which can be used as a guide for performance analysis and conceptual design of vapor permeation modules.

The following examples illustrate the validity of Table 3.3 with the base case as reference and the results of the exercises are summarized in Table 3.4. Membrane length and feed flow rate are

Table 3.2: Variation of polarization as functrion of permeance and perm-selectivity

Simulation	Q_{water} $(kg/h \cdot m^2 \cdot bar)$	α_i	Polarization resistance	Remarks
1	11.08	25	21.7%	Base case
2	15.49	50	26.4%	as *1* with α_i = 50
3	22.03	100	31.7%	as *1* with α_i = 100
4	11.08	25	48.7%	as *1* with module feed shell side
5	15.49	50	54.9%	as *4* with α_i=50
6	22.03	100	61.2%	as *4* with α_i=100
7	11.08	25	12.3%	as *1* with P= 1.5 bar
8	15.49	50	15.4%	as *7* with α_i=50
9	22.03	100	19.4%	as *7* with α_i=100
10	11.08	25	24.0%	as *1* P=6 bar and feed =100 kg/h
11	15.49	50	29.0%	as *10* with α_i=50
12	22.03	100	34.4%	as *10* with α_i=100
13	0.1108	25	0.3%	Lower Q_{water} than *1*
14	1108	25	66.5%	Higher Q_{water} than *1*
15	0.2203	100	0.3%	Lower Q_{water} than *3*
16	2203	100	64.2%	Higher Q_{water} than *3*

increased to 1 m and 100 kg/h for Example 1a. Example 1b is an extension of the previous one, increasing the perm-selectivity to 100. In Example 2a the feed side pressure is increased to 6 bar and the internal tube diameter is reduced to 1 mm, keeping Re-number similar to that of the base case (around 7000). The difference of Example 2b in comparison with 2a, is that the feed flow rate is kept as in the base case (50 kg/h).

According to Table 3.3 polarization resistance decreases and pressure drop in both sides increase for Examples 1a and 1b. For Example 2a the feed flow should be increased in order to obtain similar Re-number as in the base case. This will decrease concentration polarization. In Example 2b, feed is kept constant, then Re-number will be lower than in the base case and polarization will increase. For both cases (2a and 2b) pressure drop on both sides of the module will increase, due to the decrease in tube diameter. All these results agree with what is stated in

Table 3.3: Module performance indicator

Variable **increasing**	Polarization resistance	ΔP feed side	ΔP permeate side
Feed Flow	Decreases	Increases	Increases
Feed Pressure	Increases	Decreases	Increases
Tube Diameter	Increases	Decreases	Decreases
Tube Length	Constant	Increases	Increases
Memb. Permeance	Increases	Constant	Increases
Perm-selectivity	Fairly constant	Fairly constant	Fairly constant
Module feed	tube < shell	tube > shell	tube > shell

Table 3.4: Example inputs and results

	Input / Output	Base Case	Example 1a	Example 1b	Example 2a	Example 2b
Flow (kg/h)	I	50	100	100	220	50
Length (m)	I	0.5	1	1	0.5	0.5
d_{in} (m)	I	0.01	0.01	0.01	0.001	0.001
P_{feed} (bar)	I	3	3	3	6	6
α_i	I	25	25	100	25	25
Polarization (%)	O	21.7	13.7	13.7	5.5	25.8
Re	O	7100	14900	14900	6900	1400
ΔP_{feed} (mbar)	O	0.20	1.30	1.31	96.95	4.65
ΔP_{perm} (mbar)	O	0.003	0.014	0.013	1.097	0.406

the performance guidelines.

This analysis illustrates that expectations with respect to the flux enhancing effect of an operation at high feed pressures could be too optimistic, because concentration polarization also increases. It is demonstrated as well that the tube-side pressure drop is the limitation for modules with small diameter tubes and that concentration polarization doesn't change with longer modules. Finally, the effect of perm-selectivity is rather small on concentration polarization and pressure drop for the range studied in this work (α between 25 and 100). However, it might be that becomes important for small diameter tubes and/or high-flux membranes.

The optimization of a membrane module is a difficult and complex task because, as usual with mass transfer contactors, designing a membrane module implies making a tradeoff between separation efficiency and pressure drop and every case is different in this respect. That is why the predictive model described here can be a useful tool for module/process design.

3.6 Conclusions

A versatile predictive model describing the relation between design/operating variables and the performance of a vapor permeation module has been introduced. The capabilities of the model to serve as a process analysis and process design tool are demonstrated for system ethanol/water. A parametric study was carried out to illustrate the effects of variations in design and operating variables with particular emphasis on the contribution of concentration polarization because it may become the limiting resistance for mass transfer.

Concentration polarization is mainly affected by the feed flow rate in conjunction with the tube diameter and the feed pressure. Module length and membrane perm-selectivity are less influential in this respect. It is always desirable to operate at the highest possible Re-number i.e. that associated with an affordable pressure drop. Pressure drop depends strongly on the tube

diameter, flow rate, position of the feed in the module (feed in the tubes or in the shell) and tube length. Simulations demonstrate that the highest pressure drop is located on the tube side, regardless of the feed side, which means that the modules with small diameter tubes are less suitable for high pressure operation.

Chapter 4

Vapor permeation with single tube ceramic membranes. Preliminary study of integrated process for ethanol dehydration

A rather new alternative for separating azeotropic mixtures is coupling membranes with distillation. So far this proved to work with pervaporation, which implies total condensation of the vapors leaving the top of the distillation column. Vapor permeation has emerged as a very attractive alternative for ethanol dehydration since the vapor at the distillation top can be directly fed to the membrane module. Another beneficial feature of vapor permeation over pervaporation is the reduction of concentration and temperature polarization; these characteristics may play an important role when determining membrane area and extra equipment required.

Vapor permeation lab-scale experiments were performed to identify the most suitable membrane for industrial implementation. Two single tube, multilayer ceramic membrane tubes were tested

with the water/ethanol mixture. One of them displays high flux and low selectivity; the other shows lower flux but high selectivity. Process parameters were extracted from the experimental results and simulated successfully using a subroutine describing performance of the membrane as function of component partial pressure and temperature.

An integrated distillation/membrane process was simulated to identify which membrane is more convenient to use for industrial applications. From the simulation results it appears that working with high flux / low selectivity membranes at high column pressure and membrane feed concentration below the azeotropic composition seem the most promising conditions for the hybrid process.

4.1 Introduction

Considering that the membrane is the heart of a vapor permeation process, it should comply with several requirements regarding stability, endurance, adaptability to fit into modules and of course the best combination of flux and selectivity for the specific application. This chapter aims to recognize the most appropriate membrane performance characteristics for the dehydration of ethanol.

Membrane based separation processes have been intensively studied for separation of aqueous / organic mixtures in view of their ability to separate azeotropic mixtures and the promise of an overall economic advantage. Two types of materials have been mainly studied in the last years for membrane production: polymers and ceramics. The fabrication of a suitable membrane with high flux, good selectivity, sufficient mechanical strength and chemical stability is a challenge for membrane developers. Most polymeric materials have an excellent selectivity but their flux hardly reaches 1 $kg/h \cdot m^2$ and their chemical and mechanical stability is a disadvantage for applications that involve solvents. Yet, they are easy to made and very cheap and their characteristics

are being improved through continuous research. Ceramic membranes offer a solution for the drawbacks of polymeric membranes, but they are not widely used because they are expensive. As a consequence it is relevant to search the membrane characteristics and process conditions that still offer an (economically) affordable process.

4.1.1 Polymer materials

The polymeric materials that are currently under investigation for use in ethanol dehydration are among others chitosan, polysulfone and polyvinyl alcohol. In a number of cases membrane materials are modified to obtain better operating properties. These modifications include the inclusion of certain ions, cross-linking, creation of mixed-matrices and some more.

Kanti e.a. [58] used a membrane made out of biopolymers (chitosan and sodium alginate) for the pervaporation of ethanol/water mixtures. The combination of the two membrane materials resulted in a moderate flux (max. 1 $kg/h \cdot m^2$), high selectivity (max. around 2000) and good mechanical properties (the combined membrane exhibits a higher tensile strength than either chitosan or sodium alginate). Sorption studies revealed that the polymer had greater affinity towards water than ethanol. The membrane performance was found to be affected substantially when increasing feed water concentration. This was observed as an increase in the extent of swelling of the polymer, which resulted in a rise in flux but a reduction in selectivity. The crosslinked blends were found to show promising performance for dehydration of ethanol containing smaller amounts of water (less than 12 % wt). Increasing membrane thickness decreased the flux but had a less profound effect on the selectivity. Higher permeate pressure caused a reduction in both flux and selectivity. Uragami [141] prepared membranes with chitosan and polyethersulfone and used them for the vapor permeation of water/ethanol mixtures. The influence of feed temperature and pressure was investigated for the prepared membranes. Experiments were performed from 2

to 4.5 bar and from 100 to 130 °C. It was found that the permeation flux increased with increasing feed vapor pressure and decreased with the increasing feed temperature. The maximum flux found was approximately 0.7 $kg/h \cdot m^2$ at 3.5 bar and 120 °C. The selectivity of the experiments was not reported.

Hung [53] dehydrated alcohol by pervaporation using a modified polysulfone membrane modified with sodium sulfonate. The addition of sodium ions successfully improved the pervaporation performance of polysulfone membrane. The introduction of a sodium group into the polymer unit increased the hydrophilicity of the polysulfone membrane. They showed a membrane that can be used at the entire range of composition with a stable flux (approx. 0.7 $kg/h \cdot m^2$) and with an increase in selectivity from 500 to 2000 when increasing ethanol concentration. On the other hand the selectivity decreased when increasing operating temperature. This may be because at high temperatures more water and ethanol were sorbed into the membrane, and the coupling effect of the flux resulted in more ethanol transport through the membrane. These phenomena induced the loss in the selectivity at higher temperatures. Chen [20] (from the same research institute as Hung [53]), found similar results sulfonating a polysulfone membrane with chlorosulfonic acid. They found that sulfonation improved the pervaporation performance of polysulfone membrane because introducing a sulfuric group in the polymer unit increased the hydrophilicity of polysulfone membrane. The increase in flux and selectivity with the increase in the degree of substitution was similar as for reference [53]. The fluxes found by Chen [20] were in the range of 0.7 to 0.9 $kg/h \cdot m^2$ and selectivities from 200 to 1500. In another article by Chen and coworkers [21] they used a lithiated polysulfone membrane. Again they found that the separation performance of water and ethanol strongly depend on the degree of substitution of the polysulfone membrane. The lithium content decreased the water permeation rate, but increased the selectivity. For these membranes the permeation flux was lower that for the previous experiments [53, 20], ranging from 0.25 to 0.5 $kg/h \cdot m^2$ and selectivity from 200 to 1800.

The permeation flux is strongly dependent on the operating temperature and, the selectivity decreased with increasing the operating temperature. Hsu [51] (yet from the same group as Chen and Hung), used a polysulfone membrane modified with poly ethylene glycol (PEG). Increasing PEG content had hardly any influence on the selectivity (around 300). Just high amounts of PEG decreased selectivity down to 50. On the other hand the PEG content did have a positive effect on permeate diffusion improving the flux from 0.45 $kg/h \cdot m^2$ without any PEG to 1.5 $kg/h \cdot m^2$ with 25 % wt PEG. The reason for this behavior was the polar-polar interaction among PEG, water, and ethanol that played an important role in diffusion and selectivity in the membrane.

The modification of poly vinyl alcohol (PVA) membranes was investigated by Rafik [105]. The ability of the modified membranes for dehydrating the water/ethanol azeotropic mixture by pervaporation was studied at 25, 40 and 60 °C. The best selectivity (250) was obtained in the case of the allyl alcohol treatment. However the flux was substantially lowered by this modification (from an original 0.12 to 0.04 $kg/h \cdot m^2$). In contraposition the modification with acrylic acid increased the membrane flux (to 0.144 $kg/h \cdot m^2$) but had low selectivity (around 22).

Toutianoush [135] proved that at low water content in the feed ($\leq$ 20 % wt), the strongly hydrophilic poly vinyl amine (PVAm) / poly vinyl sulfonate (PVSu) membrane is best suited for separation, while at higher water content the less hydrophilic PVAm / poly acrilate (PAA) membrane exhibits the best separation. The reason for this may lay in the hydrophilicity of the sulfonate group and thus becomes strongly hydrated even at a very low water content of the feed solution. Consequently, the PVAm/PVSu membrane exhibits the highest flux and separation at low water concentrations of the feed solution. When increasing feed water concentration swelling appears, the flux becomes very high but the separation gets worse. It is shown that when increasing the number of layers of a membrane (from 10 to 60), improves the water content in the permeate (from 25 to almost 100 % wt) but decreases the total flux (from 0.94 to 0.1 $kg/h \cdot m^2$).

Other polymeric materials also have been successfully used for the dehydration of ethanol,

for example: crosslinked poly butyl methacrylate-co-methyl methacrylate [69], modified poly acrylonitrile [151] and modified poly tetrafluoroethylene [52]. Current problems with polymeric membranes are a low thermal and chemical stability. Furthermore the hydrophilic character of the membranes can cause excessive water absorption causing swelling and resulting in lower selectivity due to plasticization effect [58]. Yet we observe that the permeation fluxes in polymer membranes are seldom higher than 1 $kg/h \cdot m^2$.

4.1.2 Ceramic materials

Far fewer papers have been recently published about ceramic membranes for dehydration of ethanol than for polymeric membranes, anyhow most of the current development with ceramic membranes will be presented.

Sekulic and coworkers [116] have investigated silica and doped silica membranes in pervaporation for the system propanol/water. It was found that depending on the nature and amount of dopant, membranes with improved pervaporation characteristics and chemical stability were obtained. Doping with zirconium and titanium led to a moderate improvement in stability while doping only with zirconium improved pervaporation performance of the membrane. The chemical stability of amorphous silica and the doped silicas were investigated by solubility tests with the unsupported material at room temperature. The addition of alumina has a negative effect on the chemical stability, while zirconium and titanium give clear improvements at high pH. It was found that while pure silica is stable at pH range 2 to 8, the addition of 10 % mol of zirconium or titanium leads to a stable material in the pH range 2 to 10.

Cuperus et.al. [23] investigated the influence of hydrodynamics on a limited Reynolds region using silica membranes for pervaporation of water/alcohol or water/acetic acid mixtures. A flux of 1 $kg/h \cdot m^2$ was found for the system IPA / water at 70 °C with a selectivity of 100. When the

temperature of the feed is increased the water flux also increases. They mentioned that the reason is that upon temperature increase the diffusion of water is becoming faster which together with the decrease in boundary thickness yields a higher flux. They found a considerable influence of hydrodynamics on the performance of the membranes, which is attributed to mass transfer phenomena during operation. For a module with the same initial conditions and working at Re = 48, the increase of flux is considerable at Re = 1688 (0.3 and 0.5 $kg/h \cdot m^2$, respectively). They studied membrane performances up to a Re = 1688 and expect that the use of higher Re than 3500 won't yield a better operation in practice. They claim that at Re around 3500 the flow inside the membrane tube has become turbulent, and the influence of flow velocity in mass transfer won't increase significantly after this value of Reynolds.

Navajas [87] observed the influence of preparation methods on the pervaporation performance for mordenite membranes. The synthesis time and the level of dilution in the synthesis gel influenced the mordenite membrane performance. The membranes used had a water/ethanol selectivity around 150 and water fluxes of approximately 0.20 $kg/h \cdot m^2$, with maximum values of 0.33 $kg/h \cdot m^2$ and a selectivity of 310.

In the last years Pervatech membranes, as the ones used throughout this thesis, have been subject of different studies and their results reported. Casado et.al. [18] studied the dehydration of isopropanol and acetone with single tube. They report an extraordinary flux for the dehydration of isopropanol (as high as 14 $kg/h \cdot m^2$) and they confirm the logarithmic behavior of flux versus temperature for this membrane. Fontalvo [39] performed a thorough research on Pervatech single tube and multi tube modules for the dehydration of several solvents as dimethylformamide, methanol, ethanol, dioxane, isopropanol and acetonitrile. The fluxes vary a lot depending on the conditions, but they are always higher than 1 $kg/h \cdot m^2$. They showed that the stability of the membrane is a problem. Kuhn [65] analyzed the pervaporation performance with multiphase flow. The main purpose of this research was to enhance turbulence inside the membrane tubes

and in this way decrease the detrimental effect of polarization. At the beginning of his experiments he found fluxes around 3.5 $kg/h \cdot m^2$, but after 100 hours of operation fluxes were never higher than 1.5 $kg/h \cdot m^2$, indicating a severe deterioration of the membrane properties. The reasons for this deterioration were not found.

The Energy Research Center of the Netherlands (ECN) produces silica / alumina membranes for pervaporation or vapor permeation applications. They have tested several solvents with their isothermal concentric tube module concept [146]. They performed several binary mixture permeation experiments with a total of 34 organic solvents at 10 % wt water and 10 mbar permeate pressure and found fluxes up to 4.5 $kg/h \cdot m^2$ and selectivity up to 65 for the case of ethanol dehydration [146]. ECN has devoted a lot of effort in the development of their ceramic membranes in the last years and has tested them for different applications, such as organic solvent dewatering, the production of esters of resins and the separation of organic / organic mixtures. These membranes have been tested specifically for the dehydration of ethanol in [147]. In that study they achieved a pervaporation flux up to 1.5 $kg/h \cdot m^2$ at atmospheric pressure and 70 °C with a selectivity of 350.

There are some cases in which polymer and ceramic membranes are combined. Okumus [92] used a polyacrylonitrile (PAN) membrane filled with different zeolites (3A, 4A and 13X) for the pervaporation of water/ethanol mixtures. It was concluded that the zeolite content determines the membrane morphology and the dominant layer controlling the transport mechanism while the polymer gives the body to the membrane. The addition of zeolite particles affects the membrane performance differently in three different zeolite concentration zones. At low zeolite contents (0-30 % wt), the permeation rate is controlled by the zeolite-free polymer layer. At moderate zeolite contents (30-35 % wt), the permeation rate is controlled by the hydrophilic corridor of the zeolite particles. At high zeolite contents (above 35 % wt), zeolite particles loosens the membrane structure that causing complete loss of selectivity. The increase of 32 % wt zeolite,

Table 4.1: Fluxes gathered from literature review for the system ethanol / water

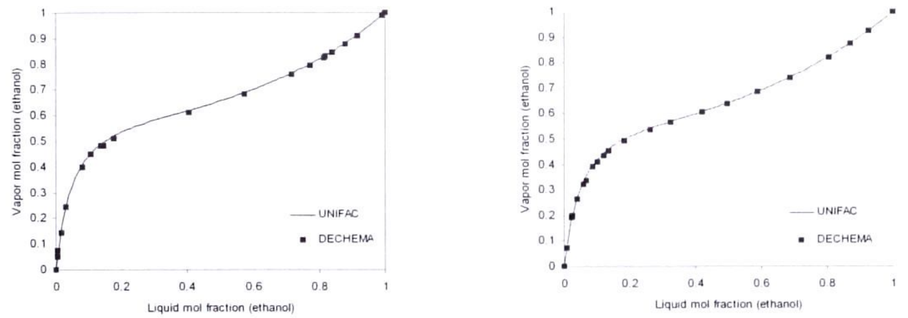
Membrane	PV or VP	Selectivity	Flux $kg/h \cdot m^2$	Ref.
biopolymer	PV	2000	max. 1	[58]
chitosan + PSu	VP	n.a.	max. 0.7	[141]
PSu + Na-sulfonate	PV	500 - 1200	0.7	[53]
PSu + chlorosulfonic acid	PV	200 - 1500	0.7 - 0.9	[20, 21]
PSu + PEG	PV	300	0.45 - 1.5	[51]
PVA + allyl alcohol	PV	max. 250	0.04 - 0.12	[105]
PVA + acrylic acid	PV	22	0.14	[105]
PVAm + PVSu	PV	n.a.	0.1 - 0.94	[135]
Methylated silica	PV	max. 65	max. 4.5	[146]
Mordenite	PV	150 - 310	0.20 - 0.33	[87]

increased flux about nine-fold with a loss of selectivity around seven-fold relative to the base PAN membranes.

Finally, it is worth to mention the Ph.D. study of Fakhri [33] in the Laboratory for Process Equipment, because he found that for an isopropanol dehydration plant (20 kton anhydrous IPA per year), the process distillation / vapor permeation showed lower operating costs than the azeotropic distillation. However, he found membrane areas in the range of 1000 m^2 using polymer membranes.

4.2 Model Description

The potential of ceramic membranes implemented in a distillation / vapor permeation process for ethanol dehydration can be evaluated with the help of a mathematical model of a membrane module. The proposed model has been developed and linked to a process simulator to enhance the flowsheeting capabilities and study the feasibility of integrated processes [100, 98]. A brief description of the model used throughout this thesis is given in what follows.



(a) 1.013 bar (b) 3 bar

Figure 4.1: Experimental and simulated ethanol / water VLE data

4.2.1 Thermodynamics

Thermodynamic equilibrium is extremely important to identify the possibility of separation of any mixture. The computer simulated equilibrium data were compared with the experimental data from Dechema data series [42]. It is clear from Figure 4.1 that UNIFAC thermodynamic model represent adequately the vapor - liquid equilibrium (VLE) for the system ethanol / water at different pressures, accordingly UNIFAC will be used throughout the present study.

4.2.2 Working Equations

Membrane performance is usually quantified by two parameters: membrane flux (J_i) and selectivity (α). The difference in fugacity in the feed and permeate side is the driving force for vapor permeation. Therefore the membrane flux can be defined as

$$J_i = Q_i \cdot (f^v_{i,per} - f^v_{i,ret}) \tag{4.1}$$

where J_i is the molar flux and Q_i is membrane permeance of component i. The vapor fugacity

in a real mixture is the effective partial pressure

$$f^v_i = \varphi^v_i \; y_i \; P \tag{4.2}$$

where the correction factor φ^v_i is the fugacity coefficient, P is the absolute pressure and y_i the molar fraction of component i. For a vapor at moderate pressures, φ^v_i is close to unity.

Accordingly, for vapor permeation, the driving force can be expressed as the partial pressure difference and the membrane permeance determines the magnitude of the flux at a given driving force for every component. As a consequence, flux can be defined as

$$J_i = Q_i \cdot \left\{(Py_i)_{feed} - (Py_i)_{permeate}\right\} \tag{4.3}$$

Membrane permeance varies with temperature. Permeance is an activated process that is well described by the Arrhenius-type equation

$$Q_i = Q^o_i \; EXP \left\{\frac{-E^{app}_{act,\,i}}{R} \cdot \left(\frac{1}{T_{ref}} - \frac{1}{T}\right)\right\} \tag{4.4}$$

where Q_i is the calculated membrane permeance, Q^o_i is the permeance at the reference temperature, $E^{app}_{act,\,i}$ is the apparent activation energy, R is the universal gas constant and T the system temperature.

The apparent activation energy ($E^{app}_{act,\,i}$) is a term that lumps and simplifies the adsorption and diffusion terms of the simplified Maxwell-Stefan equation (see Appendix 1). If the membrane permeance for a certain component is determined at several temperatures the numerical value of $E^{app}_{act,\,i}$ can be obtained constructing a plot of $ln\ Q_i$ versus $1/T$. If the permeation rate obeys the Arrhenius equation, a straight line plot of the experimental data is obtained with the slope of this line is equal to $E^{app}_{act,\,i}$. De Bruijn [25, 26] studied thoroughly the modeling of the transport

across silica membranes using a rigorous thermodynamic model using chemical potentials and compared with the simpler model using partial pressure difference and the Arrhenius approach. He concluded that the results are pretty similar and both approaches can be used to predict the performance of a membrane but the rigorous approach gives more information on the molecular phenomena occurring during permeation.

The membrane allows the separation of certain molecules. To quantify the degree of separation selectivity is calculated as follows

$$\alpha = \frac{y_A / y_B}{x_A / x_B} \tag{4.5}$$

where α is selectivity, y_i is the mol fraction of i in the permeate side and x_i is the mol fraction of i in the feed side.

According to the above described equations, there are some parameters that should be obtained from experiments, namely the activation energy, reference permeance and reference temperature for the different components. The necessary membrane parameters for the program were retrieved from membrane characterization experiments carried out at pressures up to 5 bar.

4.3 Experimental part

4.3.1 Set-up and procedure

Vapor permeation experiments were performed using a lab-scale set-up available at the Netherlands Organization for Applied Scientific Research (TNO - MEP, Apeldoorn). A diagram of the experimental set-up is presented in Figure 4.2. The mixture is stored in vessel T1 and heated to evaporation with electric heater HE1. Thereafter the vapor is superheated with heater HE2, and passes through a heated pipe to avoid temperature losses. The membrane module is kept at

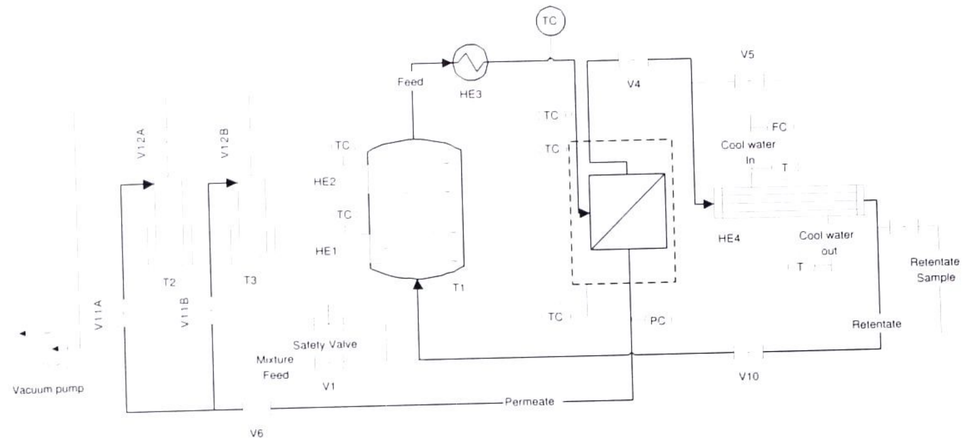


Figure 4.2: TNO experimental set-up for single tube experiments

constant temperature with an oven. The retentate is condensed outside the oven with the water-cooled heat exchanger HE4. After condensation, the retentate is fed back to vessel T1. Permeate is condensed using liquid nitrogen cold traps (T2 and T3). The permeate mass is measured with an electronic balance and the permeate composition is determined by analyzing the samples using an automated refractometer. Detailed information about the experimental work can be found in references [100, 98, 145].

4.3.2 Membrane characteristics and experimental conditions

Two multi-layer silica tubular membranes with selective layer inside the tubes were provided by Pervatech. One of them had larger selectivity (M-1) and the other larger flux (M-2). The difference is due to an extra coating step with silica for the more selective membrane. Typical characteristics of the layers are shown in Table 4.2, which shows average measures of Pervatech membranes. Unfortunately detailed information for each membrane was not available.

Tube dimensions are 225 x 10.4 x 1.68 mm (length x outside diameter x wall thickness) with

Table 4.2: Membrane tube characteristics

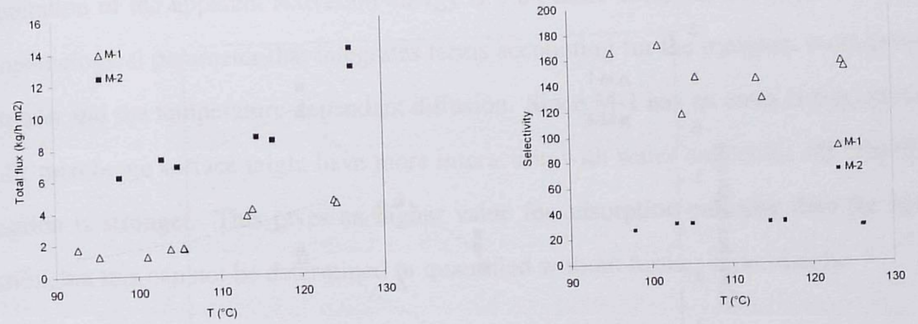
Layer	Material	Thickness	Pore size
Substrate	α-alumina	1.5 mm	3 - 12 μm
1	α-alumina	20 - 30 μm	1 μm
2	α-alumina	21 - 30 μm	100 nm
3	γ-alumina	1 - 2 μm	3 - 5 nm
4 (inside tube)	SiO_2	10 - 20 nm	0.3- 0.4 nm

the silica selective layer inside the tubes. The experiments conditions varied with temperatures in the range of 90 to 120 °C and feed pressure from 1.5 to 5 bar. The temperature at the membrane feed was always 2 °C higher than the boiling temperature to avoid condensation inside the tubes. The feed concentration and the permeate side pressure were constant at 96 % wt ethanol and 7 mbar, respectively.

4.4 Results and discussion

From experiments it was found that the membrane total flux increased with temperature from 1.22 to 4.54 $kg/h{\cdot}m^2$ for M-1 and from 6.02 to 14.01 $kg/h{\cdot}m^2$ for M-2 (Figure 4.3(a)). Selectivity is rather constant for both membranes (Figure 4.3(b)). Membrane M-2 presents the largest flux but less selectivity (around 30) compared with the "high selectivity" membrane M-1 (average 150).

Comparing the previous outcome with other results using Pervatech membranes, the fluxes are comparable to the ones reported by Casado et.al. in [18], but those ones were obtained for the dehydration of isopropanol by pervaporation with Pervatech membranes. Unfortunately they don't give any indication or data to calculate the selectivity for such large flux. Kuhn [65] also used Pervatech membranes and observed maximum pervaporation fluxes of 3.3 $kg/h{\cdot}m^2$ at 75 °C for the mixture ethanol / water. The selectivity of this membrane varies a lot with temperature,



(a) Flux (b) Selectivity

Figure 4.3: Experimental performance of M1 and M2

ranging from 60 at 50 °C to 140 at 75 °C. Comparing the results reported in literature and the present experiments it is clear that working with vapor permeation at high pressure is beneficial to obtain a larger flux, while the separation properties of the membrane are not adversely affected.

As can be seen from Equation 4.3, the driving force for vapor permeation can be represented by the difference in partial pressures in the feed and permeate sides. At turbulent conditions, the concentration in the bulk and near the wall can be assumed as the same. When the component flux is plotted against the driving force, the slope represents the membrane permeance (Figures 4.4 and 4.5). The membrane parameters used during simulations are presented in Table 4.3.

Table 4.3: Membrane parameters determined from experiments

Membrane	Q^o_{Water} $kg/h \cdot m^2 \cdot bar$	$E^{app}_{act,\,W}$ kJ/mol	$Q^o_{Ethanol}$ $kg/h \cdot m^2 \cdot bar$	$E^{app}_{act,\,E}$ kJ/mol
M-1	6.83	-14.0	0.20	0.3
M-2	17.48	1.2	1.55	3.8

The results in Table 4.3 denote a significant difference between the membranes. The interpretation of coefficient Q^o is that membrane M-2 permeates more molecules than M-1. The

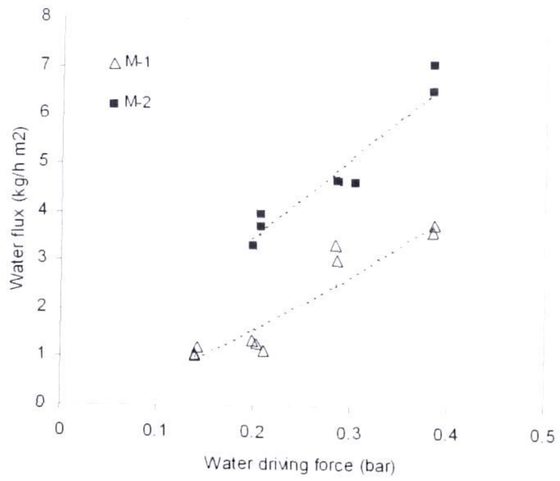


Figure 4.4: Water flux against partial pressure difference for M1 and M2

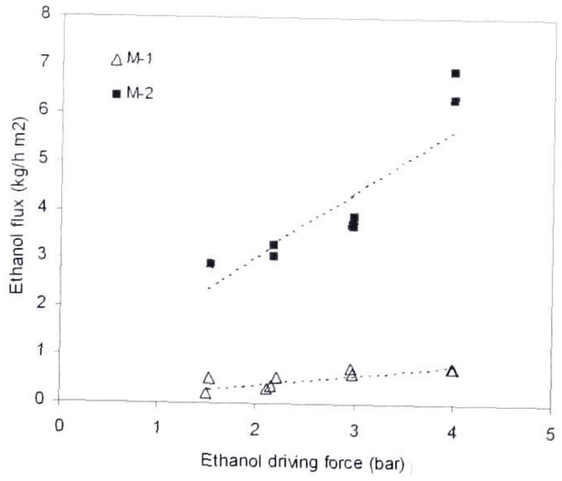


Figure 4.5: Ethanol flux against partial pressure difference for M1 and M2

interpretation of the apparent activation energy is a bit more complicated, since it is a lumped phenomenological parameter that integrates terms accounting for the transport mechanism, like adsorption and the temperature dependant diffusion. Since M-1 has an extra (silica) layer coating, the membrane surface might have more interaction with water molecules and therefore the adsorption is stronger. This gives an higher value for adsorption enthalpy than for activated diffusion, but this can not be determined or quantified without further experiments.

4.5 Model Validation

The overall model developed in Chapter 3 has been successfully validated and used also for different applications [99, 95]. Simulations using the latter model were performed with the parameters retrieved from the experimental results (Table 4.3). The model predictions are shown as dotted lines in Figures 4.3 to 4.5. Figure 4.6 shows that the predictions agree with the measured flux. These simulations do not consider polarization and support layer resistance. It is clear that the calculated values are estimated correctly for low fluxes, but the estimation deviates when increasing flux.

In other work it was demonstrated that membrane and polarization resistances are the most significant resistances for permeation [97]. Also it was recognized that membranes with high fluxes are more prone to concentration polarization [96]. If concentration polarization is accounted in our simulations, the polarization contribution to total resistance for M-1 was in the range of 12 to 18%, while for M-2 was between 28 to 35%, these numbers agree with literature [96], meaning that the deviation for large fluxes between model and experimental found in Figure 4.6 can be attributed to concentration polarization. In general the simulations show that the subroutine and the parameters can be used with confidence to represent the performance of a membrane module.

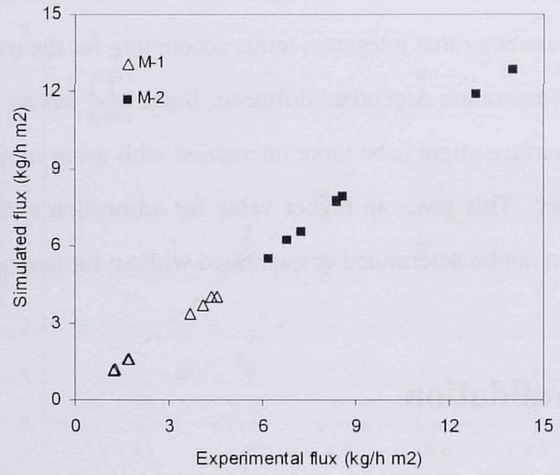


Figure 4.6: Experimental and calculated fluxes with parameters from Table 4.3

Assuming that an industrial scale module performs as the single tube, it is interesting to identify which membrane gives better results in combination with the distillation column. Nevertheless, one should note that regarding the nature of laboratory scale experiment, simulating an industrial module with the obtained data gives a too optimistic approach.

4.6 Process Simulation

The simulation study was carried out in order to discover the best conditions for the integrated process with respect to operating pressure and feed composition. An industrial scale plant was simulated following the specifications in Table 4.4 and the scheme of the simulated process can be seen in Figure 4.7.

In the present study the membrane feed composition was varied from 83 to 92 % wt ethanol and three operating pressures were considered, i.e. 1.5, 3.0 and 5.0 bar. The simulation condi-

Table 4.4: Process simulation input

Description	Unit	Value	Remarks
Production	tones/year	23400	Ethanol 99.9%
Operation time	hr/year	8000	
Feed composition	% wt et.	42.0	Column feed
Product purity	% wt et.	99.9	
Water purity	% wt	99.99	Column bottom
Permeate pressure	mbar	250	allowing CW condensation

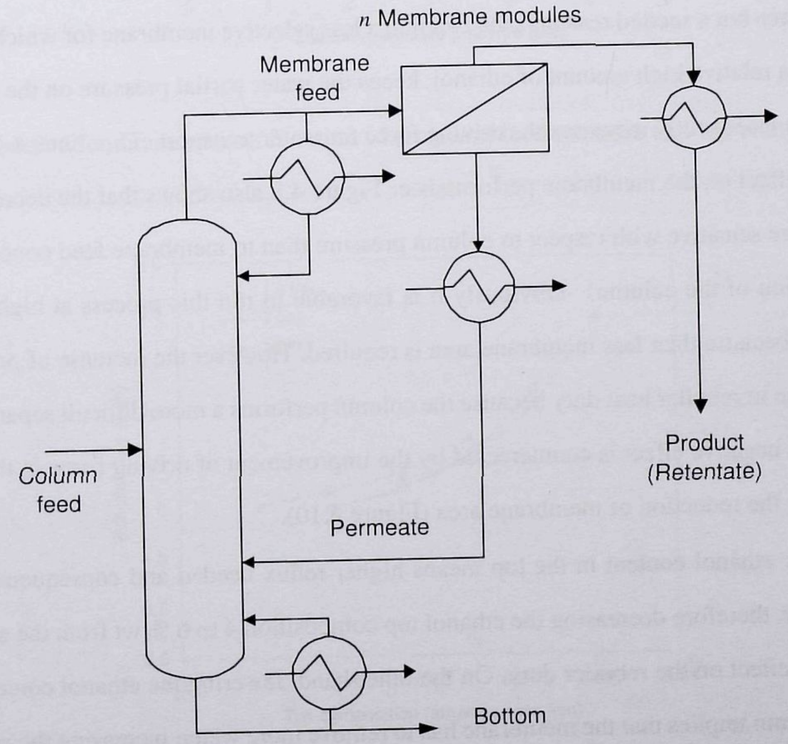


Figure 4.7: Flow scheme for process simulation

tions are shown in Table 4.5.

Table 4.5: Feed pressure and composition for process simulation

Composition, % wt	Azeotrope	83.9	85.6	87.4	89.0	90.6	92.1
1.5 bar	94.8			*	*	*	*
3.0 bar	93.4		*	*	*	*	
5.0 bar	91.7	*	*	*	*		

From Figure 4.8 it is clear that M-2 (high flux, low selectivity) requires less membrane area. It may appear obvious that for a given dewatering capacity a membrane with large flux requires a smaller area but a second reason is the fact that a less selective membrane for which the permeate contains a relative high amount of ethanol, keeps the water partial pressure on the permeate side low and consequently increases the driving force for water transport. This "internal sweep" has a positive effect on the membrane performance. Figure 4.8 also shows that the decrease in area is much more sensitive with respect to column pressure than to membrane feed concentration (top composition of the column). Obviously it is favorable to run this process at highest operating pressure, because then less membrane area is required. However the increase of pressure brings an increase in reboiler heat duty because the column performs a more difficult separation (Figure 4.9). This negative effect is counteracted by the improvement of driving force in the membrane and hence the reduction of membrane area (Figure 4.10).

Higher ethanol content in the top means higher reflux needed and consequently higher reboiler duty, therefore decreasing the ethanol top composition 4 to 6 % wt from the azeotrope has a positive effect on the reboiler duty. On the other hand, lowering the ethanol content in the top of the column implies that the membrane has to remove more water, increasing the area required.

The effect of top composition on the required membrane area is rather small. The reason for the small influence is that most of the membrane area is required when ethanol concentration

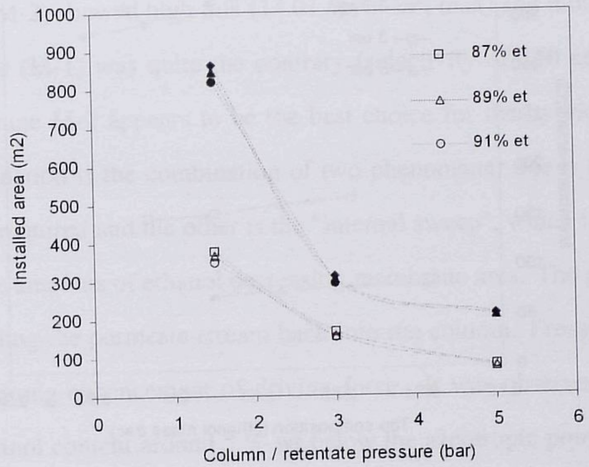


Figure 4.8: Membrane area as function of (column) feed pressure and top composition

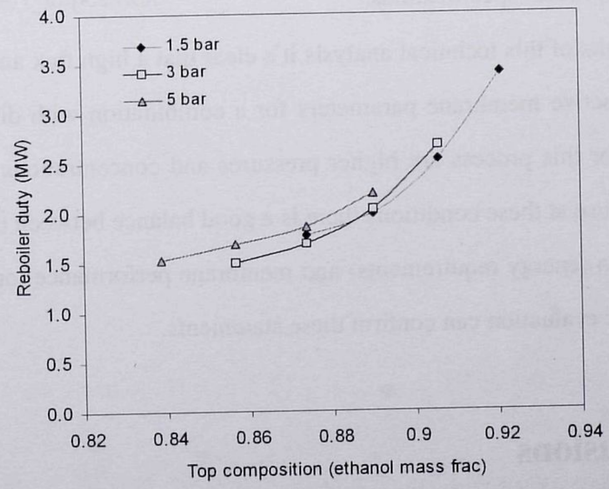


Figure 4.9: Column reboiler heat duty required for different pressures

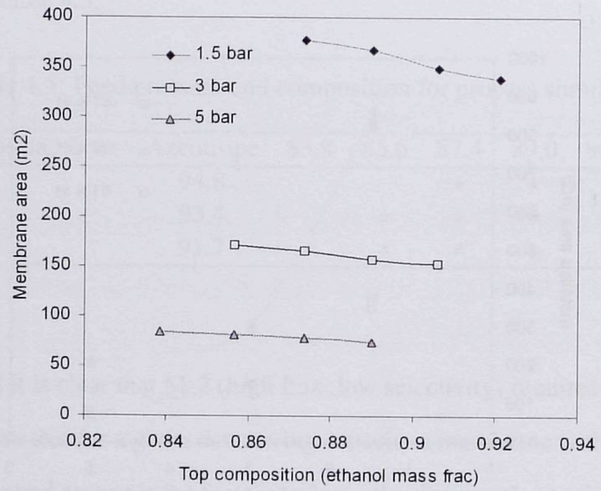


Figure 4.10: Membrane area required for different operating pressure

is larger than 98-99%, where water driving force becomes small and a lot of membrane area is required to reach process specifications.

From the results of this technical analysis it's clear that a high flux and moderate selectivity are the most attractive membrane parameters for a combination with distillation. The conditions beneficial for this process are higher pressures and concentrations below the azeotropic composition because at these conditions there is a good balance between the performance of the distillation column (energy requirements) and membrane performance (area required). A more detailed economic evaluation can confirm these statements.

4.7 Conclusions

Vapor permeation experiments were carried out for the first time with the ceramic membrane tubes used in this project and tested at different pressures and temperatures. The single tube

experiments give a good indication of the overall performance of both ceramic membranes. One of the membranes (M-2) showed high flux (14.01 $kg/h \cdot m^2$, max) and moderate selectivity (30), the other membrane (M-1) was quite the contrary (selectivity of 150 and max. flux of 4.54 $kg/h \cdot m^2$). Membrane M-2 appears to be the best choice for the hybrid ethanol dehydration process. The explanation is the combination of two phenomena; one is the fact that high flux implies lower area required and the other is the "internal sweep", which increases driving force by permeating large amounts of ethanol decreasing membrane area. The permeated ethanol can be recovered recycling the permeate stream back into the column. Pressure affects the process positively with a strong enhancement of driving force. It was observed that the column top stream with an ethanol content around 5 % wt below the azeotropic point is also beneficial for the combined process because on one hand reduces the energy used for distillation and on the other hand increases the difference in concentration across the membrane. Therefore conditions recommended for this process are pressures between 3 to 5 bar and concentrations 4 to 6 % wt below the azeotropic composition.

Chapter 5

Vapor permeation with multitube ceramic modules. Pilot-scale study of integrated process for ethanol dehydration

The current study makes an evaluation of a combined distillation / membrane process based on a pilot-scale set-up equipped with a commercial 7-tube ceramic membrane module. The module was tested in a long term experiment and the performance when changing feed concentration and superheating was studied. The membrane showed a flux of 5.1 kg/h m^2 and selectivity of 5.5 performed at base case conditions (3 bar, 91 % wt ethanol feed and 109.5 °C). Simulations of the combined process demonstrate that due to the low selectivity of the membrane the permeate stream back to the column is too large therefore the heating and cooling requirements of the column are comparable to those of an azeotropic distillation process with three columns (from a previous study [128]). Still certain benefits can be found in the proposed hybrid process.

5.1 Introduction

The removal of water from solvents is one of the most frequently operations in chemical industry, either in the solvent production process or when solvents are used. For the solvents that form azeotropes with water, like ethanol, reutilization is complicated since they have to be first dehydrated.

Anhydrous ethanol is widely used in organic synthesis and in many industrial products. During the production process of ethanol a mixture with water is obtained, conventional separation by means of distillation can only separate this mixture up to an ethanol concentration of 95.57 % wt at atmospheric pressure and 78.13 °C since a minimum boiling point azeotrope is formed. To obtain absolute ethanol (99.9 % wt) two processes are currently in use: azeotropic distillation and pressure swing adsorption.

A rather new alternative for breaking azeotropes is coupling membranes with distillation. So far this proved to work with pervaporation [56, 35, 70, 49, 120, 7], which however implies total condensation of the vapor leaving the top of the distillation column. Pervaporation has the disadvantage of a strong temperature decrease during operation, which affects adversely the flux through the membrane. This performance deteriorating effect is avoided if vapor is feed directly to the membrane coupled with the distillation column. This and other beneficial features make vapor permeation a very attractive alternative for ethanol dehydration [112, 54].

5.2 Industrial dehydration processes

Ethanol is one of the largest volume organic chemicals used in industrial and consumer products. The main uses for ethanol are as intermediate in the production of other chemicals, as a solvent and very recently as fuel (either pure or blended with gasoline). A description of the currently

available technologies applied for the production of pure ethanol follows.

5.2.1 Distillation-based processes

In azeotropic distillation a third component (entrainer) is added to the ethanol / water mixture. The entrainer breaks the azeotropic mixture, most of the times forming a new azeotropic mixture with lower boiling point than the original one. However, the recuperation of entrainer, for further reutilization, is achieved in a separate column. For this reason the process contains at least three distillation columns: the pre-concentration column, the azeotropic column and the entrainer recovery column. The dehydration of ethanol presents a difficult problem, since most of the entrainers form binary, or even ternary, azeotropes with ethanol. A number of liquid entrainers have been tested for ethanol dehydration such as benzene, pentane, cyclohexane, isooctane, diethyl-ether and toluene [60, 140, 38]. From these entrainers benzene was the most utilized, but due to its carcinogenic nature the use is diminishing and most of the times replaced by cyclohexane. Several technical developments have been implemented to the old benzene-based process. Nowadays the azeotropic column is very efficient and the supply of entrainer is carefully monitored by a combination of two control systems so that no benzene reaches the lower plates [60].

Another method is to distil the mixture at high pressure in the first column almost reaching azeotropic composition. The distillation in the second column is carried out at low pressure where the azeotropic point is at a different concentration and the solvent can be distilled without problems. Obviously this method only works when the azeotrope varies with pressure. The disadvantage of this method is the energy requirement because the specification in the first column is very close to the azeotrope, as a consequence high reflux and reboiler duty are needed. In the second column there can be some inconvenients as when there is a very narrow temperature

distribution, but this depends upon the system.

An alternative process to produce anhydrous ethanol is the extractive distillation using soluble salts as separation agents [40]. The advantages of the salt distillation are the lower toxicity levels than with liquid entrainers, an entrainer free product and lower energy consumption. Ligero, et.al. [68] investigated the salt extractive distillation process using potassium acetate. He performed process simulations with two cases, one with dilute ethanol feed (2.4 % mol), the other with concentrated ethanol feed (60 % mol). The simulation results showed that the concentrated ethanol feed process is the most advantageous alternative, because compared with dilute ethanol feed process, it requires lower reflux ratio, lower column diameter and lower salt consumption. It was concluded that the conversion of existing benzene extraction plants to potassium acetate extraction plants can be quite easy.

5.2.2 Adsorption-based processes

Adsorption is the selective collection and concentration on solid surfaces of particular types of molecules contained in a liquid or a gas [60]. With adsorptive separation, contaminants can be removed to nearly undetectable levels. The simplicity of the physical adsorption process reduces capital costs, operating costs and adds flexibility and high reliability to the complete process.

Pressure Swing Adsorption is a semi-batch method based on the difference in adsorption of water and ethanol on a selective material (adsorbent). A mixture of water and ethanol is led into a selective absorbent bed, where water is absorbed selectively. A high concentration ethanol stream is thus obtained. Once the bed is saturated with water it must be regenerated. This is done by desorption under vacuum. Due to the regeneration step multiple beds are necessary for continuous operation. The molecular sieves that have been found suitable for ethanol dehydration are zeolites 3A, 4A, NaX and NaY4. The favorable properties of molecular sieves in adsorptive separation applications are their high capacity at low adsorbate concentration, the ability to maintain their capacity at (moderately) elevated temperature and their selectivity based on size, configuration and affinity.

Guan et.al. [46] performed pressure swing adsorption simulations for dehydration of mixture of ethanol 93.54% and water 6.46 % wt at feed pressures from 2 to 5 bar and operating temperature between 120 and 150 °C. He found that raising feed pressure increases product purity, recovery and productivity. The optimized condition for desorption is a vacuum pressure of 0.4 bar. Recently, efforts have been made in the mathematical modeling of cyclic adsorption processes. In this respect Jiang et.al. [55] refined previous algorithms and simulated two non-isothermal industrial applications (oxygen-from-air with Vacuum Swing Adsorption and hydrogen from hydrocarbon mixtures with Pressure Swing Adsorption). He succeeded to speed up the optimal design and operating conditions for the simulated processes.

5.2.3 Membrane-based processes

Ethanol dehydration by pervaporation is one of the emerging commercial applications of membrane technology these days [112, 9, 113, 137, 83, 57]. Unlike other methods, membrane separation doesn't suffer from vapor-liquid equilibrium or batch configuration [119] and although investment cost can be high, their operating costs often offer significant savings [70].

First steps in the application of membranes for commercial purposes were made using well-established polymer membranes, which however proved to be prone to swelling and thermal decomposition [112, 54, 85]. In this respect ceramic materials are a natural choice and a great deal of recent effort went into development of ceramic membranes [147, 41, 122, 18]. An obvious advantage is the thermal stability of ceramics that allows utilization of high temperature, enhancing driving force and reducing membrane area. Since dealing with distillation implies handling

saturated vapors and liquids, the temperature of the vapor depends directly on the operating pressure. Certainly, with increasing pressure the membrane driving force increases, however on the distillation column side this leads to a number of negative and positive effects (column configauration, materials and higher rebolier duty due to more difficult separation, among others). These should be balanced in a way to arrive at an optimized integrated process.

5.2.4 Future direction in the ethanol industry

New technologies to produce ethanol are being studied and developed preferably from renewable sources to face the oil shortage in the future and to reduce fuel prices. The United States wants to double the use of renewable fuels by 2012 [32] and in Europe countries like Sweden and Spain are already adding ethanol to car petrol [115]. The aim in Europe is that all fuels contain at least 1% of bio-fuels by from 2009 onwards [115]. At the moment ethanol shortage in the US has caused ethanol doubles its price in the past year (to 2.95 USD per gallon or 0.57 euro per liter) [32].

There are several steps in the production of ethanol from fermentation. Each of them is being studied deeply at the moment and promising solutions have been detected. Anyhow, a lot of research and development is needed to bring these new solutions to full commercial applications. Ethanol is produced by fermenting sugar into grain alcohol, but the production of fuel-grade ethanol from corn showed to be difficult and costly (at least in the USA). However, whereas the USA primary uses corn starch for fermentation, Europe uses a wide range of raw materials, including other grains (wheat, barley), sugar beet and molasses. New efforts are being made in the research of producing alcohol from cellulose, this method treats any plant matter with ammonia at 93 °C and 17 bar for five minutes, but this method (as many others) is still on laboratory scale.

After this step the long cellulose molecules are broken into sugars by enzymes. A method that is now in research to speed up this process is the use of ultrasound waves to break corn kernels [45], releasing corn sugar more efficiently than grinding and smashing corn. Ultrasound can break corn into very fine particles, that expose more of the corn's starch to the enzymes to convert it into sugar. Although the price of enzymes has decreased dramatically (from 0.96 down to 0.05 euro per liter of ethanol produced) the price should be least 0.02 euro per liter to make it economically attractive. The next step is to separate and distil the ethanol from the fermentation broth, which consist mainly of water. The overall fermenting and distilling process needs to get twice as efficient. It is estimated that about 5% of the total energy consumption in Canada and the USA can be attributed to separation processes [1]. There is yet another problem: transportation. The transport of raw material to the plant and of the ethanol to the final consumer will be expensive and difficult. Since ethanol has less energy content than gasoline (but it weights about the same), it may consume more of its own content in the process of being delivered.

In the coming years there are a lot of challenges and possibilities to explore in every step of the ethanol production. With a lot of questions still unanswered there is plenty of room for the research and development of economical and energy efficient biofuels (like ethanol).

5.3 Model Description

The model used for calculations in this chapter has already been used and described in the previous chapters (3 and 4). For the detailed description please refer to those chapters.

5.4 Experimental part

5.4.1 Set-up and procedure

Figure 5.1 shows the pilot-scale set-up built at our installations. It consists mainly of a five-meter distillation column (3 m packed) and a membrane unit inside a heated box. The start and end point of the cycle is a 50 liter buffer tank (T2), from which the mixture ethanol / water is fed to the column (C1) from one of the possible feed locations. The mixture is boiled by the steam heated reboiler HE1 (up to 10 kW), part of the boiling liquid leaves the column towards T2, while the vapors pass through the column and condense on the water condenser HE2 (8 U-tubes). Vapor is retrieved from the column top and conducted to the membrane feed. Electric tracing HE6 avoids condensation on the tubes and allows for superheating when necessary. Membranes are kept at the desired temperature by means of hot air in the isolated box T7. Then the membrane retentate and permeate are condensed in the water-cooled HE3 and HE4, respectively. Afterwards both streams are kept in buffer tank T3 and T4, respectively (10 liter each approximately) before they are pumped back to T2 to complete the cycle. There are five sample ports: tank T2, column bottom, column reflux, retentate and permeate. Samples were analyzed with both Karl-Fischer titration (Metrohm 756 KF coulometer) and refractive index.

Before taking any membrane measurements, the set-up was operated at least 5 hours to warm up and arrive to steady state. After temperatures and concentrations were stable for at least 2 hours the distillate stream was directed through the membranes. After at least 30 minutes, the permeate line was drained and samples were taken from all ponts. Samples were taken again at different intervals, depending on process conditions. All experiments were made in duplicate, and if the points were too different, a third and even a fourth experiment was carried out at the same conditions. After experiments, the set-up was slowly cooled down until reaching 1.1 bar, the membrane circuit was closed and kept under vacuum and the rest of the equipment shut

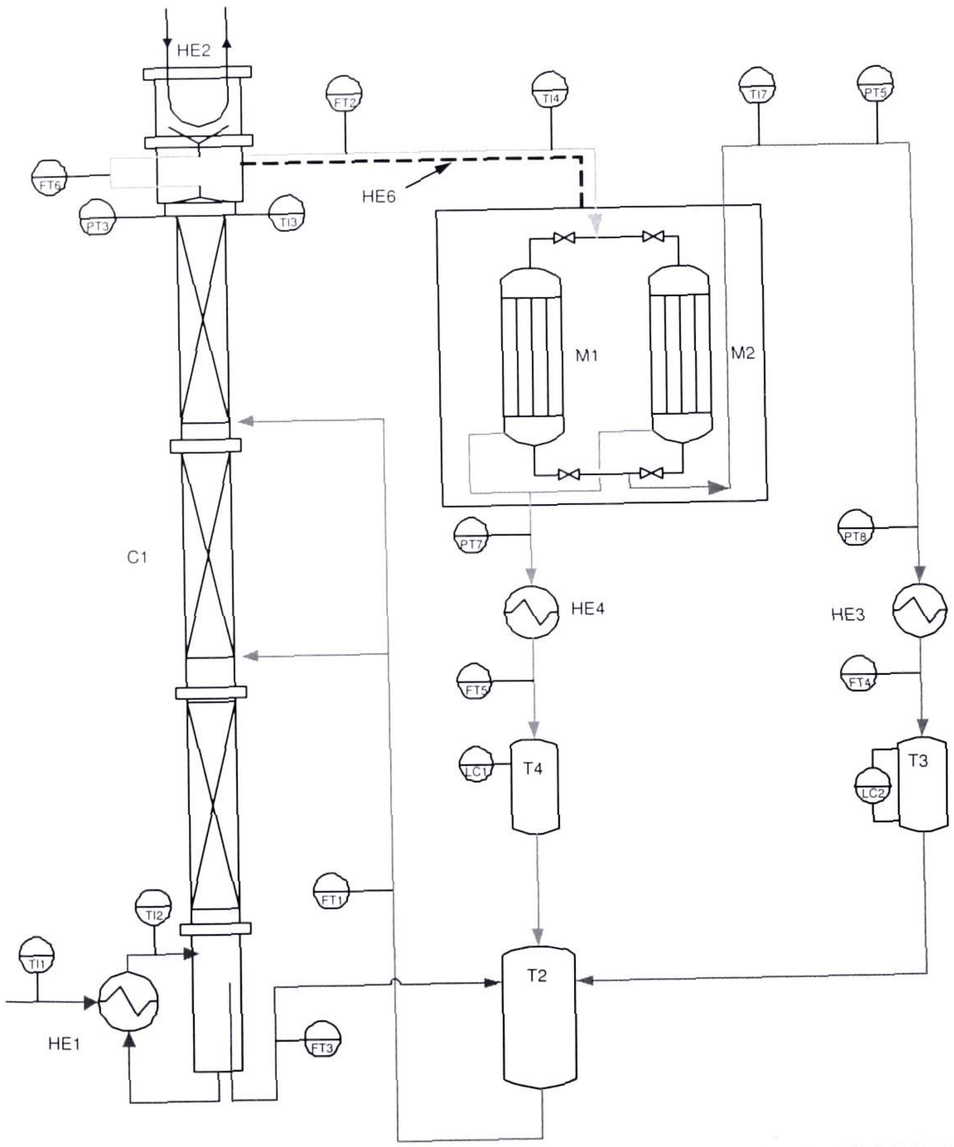


Figure 5.1: TU Delft distillation / membrane pilot-scale set-up used during experiments

Table 5.1: Initial pervaporation performance of the module (measured by producer)

Mixture	Composition % wt	Temp. °C	P_{perm} mbar	Total flux $kg/h \cdot m^2$	Select. α
IPA / W	95 / 5	70	10	4.2	99

down. With this working procedure, it was possible to retrieve only a couple of experimental data per day.

5.4.2 Membrane characteristics and experimental conditions

An industrial membrane module acquired from Pervatech was tested (as the one shown in Figure 5.2). The initial pervaporation characteristics of the module are shown in Table 5.1. The structure of the tubes is the same as to the one mentioned in Chapter 4 (Table 4.2).

The membrane module had seven tubes in hexagon, with one tube on each vertex and one in the middle. Module inside and outside configurations are shown in Figure 5.3. The tube dimensions are 500 x 10 x 7 mm (length x outside diameter x inside diameter) with the silica selective layer inside the tubes.

Membrane feed concentration was in the range of 90 to 95 % wt ethanol to study the effect of driving force. Membrane feed temperature was changed from 0 to 10 °C superheating to avoid condensation inside the tubes and to study the effect of superheating. Experiments were always conducted at 3 bar pressure and the permeate side pressure was kept constant at 200 mbar, this allowed the use of cooling water for permeate condensation.

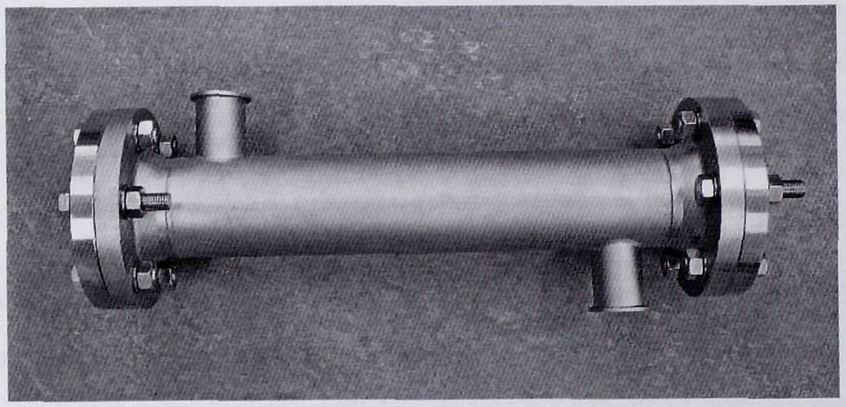


Figure 5.2: Photo of the 7-tube membrane module used for experiments

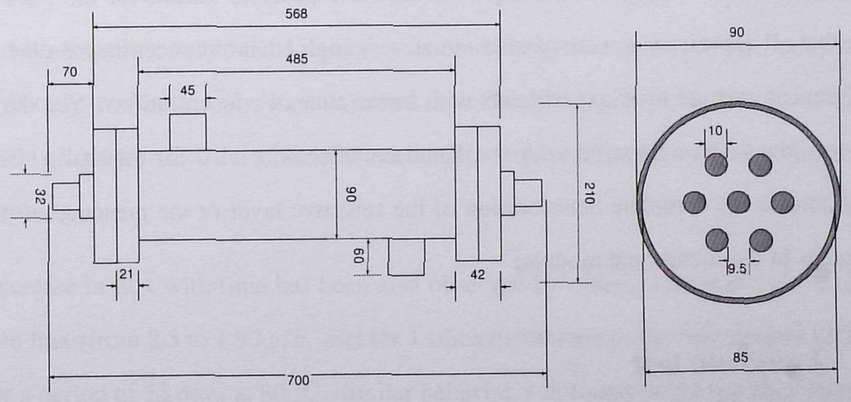


Figure 5.3: Membrane module used in pilot plant experiments (measures are in mm)

5.5 Results and discussion

The experiments with the pilot-scale set-up were performed to identify the effect of varying operating variables, e.g. feed concentration and superheating temperature, in the membrane performance. Also a long-run test was carried out.

5.5.1 Base case experiments

Table 5.2 presents the operating conditions that were used as base case throughout the whole experiments. Accordingly a flux of 5.1 $kg/h \cdot m^2$ ($\pm$ 0.45 $kg/h \cdot m^2$) and a selectivity of 5.5 ($\pm$ 0.64) was obtained. Comparing these results with those obtained for other ceramic membranes separating ethanol / water [39, 147, 65], it is clear that the module presents an average flux (for ceramic material) but poor selectivity.

A possible reason for the poor selectivity is that one (or several) membrane tubes might present defects in the selective layer, because even one small pinhole or a bad sealing affects strongly selectivity without increasing flux. Another possible reason for the poor separation can be that all experiments were carried out at very high ethanol concentrations, while most of the references execute their experiments with lower ethanol concentrations. Yet, the selectivity is not too low to be compared with the Knudsen selectivity (1.6 for ethanol / water), which would indicate the complete deterioration of the selective layer or the presence of huge cracks or leakages in the membrane module.

5.5.2 Long-run test

The long-run test was carried out operating non-stop with the membrane for approximately 20 hours. Figure 5.4 shows the membrane performance during operation. One of the test was carried out for 20 hours (triangles), the duplicate (squares) was only 10 hours due to an electric failure

Table 5.2: Base case conditions for pilot-scale set-up

	Unit	Value	Remarks
Column			
Pressure	bar	3	at column top
Feed	kg/h	45.5	at boiling point
Ethanol	% wt	90	
Membrane			
Feed	kg/h	41.2	
Pressure	bar	3	feed side
	bar	0.2	permeate side
Temperature	°C	109.5	1.5 °C superheating

in our lab the night of the experiment. A decrease in flux was observed, similar to other ceramic membranes, from around 5 to 2 $kg/h \cdot m^2$. The recovery of the membrane flux for the begining of the second experiment suggests a partially reversible interaction between the alcohol and the silica layer, as reported by Fontalvo [39] for the same kind of membrane but for a different application. The observed flux decline with time is likely to be due to interactions of water and alcohol with the silica material. Although silica has a high thermal stability, its hydrothermal stability is only moderate, and water may react with the silanol groups on the silica surface [39]. This would cause densification of the silica and as consequence the decrease in both permeability and selectivity.

A decrease in flux with time has been also observed by others. Reference [147] reports the decline in flux (from 2.5 to 1.9 $kg/h \cdot m^2$) for a silica membrane in the dehydration of 95.5 % wt IPA over a period of 73 days at 80 °C. Similar behavior was found in [123] with a mixture 95 % wt IPA / 5 % wt water over a period of 4 hours at 80 °C. This time the flux decreased from 3.7 to 2.5 $kg/h \cdot m^2$. Then the membrane performance stabilized and stayed constant. Subsequently, in the same mixture no further reduction in flux occurred over a period of several weeks.

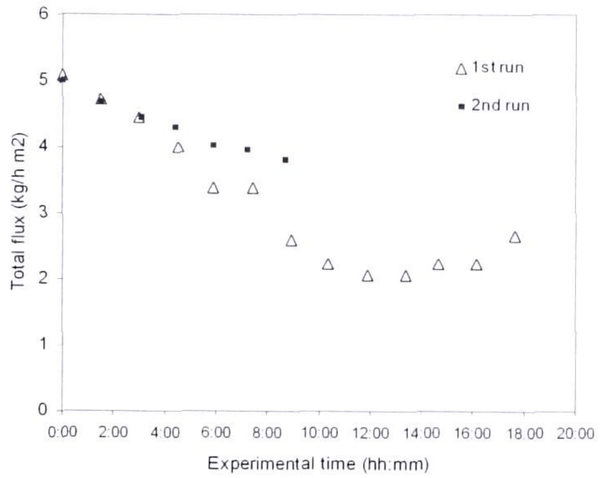


Figure 5.4: Variation of flux during the long-run test

5.5.3 Effect of superheating

Superheating experiments were performed for temperatures ranging from 0 to 10 °C above the mixture boiling temperature at 3 bar (108 to 118 °C). Figure 5.5 shows the total flux as function of superheating. Two series of experiments were performed for this figure, one increasing superheating (starting at boiling point conditions for several hours), and the other decreasing superheating (starting at 118 °C). A small increase of flux is noticed from zero to five degrees superheating, after which the flux decreases again to values close to boiling point conditions. The explanation can be because mass transport depends on two phenomena, namely adsorption and diffusion. One of them increases with temperature (diffusion), while the other decreases (adsorption). The total sum of the effects is reflected in the flux.

This effect has also been reported by Sommer [123] when he studied the effect of superheating for the systems ethanol / water and IPA / water with inorganic and polymer membranes and

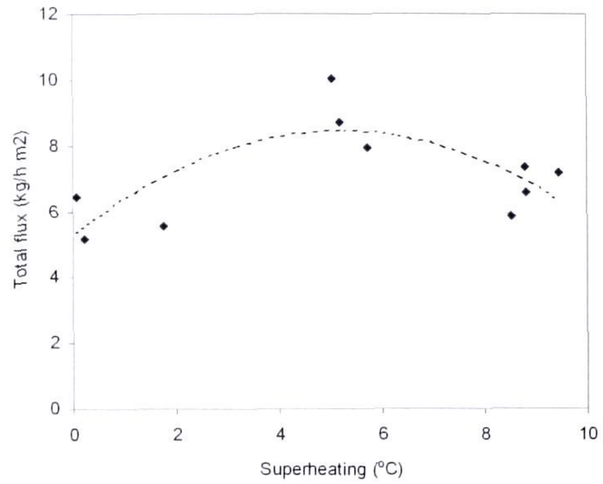
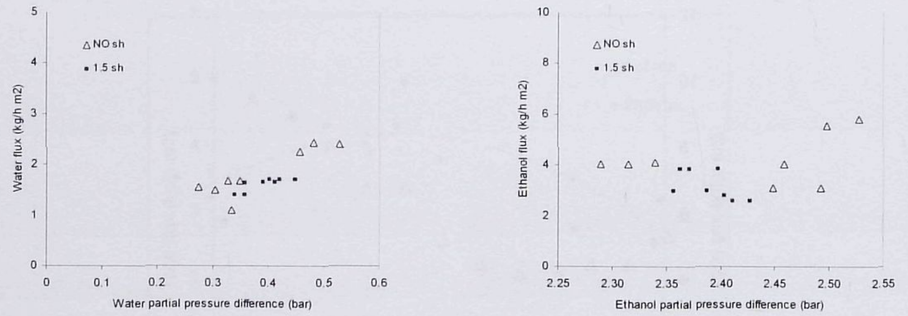


Figure 5.5: Variation of flux with superheating temperature (line is only an eyeguide)

encountered the same behavior for inorganic membranes. He found that a superheating of only 5 °C leads to an average flux decline of about 50% for polymer membranes, while superheating of the vapor feed improves performance for inorganic membranes. According to Sommer, the reason for this different behavior is the absence of membrane swelling in the rigid inorganic structure.

5.5.4 Effect of feed composition

At constant feed temperature, the membrane driving force was varied by changing the composition in the membrane feed. Ethanol composition was varied from 90 to 95 % wt at two superheating temperatures (0 and 1.5 °C). Figure 5.6 shows the water and ethanol fluxes as function of their own driving force. It is clear that water flux increases with its driving force roughly at the same rate regardless the superheating temperature (Fig. 5.6(a)). Looking at Figure 5.6(b) it



(a) Water flux (b) Ethanol flux

Figure 5.6: Flux as function of partial pressure for two different superheating (sh) temperatures

seems that ethanol flux is "independent" of driving force (with an average value of 3.5 $kg/h \cdot m^2$). Taking into consideration the poor selectivity of the module, it is believed that the selective layer has some cracks or pinholes, which allow the permeation of ethanol with viscous flow. This kind of mass transport mechanism takes place in wide pores and is the result of convective flow in the direction of an absolute pressure gradient. Viscous flow depends on pressure gradient, on membrane morphology, on the properties of the stream and not on concentration gradient. That might explain the constant ethanol flux because all experiments were performed at constant pressure difference. The macroscopic consequence of the above discussed behavior is that the module selectivity will be worse at the outlet than at the inlet.

Figure 5.7 shows the same data plotted against the ethanol feed concentration. Here we notice that once the azeotropic composition was passed water flux follows the same trend but the trend of ethanol flux changes. This behavior is not yet understood and should be studied further.

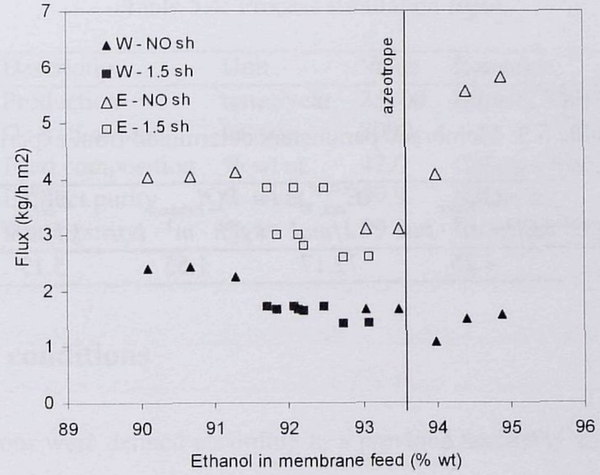


Figure 5.7: Variation of flux as function of ethanol (membrane) feed concentration for two different superheating (sh) temperatures

5.6 Process Simulation

With these experimental results it is interesting to assess if an industrial scale process equipped with membrane modules with similar performance to the one shown in the previous section is competitive for industrial applications.

5.6.1 Model parameters

Model parameters were retrieved for process simulation from the experiments described in section 5.5. Table 5.3 shows the model parameters used for the simulations of the membrane modules. Figure 5.8 shows the parity plot for simulations using these parameters.

Table 5.3: Membrane parameters determined from experiments

Q^o_{Water} $kg/h \cdot m^2 \cdot bar$	$E^{app}_{act,\,W}$ kJ/mol	$Q^o_{Ethanol}$ $kg/h \cdot m^2 \cdot bar$	$E^{app}_{act,\,E}$ kJ/mol
4.25	72.17	1.55	5.17

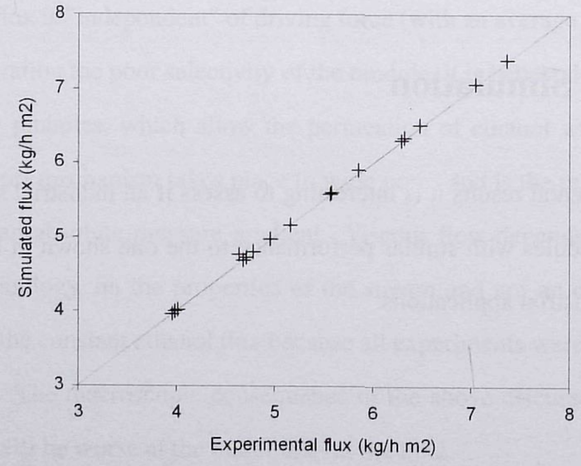


Figure 5.8: Experimental against calculated fluxes with parameters in Table 5.3

Table 5.4: Process simulation input

Description	Unit	Value	Remarks
Production	tones/year	23400	Ethanol 99.9%
Operation time	hr/year	8000	
Feed composition	% wt et.	42.0	Column feed
Product purity	% wt et.	99.9	Retentate
Water purity	% wt	99.9	Column bottom

5.6.2 Process conditions

Process specifications were defined according to a previous feasibility study for ethanol dehydration with membranes [128]. These specifications are shown in Table 5.4 and the scheme of the simulated process can be seen in Figure 5.9.

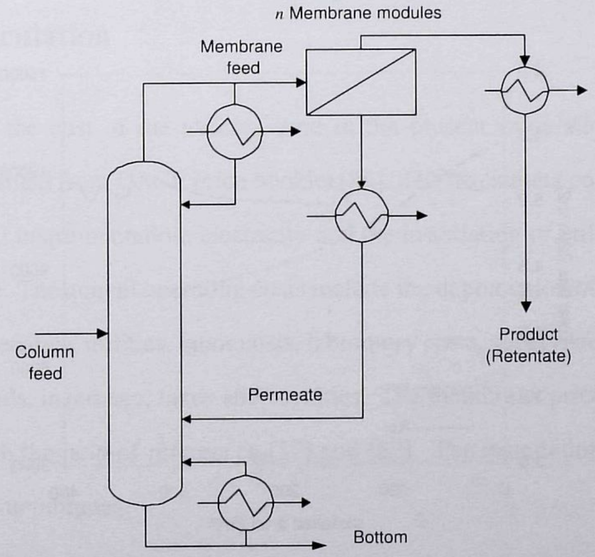


Figure 5.9: Flow scheme for process simulation

5.6.3 Simulation results

The combined process is able to reach process specifications when the installed membrane area reaches 393 m^2. Due to pressure drop, the velocity inside the tubes decreases, consequently Reynolds number as well. Since a constant Reynolds number between 10,000 and 12,000 is desired (to avoid concentration polarization), the number of parallel modules should be modified after certain length. Figure 5.10 shows the variation of Reynolds in the tubes and the total flux from beginning to end of the membrane separation section. It is clear that the variation of parallel modules was a good measure to keep Reynolds roughly constant. The decrease in flux is due to the decrease in driving force caused by two factors: water depletion and pressure drop. Figure 5.11 shows the decrease driving force as well as the water profile as the feed stream gets in contact with membrane area. The pressure drops steadily from 3 bar at the beginning to around 2.96 bar at the end of the complete module separation section.

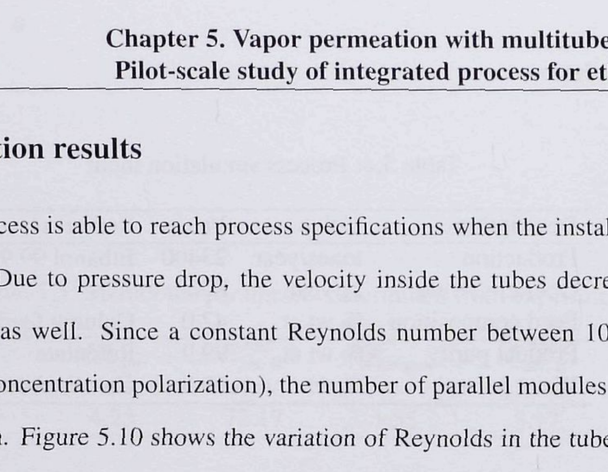


Figure 5.10: Total flux and Reynolds profile along membrane modules

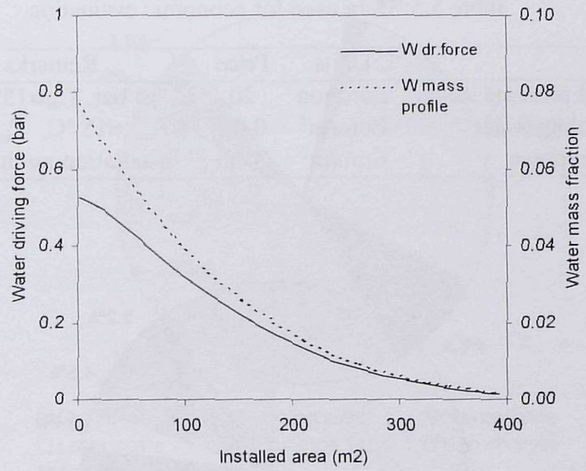


Figure 5.11: Water depletion and driving force profile along membrane modules

5.6.4 Cost calculation

Table 5.5 presents the cost of the utilities used in the present calculation. The price of the equipment was obtained from DACE price booklet [86]. The investment costs include equipment erection, piping and instrumentation, electricity and the installation of utilities and any building or process structure. The annual operating costs include the depreciation of equipment (10 years, 5% interest), maintenance, utilities, labor costs, laboratory costs, supervision, manufacturing and production overheads, insurance, taxes and royalties. The membrane price and installation cost were estimated with the help of references [17] and [82]. The installation cost considered was 50% of the cost of membranes.

Figure 5.12 shows the contribution to the investment cost of the most important pieces of equipment including installation. The total investment cost is 1.67 million euro and it is clear that the membrane is the most expensive part of the equipment. Maloncy et.al. [75] also found the

Table 5.5: Data used for economic evaluation

	Units	Price	Remarks
Mid pressure steam	Euro/ton	20	5 bar, T_{ini}=152 °C
Cooling water	Euro/m^3	0.05	ΔT_{max}=15 °C, T_{ini}=25 °C
Membrane	Euro/m^2	2000	Installation not included

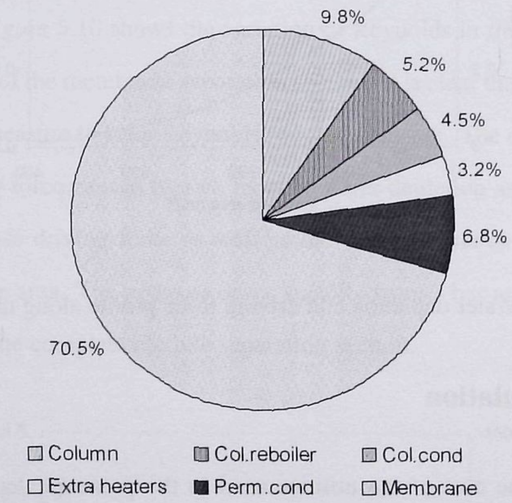


Figure 5.12: Contribution of the most important equipment (including installation) to the total investment cost (1.7 Meuro)

same for his membrane-based heptane hydroisomerization process. Though for his estimation membranes accounted just for 42% of the equipment costs.

Membranes should be replaced after some years (an optimistic lifetime of 5 years was considered in this study), increasing the operation costs. The membrane in the present study has a good flux, but the reason of the huge membrane investment lays mainly in the fact that the selectivity is so poor that the permeate stream contains on average more than 85 % wt ethanol. Although ethanol is recycled to the column and recovered, the permeate stream is so large that the column

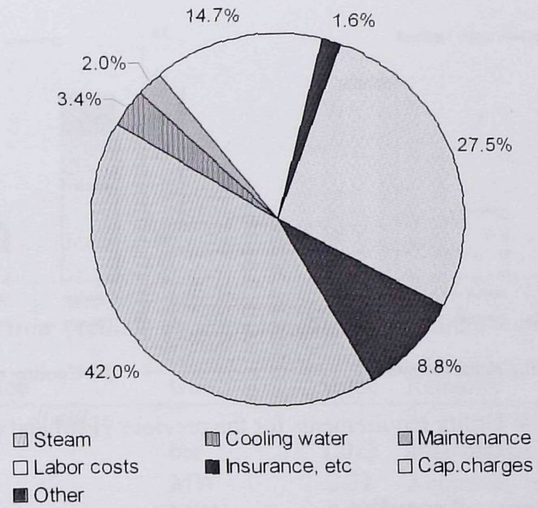
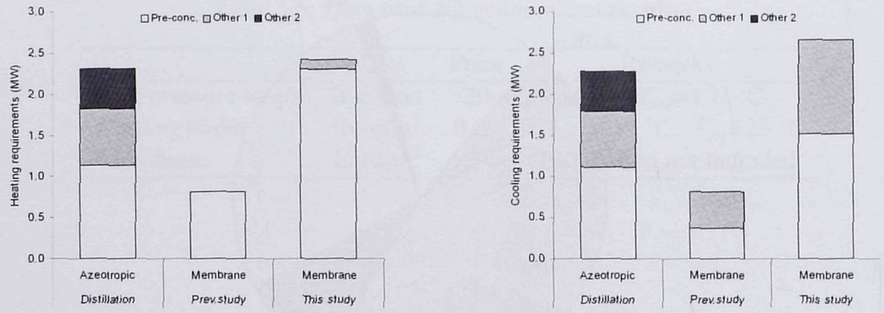


Figure 5.13: Distribution of the annual production cost (1.2 Meuro) for the combined distillation / membrane process

make use of a lot of utilities to warm up and cool down the internal column streams. From the point of view of membrane costs, it is convenient to run the process at high pressure, but from the column point of view this is less convenient, since the separation becomes difficult and the boiling points increase, requiring consequently more utilities for distillation. A possible option could be to distil atmospheric and increase pressure before the membrane, but as compressors are such sophisticated and expensive machines this option seems not feasible in practice.

Figure 5.13 shows the contribution to the annual operating cost (1.25 million euro) for this process. Here it's clear that the process uses a lot of energy and that accounts for roughly 45% of the operating cost. For "Capital cost" is considered the 15% of the investment cost for columns and heat exchangers, but for membranes 30% is considered. "Insurance" includes also taxes and royalties, while "Labor" includes also project supervision costs. Miscellaneous materials, lab costs and plant overheads are accounted under "Other".



(a) Heating requirements

(b) Cooling requirements

Figure 5.14: Utility requirements for the previous [128] and current studies

5.6.5 Comparison of results

If the results of the previous section are compared with the results of the feasibility study of the hybrid process carried out in [128] (Table 5.6) some interesting results catch the eye.

The present study requires roughly the same amount of energy as the azeotropic distillation process, while the membrane process in [128] uses only 35% of that energy (Fig. 5.14). The total amount of heating utilities is depicted in Figure 5.14(a). The legend "Other 1" for the membrane process is the amount of extra heating needed to pre-heat the permeate back into the column, while for the azeotropic process is the reboiler duty of the second column. "Other 2" is the reboiler duty of the third column for the azeotropic process. The total amount of cooling utilities is presented in Figure 5.14(b). "Other 1" for the membrane process means the permeate condenser duty, while for the azeotropic process is the condenser duty of the second column. "Other 2" is the condenser duty of the third column.

The revised investment cost of the hybrid process with ceramic membranes in [128] is roughly the half to that of the azeotropic distillation (Figure 5.15), while the hybrid process in the present study is more expensive than the azeotropic distillation in [128] particularly due

Table 5.6: Results from preliminary study for ethanol dehydration with membranes [128]

Description	Unit	Value	Remarks
Azeotropic distillation			
Pressure	bar	1.013	atmospheric
Steam	MW	2.32	3 columns included
Cooling water	MW	2.28	3 columns included
Membrane process			
Pressure	bar	4	–
Steam	MW	0.82	all heaters included
Cooling water	MW	0.82	all condensers included
Membrane area	m^2	91	ceramic membrane
Water permeance	kg/h m^2 bar	10.67	selectivity = 75
Ethanol permeance	kg/h m^2 bar	0.14	–
Present study			
Pressure	bar	3	–
Steam	MW	2.42	all heaters included
Cooling water	MW	2.45	all condensers included
Membrane area	m^2	393	–
Water permeance	kg/h m^2 bar	4.25	from Table 5.3
Ethanol permeance	kg/h m^2 bar	1.55	selectivity = 5.5

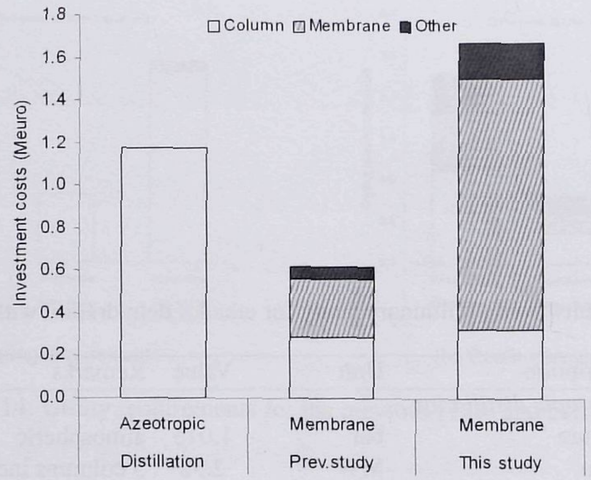


Figure 5.15: Total investment for the previous [128] and current studies

to the membrane cost. The extra heaters and permeate condensers are accounted under "Other", while all columns, reboilers and condensers are accounted for the azeotropic distillation in Figure 5.15. The investment cost of the hybrid process depends strongly on membrane performance and price. The reason for the differences in the previous and the current study is mainly the variation in membrane performance. The water permeance in the previous study is 2.5 larger than for the current study and the selectivity 15 times larger. Also the system pressure is higher (4 against 3 bar). These variables affect greatly membrane performance and ultimately the process economy.

Looking at the annual costs (Figure 5.16) some interesting results turn up. Comparing the present membrane process with the azeotropic distillation, most of the costs are smaller or similar for both cases. Membrane capital costs have a huge impact of the annual costs. The overall annual cost can be more convenient with cheaper membranes, with longer lifetime or with higher selectivity.

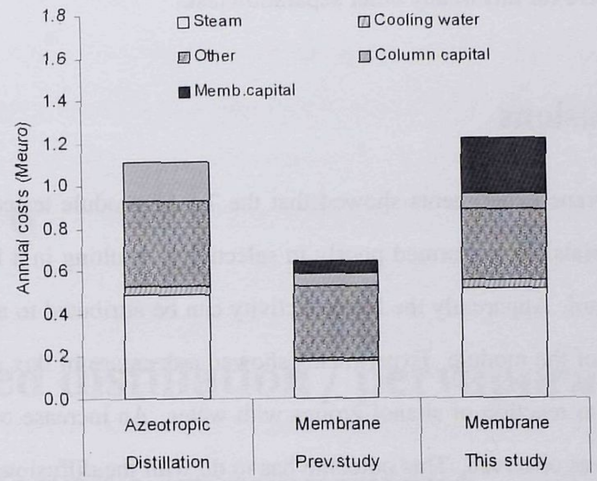


Figure 5.16: Annual cost for the previous [128] and current studies

The calculations of the hybrid process in the previous study did not take into consideration any detrimental effect of membrane performance, such as concentration polarization and pressure drop. For the current study concentration polarization was minimized with high Reynolds number and the module configuration appears to be very important to avoid excessive pressure drop while keeping constant Re inside the tubes (as shown in Figure 5.10). All these aspects count for a more realistic analysis to calculate the required area and predict the proper behavior of an industrial installation.

Despite the negative first impression of the last results, there are some positive points for the combined process simulated in this study. The utility requirement may be the same but the membrane process doesn't introduce any entrainer, therefore saves the purchase, storage and use of entrainer and at the same time avoids product contamination. Finally, if the conditions of the hybrid process improve in different fronts as new membrane materials with an increased lifetime, high (constant) flux and, above all, if they become cheaper, hybrid processes will become a very

attractive alternative for this or any other separation task.

5.7 Conclusions

Pilot-scale membrane experiments showed that the 7-tube module tested had an average flux for ceramic materials but performed poorly in selectivity, resulting in a large permeate stream with a lot of ethanol. Apparently the low selectivity can be attributed to a leakage in one of the tubes or sealings of the module. Experiments showed a decrease in flux after certain operation time, maybe due to reaction of silanol groups with water. An increase of flux with superheating temperature was observed. This outcome has to do with the diffusion and adsorption of the membrane. All results in the experiments agree with literature observations for ceramic membranes. The complete simulation of the combined process fulfilled the expectations just partially because it requires the same amount of utilities and shows larger investment than the azeotropic distillation process. The membrane process in the previous study [128] showed a reduction in energy requirements, investment and operation costs. The current study didn't exhibit the desired results because the membrane performance was different (in detriment of the present study) and the membrane prices have not decreased, as it was expected. Finally, the process in the present study becomes more attractive with cheaper membranes, with longer lifetime and / or with higher selectivity.

Chapter 6

Combined distillation / pervaporation process for the improvement of acetone production

High performance membranes are required for successful commercial implementation. In addition to large flux and selectivity, membrane stability at higher temperatures and harsh chemical environment is quite important, considering that pervaporation at higher temperature gives larger fluxes, resulting in smaller membrane areas. In this respect, inorganic porous membranes could find a wider application in practical separation and purification processes where polymer membranes can not be used. This chapter deals with the pervaporative dehydration of the mixture isopropanol (IPA) / acetone / water, which appears during the production of acetone from isopropanol. Compared with the available literature, ternary pervaporation experiments showed rather large fluxes at atmospheric pressure (0.5 to 3 kg/h m^2) for different water concentrations (5 to 20 % wt) in the range of 60 to 75 °C. From characterization experiments model parameters were retrieved and used to simulate the performance of a pervaporation module coupled to a

distillation column. The purpose of this flowscheme is to separate pure acetone as overhead and almost pure IPA (95 % wt) at the bottom of the column, while water can be retrieved as permeate. A parametric study shows the best characteristics for the combined process regarding reboiler heat duty, side stream flow and the position of the feed and retentate streams. Rough economic calculations show that the hybrid separation process is competitive against the current process that makes use of two distillation columns.

6.1 Introduction

Acetone is a the simplest and most important of the ketones. It is used as solvent, as intermediate for other chemicals, and as raw material for the chemical synthesis of a wide range of products such as methyl metacrylate, methyl isobutyl ketone, some glycols and more.

The oxidation of cumene to phenol (plus acetone) [37, 132, 131], the catalytic dehydrogenation of isopropanol [134, 133, 28] and the direct propene oxidation [140] are the main processes for the production of acetone. These methods account together for over 95% of the acetone produced worldwide.

However, there are several other processes to produce acetone [140, 60]. Some of these processes are in their developing phase [93, 29, 47], others are used for small scale production (isopropanol oxidation, fermentation process, etc) or are outdated (distillation of calcium acetate, direct oxidation of hydrocarbons). The present chapter focuses on the separation of the acetone / isopropanol / water mixture that occurs after the reactor during isopropanol dehydrogenation.

6.1.1 Isopropanol dehydrogenation process

In this process a recycled azeotropic mixture of water and isopropanol (87.8 % wt isopropanol) is evaporated and fed to a catalytic tube-reactor specially designed for effective heat transfer. The

reaction produces hydrogen ($\geq$ 99% purity) as a valuable by-product. A part of the hydrogen can be recycled to prevent catalyst fouling. The dehydrogenation reaction is endothermic and the main side reactions are the dehydration of IPA to propene, the self-condensation of acetone to di-acetone alcohol and the production of carbon oxides. A large number of catalyst can be used, including zinc, copper, manganese or magnesium oxides. However, catalysts presenting the highest activity contain platinum and ruthenium. All catalyst should be regenarated periodically due to the buildup of carbon deposits, this has to be compensated by increasing reactor temperature as the catalyst ages.

The reactor mixture is cooled and the non-condensables scrubbed with water. The liquid stream is distilled, taking acetone overhead and a mixture of isopropanol and water as bottoms. Currently this bottom stream is wasted or distilled again to concentrate isopropanol until azeotropic composition ($\approx$ 88 % wt) for recycle to the reactor. Figure 6.1 [138] shows the complete process to produce acetone via isopropanol dehydrogenation. This process is still under study and some optimizations have been reported recently, including a new membrane reactor [136] and new types of catalyst [111].

New approach

Low (atmosferic) pressure is preferred in the separation of acetone by distillation because it improves the relative volatility of the mixture and, since acetone is the most volatile component, enhance recovery.

The isopropanol dehydrogenation process can be improved by withdrawing a side stream from the column, removing most of the water with membranes and returning the retentate back to the column. In this way the separation (and recovery) of acetone, IPA and water will be almost 100% using only one column.

In the combined process, pervaporation membranes make use of the saturated liquid from

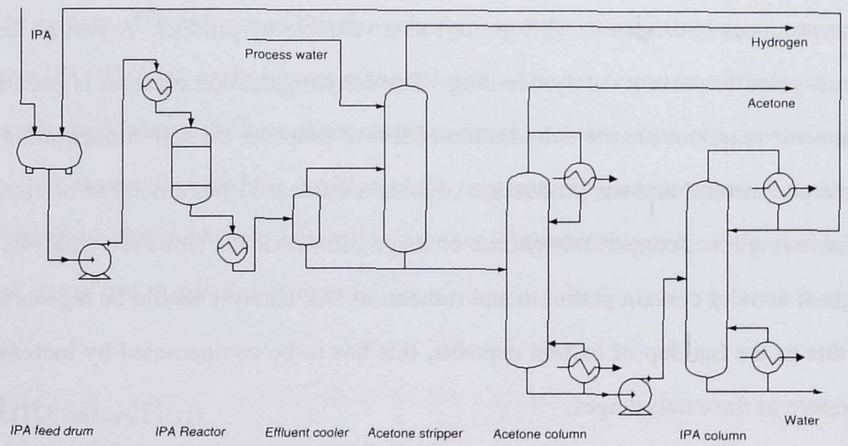


Figure 6.1: Acetone production process via isopropanol dehydrogenation

the column side stream and, for this application, in the stripping section of the column where the water driving force is larger. Sending the retentate back to the column intensifies the process, using the same column to purify the original column feed and the retentate, instead of sending the retentate to an extra column.

The combination of distillation and membranes in the acetone production process has been studied already by Kreis [62, 61]. He used capillary composite polymer membranes made with a polyethersulfone support and polyvinyl alcohol selective layer. In his work he presents a technical and economic evaluation of the combined process. However he concluded that the combined process was not economic attractive with these membranes, but he expects that the pocess will be economically feasible if the membrane separation performence can be further improved. The following section gives an overview of the membrane separation performance for acetone or IPA dehydration reported in literature.

6.1.2 Review of dehydration of acetone or IPA with membranes

Table 6.1 show the experimental fluxes reported for silica membranes for isopropanol or acetone dehydration by pervaporation. From the table it is obvious the convenience to use ceramic membranes for this application. The following paragraphs give a detailed description of what is reported in Table 6.1.

Polymer membranes (PEBA 2533) were tested by Liu [71] for the pervaporation of binary aqueous mixtures of acetone, butanol, ethanol and the quaternary mixture of these components. The hydrophobic polymer polyether-block-amine was used for their process because it was desired a membrane with high organic flux. Acetone flux increased linearly with increasing acetone concentration (1 to 5 % wt), but it was pretty low (0.001 to 0.004 $kg/h \cdot m^2$), while water flux remained constant (approximately 0.030 $kg/h \cdot m^2$) at 23 °C. When tested with a quaternary mixture, the membrane showed similar results as those obtained for binary mixtures. From an application point of view, the butanol recovery from the fermentation broth could be a niche application for the membrane. It was shown that this membrane was particularly selective to butanol (selectivity around 10), which is the primary product but at the same time slows down the fermentation process.

The pervaporative dehydration of water / organic mixtures was studied by Ray [108] using an acrylonitrile-maleic anhydride copolymer membrane at 30 °C. He obtained a total flux of 0.34 $kg/h \cdot m^2$ with a selectivity of 5.4 for acetone / water separation (10 % wt water in feed). For a mixture 85 % wt IPA, 15 % wt water, the total flux is 0.21 $kg/h \cdot m^2$ with a selectivity of 3.8. This membrane showed the best result in terms of both permeance and separation factors for the dehydration of acetone.

Silica-zirconia membranes were prepared and tested by Asaeda [4]. He worked with the pervaporation of various aqueous organic solutions (isopropanol, 1-propanol, acetone, tetrahy-

drofuran, and ethanol) at temperatures from 50 °C to their normal boiling points. The fluxes for these aqueous mixtures, with the exception of aqueous ethanol, exceded 7 $kg/h \cdot m^2$ with separation factors larger than several hundreds at 10 % wt water in the feed. Experimental fluxes at boiling point and 10 % wt water were around 8.3 and 0.2 $kg/h \cdot m^2$, for water and IPA respectively, with a selectivity around 500. Experiments with acetone (also at boiling point) showed smaller numbers at the same conditions (flux around 6.9 and 0.3 $kg/h \cdot m^2$ and selectivity of 200), may be due to the adsorptive properties of acetone on the membrane surface.

The performance of commercially available polymeric membrane (PERVAP 2510) and a microporous silica membrane (SMS), both supplied by Sulzer Chemtech GmbH, was investigated by Gallego [41]. The dehydration of binary mixtures of isopropyl alcohol / water was chosen to perform the pervaporation experiments. The range of concentrations investigated (less than 20 % wt water) was selected according to industrial needs. The effect of temperature was investigated in the 70 to 105 °C range. For the investigated conditions, water and IPA fluxes through the SMS membrane were found to be larger (1 to 20 $kg/h \cdot m^2$) than those of the polymeric PERVAP 2510 membrane (0.3 to 6 $kg/h \cdot m^2$), resulting in selectivity of maximum 100 for the SMS membrane, while for the polymeric PERVAP 2510 membrane the selectivity drecreases from 800 to 20 (1 to 18 % wt water in the feed).

Verkerk [149] studied the dehydration performance for the separation of IPA / water mixtures with ceramic membranes provided by ECN (The Netherlands) by pervaporation. For the system investigated, these membranes appear to combine high selectivities with high permeabilities. The experimental fluxes (at 5 % wt water) varied between 0.2 to 2.4 and from 0.003 to 0.018 $kg/h \cdot m^2$ (for water and IPA, respectively), resulting in a selectivity from 1500 to 2500 (for 30 and 80 °C, respectively).

Finally, Casado [18] reported experiments with IPA / water and acetone / water with a commercial silica-alumina membrane from Pervatech (The Netherlands). Here the effect of tem-

Table 6.1: Fluxes gathered from literature review for the system acetone / water or IPA / water

Mixture	Membrane	Temp. °C	x_{water}^{feed} % wt	Flux $kg/h \cdot m^2$	Selec. α	Ref.
W / IPA	Pervatech	50	10	1.5	n.a.	[18]
			20	2.5		
		70	5	2.0		
			10	3.2		
		90	10	8.1		
			20	15		
	Sulzer SMS	70	5	1.7	1800	[149]
		70	8.2	1.9	80	[41]
		90	6.9	7.9	100	
	Silica / alumina	70	5	1.0	n.a.	[23]
		80	4.5	1.86	200	[147]
	Silica / zirconia	BP	10	8.2	500	[4]
			20	16.4	200	
	Polymer	30	15	0.2	3.8	[108]
		n.a.	15	4.3	n.a.	[3]
		n.a.	15	8.9	n.a.	[2]
	Pervap 2510	70	5	3.0	100	[41]
W / Acetone	Pervatech	40	10	0.4	n.a.	[18]
			20	0.9		
		70	10	2.7		
			20	4.6		
	Sulzer SMS	40	10	0.4	n.a.	[142]
			20	0.5		
		70	10	0.5		
			20	1.2		
	Silica / alumina	50	10	0.8	180	[147]
	Silica / zirconia	BP	10	7.2	200	[4]
			20	9.3	100	
	PEBA 2533	23	95	0.14	10	[71]
	Polymer	30	10	0.34	5.4	[108]

perature was studied in the range 40 to 90 °C. It was found that for the range of conditions investigated, water fluxes were larger than those previously reported for other commercial silica membrane [142].

6.2 Model Description

The potential of ceramic membranes implemented in a distillation / pervaporation process for the removal of water can be evaluated with the help of the mathematical model of a membrane module described in the previous sections. A brief description of the model is given in the following sections.

6.2.1 Thermodynamics

The vapor-liquid equilibrium predictions by Aspen Plus were compared against the experimental data reported in Dechema vapor-liquid equilibrium data collection [42]. Figure 6.2 show the binary equilibrium IPA / water calculated with Aspen Plus and UNIFAC thermodynamic model. It is clear that the equilibrium is correctly predicted.

Figure 6.3 shows the distillation curves calculated by Aspen for the ternary mixture Acetone, IPA, Water. There are two distillation regions (**A** and **B**) separated by a boundary line that runs from pure acetone to the IPA / water azeotrope (approx. 68 % mol or 88 % wt IPA). These results are according with the ones reported in [62, 42]. Taking into consideration the binary and ternary results, simulations with Aspen Plus can be used with confidence.

As a consequence of the ternary diagram, mixtures with the composition in region **A** can never have higher IPA content at the bottom than the azeotrope. If higher IPA composition is required, the feed should have a composition in region **B** of the ternary diagram. This can be done with the use of membranes, because the membrane switches the composition profile of the

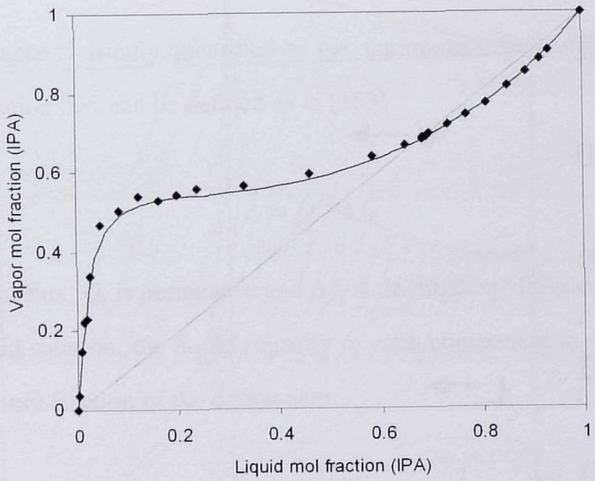


Figure 6.2: Vapor - liquid equilibrium for the system IPA / water at atmospheric pressure

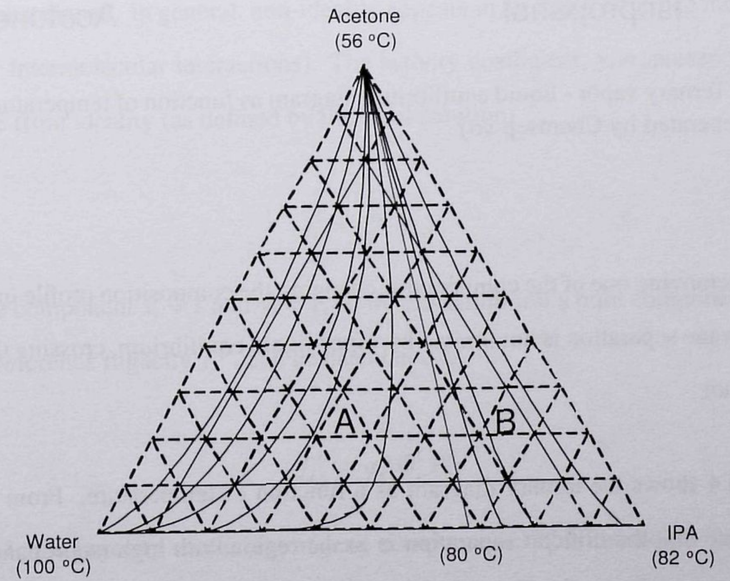


Figure 6.3: Ternary diagram for the system acetone / IPA / water

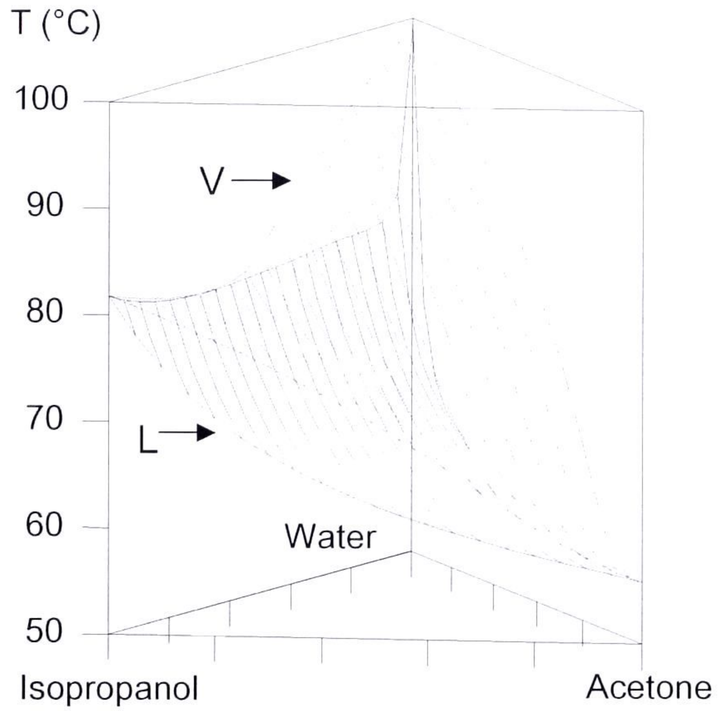


Figure 6.4: Ternary vapor - liquid equilibrium diagram as function of temperature at atmospheric pressure (generated by Chemsep v6)

column by removing one of the components, changing the composition profile in the column and, since membrane separation is not limited by vapor-liquid equilibrium, crossing the boundary line in the diagram.

Figure 6.4 shows the ternary diagram as a function of temperature. From the diagram we can appreciate that the difficult separation is in the region with high isopropanol concentration (L and V surfaces close to each other), while the acetone / water separation is quite easy. The minor boiling point azeotrope (80 °C) can also be appreciated.

6.2.2 Model Approach

Membrane performance is usually quantified by two parameters: membrane flux (J_i) and selectivity (α). Pervaporation flux can be defined as in [153]

$$J_i = Q_i \cdot \Delta f_i \tag{6.1}$$

where J_i is molar flux, Q_i is permeance and Δf_i is the fugacity difference of component i.

In an ideal liquid solution, the liquid fugacity of each component in the mixture is directly proportional to the mol fraction of the component.

$$f_i^l = f_i^{o,l} x_i \tag{6.2}$$

The ideal solution assumes that all molecules in the liquid solution are identical in size and are randomly distributed. In general, non-ideality appears in mixtures of unlike molecules (either size, shape or intermolecular interactions). The activity coefficient, γ_i, represents the deviation of the mixture from ideality (as defined by the ideal solution)

$$f_i^l = f_i^{o,l} \gamma_i x_i \tag{6.3}$$

For a pure component $x_i = 1$ and $\gamma_i = 1$, so by this definition a pure component is ideal. The liquid phase reference fugacity $f_i^{o,l}$, can be calculated as

$$f_i^{o,l} = \varphi_i^v \Theta_i^l P_i^o \tag{6.4}$$

where φ_i^v is the fugacity coefficient of pure component i, P_i^o is the liquid vapor pressure of component i and Θ_i^l is the Poynting correction for pressure. At low and moderate pressures Θ_i^l and φ_i^v are near unity, and can be ignored.

Combining equations 6.2 to 6.4 the liquid fugacity can be represented as

$$f_i^l = P_i^o x_i \gamma_i \tag{6.5}$$

and the driving force for pervaporation can be expressed as

$$\Delta f_i = \left\{ (P_i^o x_i \gamma_i)_{feed} - (P y_i)_{permeate} \right\} \tag{6.6}$$

Combining equations 6.1 and 6.6 the basic pervaporation transport equation is obtained

$$J_i = Q_i \cdot \left\{ (P_i^o \cdot \gamma_i \cdot x_i)_{feed} - (P \cdot y_i)_{permeate} \right\} \tag{6.7}$$

where P is the absolute pressure, P_i^o is the vapor pressure, γ_i is the activity coefficient, x_i the molar fraction in the feed side and y_i the molar fraction in the permeate side of component i. By selecting the driving force as defined here, the changes in permeation rate of a compound are caused mainly by the changes in temperature and composition.

Permeance is an activated process that is well described by the Arrhenius equation

$$Q_i = Q_i^o \; EXP \left\{ \frac{-E_{act,\,i}^{app}}{R} \cdot \left(\frac{1}{T_{ref}} - \frac{1}{T} \right) \right\} \tag{6.8}$$

where Q_i is the calculated membrane permeance at temparature T, Q_i^o is the membrane permeance at T_{ref}, $E_{act,\,i}^{app}$ is the apparent activation energy, T_{ref} is the reference temperature and T the system temperature. More details on the model used for simulations can be found in Chapters 3 and 4, Appendices 1 and 2 and in references [99, 96].

The model approach described above has been used by several authors [154, 30, 123, 39, 25, 11] and the results agree satisfactorily with their observations. All of them worked with binary mixtures. We believe that in the case where only one component permeates, the same model can

be used for ternary or even multicomponent mixtures. The only change is that the mixture of components will bring a different chemical potential in the mixture (which should be calculated correctly). Another difference is the interactions between membrane and the components in the mixture. Therefore a different set of parameters will be needed for every mixture, but that also is the case for two membranes even from the same manufacturer (see Chapter 4).

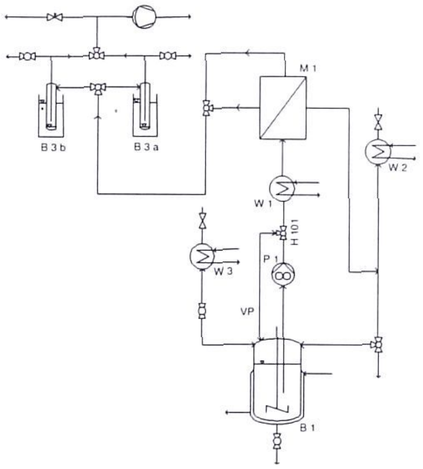
6.3 Experimental part

6.3.1 Membrane set-up

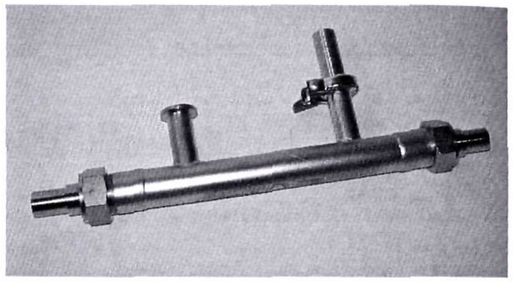
Pervaporation experiments were carried out at the Chair of Fluid Separation Processes of Dortmund University using the set-up shown in Figure 6.5(a). A detailed description of both set-up and procedure can be found in [62]. For the experiments in this study, a commercial silica / alumina membrane from Pervatech was used (see Figure 6.5(b)). The membrane tube was 25 cm long, with an inner / outer diameter of 7 / 10 mm, respectively (0.0053 m^2 membrane area). All experiments were performed at atmospheric pressure and 30 mbar permeate pressure. Temperature was varied between 60 and 78 °C and controlled with a thermal oil bath in the (jacketed) feed vessel and with an electric tracing in the module. The permeation rate was determined by weighing the permeate sample collected over a period of time. Feed and permeate samples were analyzed by gas chromatograph GC14A (Shimadzu) equipped with a FID detector. The samples were also analyzed by Karl-Fischer titration (Mettler Toledo DL31 coulometer).

6.3.2 Distillation set-up

Distillation experiments were carried out in the pilot-scale set-up present at the University of Dortmund (see Figure 6.6). Both the set-up and the procedure have been described in detail



(a) Set-up for membrane characterization



(b) Single tube module

Figure 6.5: Photo of set-up and membrane module used for experiments at Uni. Dortmund

in reference [62]. The column was packed with 33 elements of Sulzer BX (15 cm heigth). Experiments were performed at atmospheric pressure, with a natural convection reboiler (with warm oil as heating medium) and a water cooled atmospheric spiral condenser. The column has sample ports in every redistributor, where is possible to take the composition profile of the column. All samples were analyzed by the same equipment and procedure as for pervaporation experiments.

6.4 Results and Discussion

6.4.1 Pervaporation Results

Isopropanol / water pervaporation fluxes are in the range of 0.7 to 4.2 $kg/h \cdot m^2$ depending on experimental conditions (Figure 6.7(a)). They are are larger than the ones found with polymer membranes [71, 108, 62], and in the same range as those with ceramic membranes (see Table

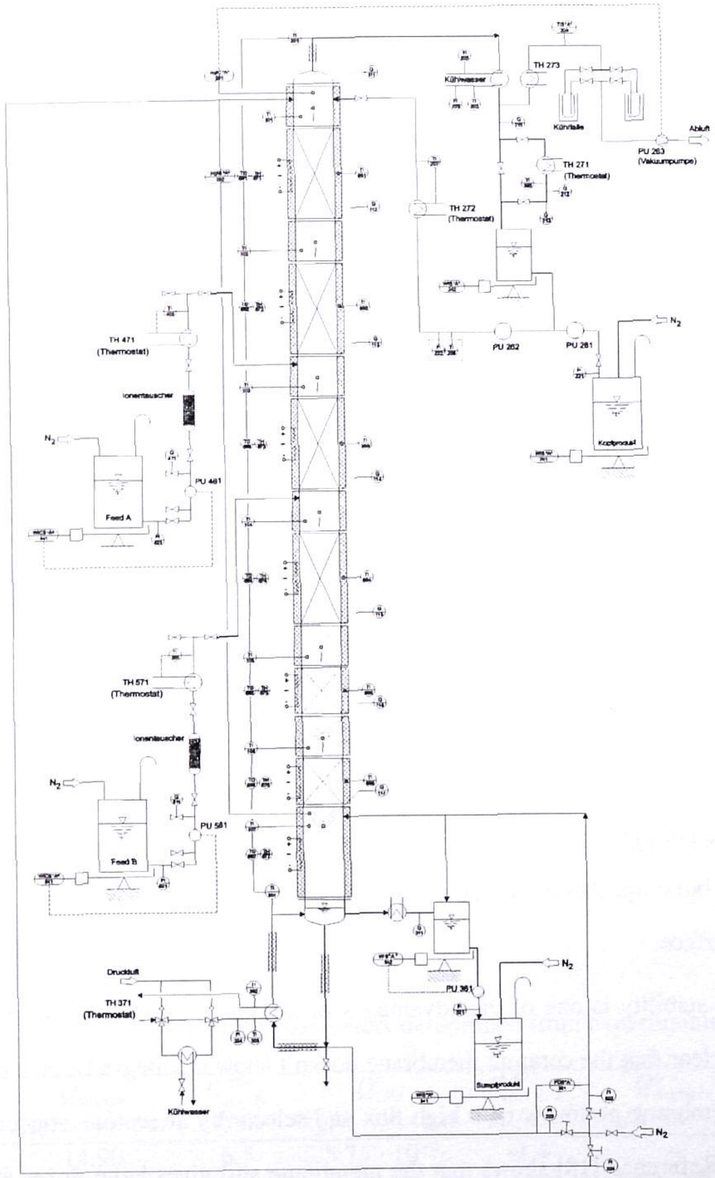
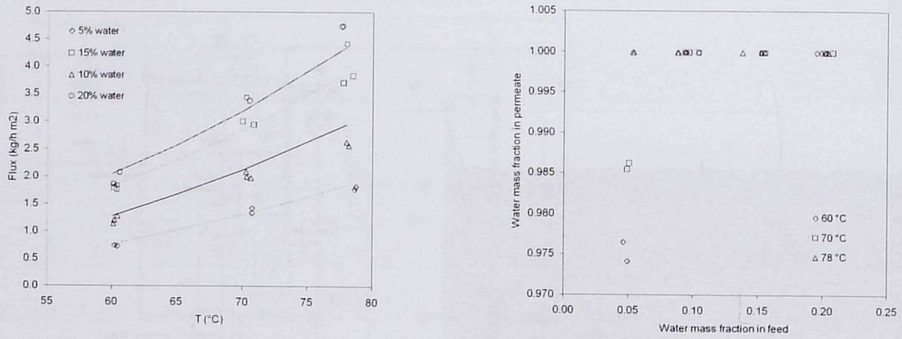


Figure 6.6: Continuos distillation set-up used for experiments (image from Uni.Dortmund)



(a) Total flux (b) Permeate composition

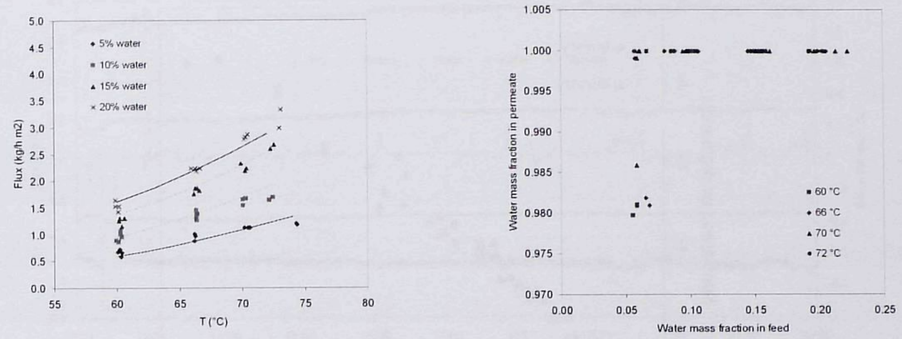
Figure 6.7: Membrane performance during experiments with IPA / water mixture

6.1), but somehow they are lower than those reported in [18] at the same conditions with a membrane from the same manufacturer. The separation is almost absolute as can be seen in Figure 6.7(b).

Pervaporation fluxes for ternary system acetone / IPA / water are smaller than for binary mixture (Figure 6.8(a)). The separation remains excellent (see Figure 6.8(b)). It is possible that acetone has a stronger interaction with the membrane wall than IPA, due to the double-bonded oxygen of the ketone group. The carbonyl groups interact stronger with polar molecules by hydrogen bonding, therefore might be preferentially adsorbed, blocking some pores at the membrane surface.

Chemical stability is one of the advantages of inorganic materials towards polymer membranes. It is clear that the ceramic membrane doesn't show any degradation caused by the acetone. The membrane performs with high flux and selectivity at acetone concentrations as high as 20 % wt. Reference [18] shows that the membrane still gives large fluxes at higher acetone composition without afecting selectivity.

Model parameters were retrieved from the experimental results for binary and ternary exper-



(a) Total flux (b) Permeate composition

Figure 6.8: Membrane performance during experiments with ternary mixture

iments (see Table 6.2). The values in Table 6.2 confirm that there is a strong interaction between the membrane and acetone as stated previously. The presence of acetone in the mixture not only causes a decrease in the apparent activation energy of water and IPA, but also on the reference permeance, with a reduction in flux as a consequence.

The predictions of the model are shown as continuous lines in Figures 6.7(a) and 6.8(a). Figure 6.9 shows the comparison experimental against calculated flux for all experiments. It is clear that most of the simulated results are predicted within 5% of the experimental value (dotted lines).

Table 6.2: Membrane parameters determined from experiments

Mixture	Q^o_{Water} $kg/h \cdot m^2 \cdot bar$	$E^{app}_{act,\,W}$ kJ/mol	Q^o_{IPA} $kg/h \cdot m^2 \cdot bar$	$E^{app}_{act,\,IPA}$ kJ/mol	$Q^o_{Acetone}$ $kg/h \cdot m^2 \cdot bar$	$E^{app}_{act,\,A}$ kJ/mol
Binary	14.90	6.5	$5.75 \cdot 10^{-4}$	-1.4	–	–
Ternary	11.73	1.5	$2.54 \cdot 10^{-4}$	-13.0	$2.84 \cdot 10^{-4}$	-34.8

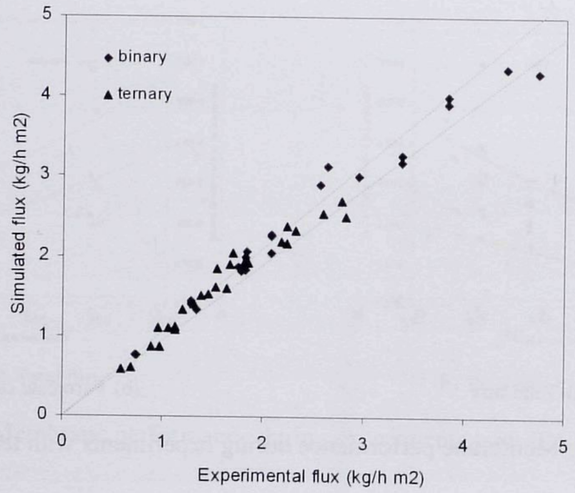


Figure 6.9: Experimental against calculated fluxes with parameters from Table 6.2

6.4.2 Distillation Results

Distillation experiments with the mixture acetone / IPA / water were performed until steady state was reached. The steady state condition was assumed when the mass balance, composition and temperature at the top and bottom were equal for at least two consecutive hours. Experiments were performed with feed flow, feed composition and reflux ratio known. Samples were taken at steady state at different column heights to determine the column profile. Operation conditions for one experiment can be seen in Figure 6.10. The column was very delicate during operation and any disturbance was immediately reflected in the column operation, for instance sampling time can be noticed in in Figure 6.10 at 16, 18, 19:30 and 21 hours.

Distillation experiments were simulated in Aspen Plus according with the experimental observations. The column feed was 1.993 kg/h at boiling point with a composition of 8.57 IPA, 78.65 acetone and 12.78 water (all in % wt). The column was simulated with 30 stages, feed on

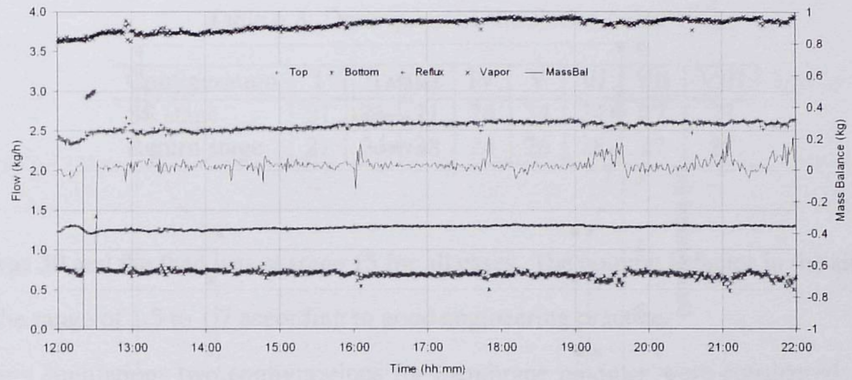


Figure 6.10: Mass balance and flows during distillation experiments

stage 15, a total condenser and a kettle reboiler, the distillate rate was 1.31 kg/h and the (mass) reflux ratio was 2. An atmospheric condenser was used and the column pressure drop was 0.003 bar. The experimental and simulated composition profiles are shown in Figure 6.11.

6.5 Process Simulation

The simulated process is the separation section of the acetone production via catalytic dehydration of isopropanol described in section 6.1.1. The simulated hybrid process is shown in Figure 6.12 and the description of the simulation study is given in what follows.

6.5.1 Process Specifications

The column feed stream was 2290 kg/h with a composition of 77.5 % wt acetone, 8.4 % wt IPA and 14.1 % wt water. The feed was at atmospheric pressure and at boiling point. It was desired to recover more than 99% of the acetone and, with the help of membranes, remove the amount of water to have a maximum water concentration at the bottom of 5 % wt. The number of column

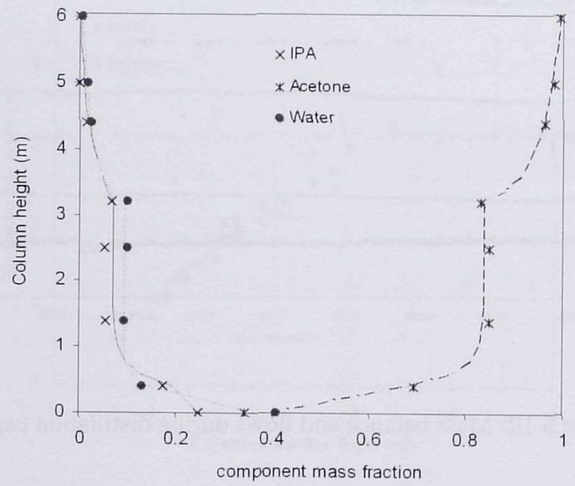


Figure 6.11: Experimental and simulated column profiles

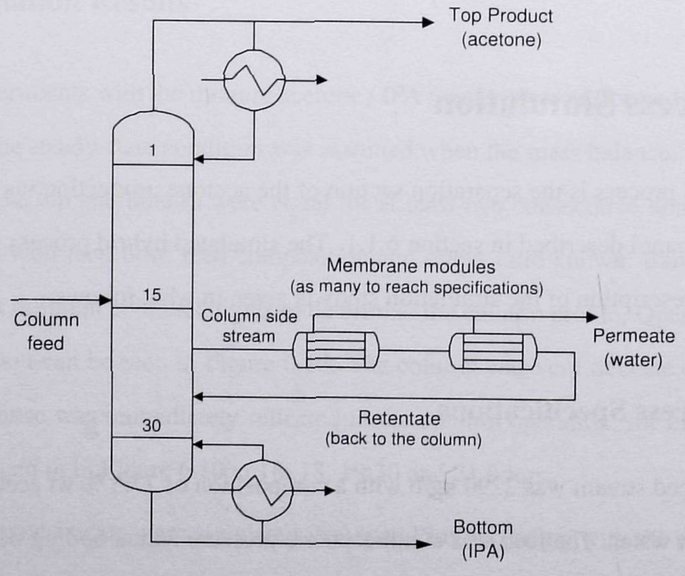


Figure 6.12: Flow scheme for process simulation

Table 6.3: Description of simulation cases

Configuration	I	II	III	IV	V	VI	VII	VIII
SS stage	21	21	21	24	24	24	27	27
Return stage	21	24	28	24	26	28	27	28

stages was 30 and the feed was at stage 15 for all cases. The column F-factor in the simulations was in the range of 1.5 to 1.7 according to good engineering practice.

During simulations two configurations for membrane modules were considered: 25 or 20 tube modules of one meter length (0.55 and 0.44 m^2 membrane area, respectively). Reynolds number in the range of 10,000 to 12,000 was achieved arranging membrane modules in parallel, trying to minimize concentration polarization.

The first studies were performed considering ideal membrane units (without pressure drop, neither concentration nor temperature polarization effects). Only the most feasible cases were simulated as real membrane modules.

A sensitivity study was carried out in order to find out the best process conditions for this process. The studied variables were

- Side stream stage,
- Retentate location (return stream),
- Side stream flow, and
- Reboiler heat duty.

In order to reduce the number of simulations, the column side streams were chosen at stages 21, 24 and 27. The return stages (retentate) for each case are shown in Table 6.3.

6.5.2 Simulations with ideal modules

While simulating, two operating limits for the column were found out:

1. The flow of the column side stream shouldn't be larger than the internal liquid stream of the column, and

2. The amount of water present in the side stream should be enough that if all water is removed from the side stream, the water concentration in the bottom of the column complies with the product specifications.

Removing water from the column, results in a change of internal streams which causes a shift of vapor - liquid equilibrium inside the column resulting in a column profile that differs from that of the stand alone column. This can be clearly seen in Figure 6.13 where the different column profiles are compared as function of membrane area for configuration III (100% is the area required to achieve product specifications).

Figure 6.14 shows the different column profiles for the configurations shown in Table 6.3 with reboiler heat duty of 2 MW (results with the smallest membrane area for each configuration). The column profile is similar for simulations with the same configuration and reboiler duty regardless the side stream flow.

Looking at the simulation results, some similarities in the results are displayed depending on the return stream stage. Accordingly, the different configurations can be grouped in three general cases:

1. Side and return streams in the same stage (configurations I, IV and VII),

2. Return stream at the middle of the stripping section (configurations II and V) and

3. Return stream at the bottom of the column (configurations III, VI and VIII).

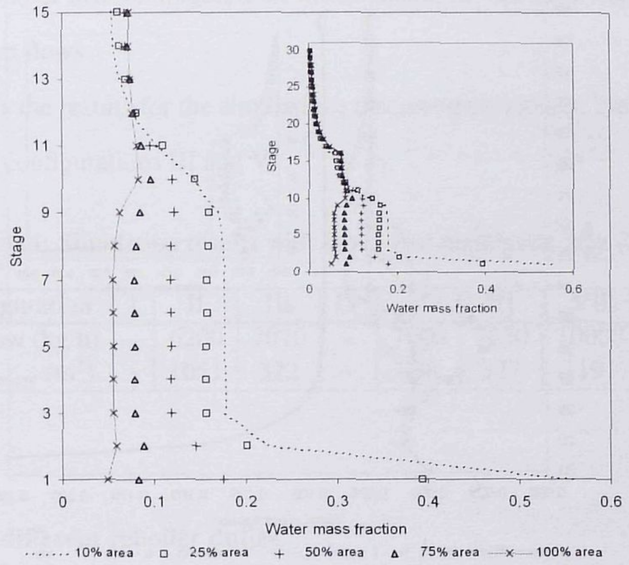


Figure 6.13: Change in column composition profile as function of installed membrane area

Simulations with side- and return streams in the same stage

Simulations were especially difficult for the cases with side and return streams in the same stage (configurations I, IV and VII). From all these, only configuration VII was successful to meet process specifications. The reason is that returning the liquid in the same stage that was taken reduces the water concentration in the side stream. The more water is removed, the lowest concentration in the feed, making the separation more difficult for membranes (more area is required). For configurations I and IV the limit case was reached, when even taking all column liquid stream, there was not enough water to reach specifications (operating limits 1 and 2 together). From simulations appears that withdrawing the side stream and returning the retentate in the same stage results in the largest membrane area needed for the combined process (around 1200 m^2 for configuration VII). However after the analysis of results it was discovered that plac-

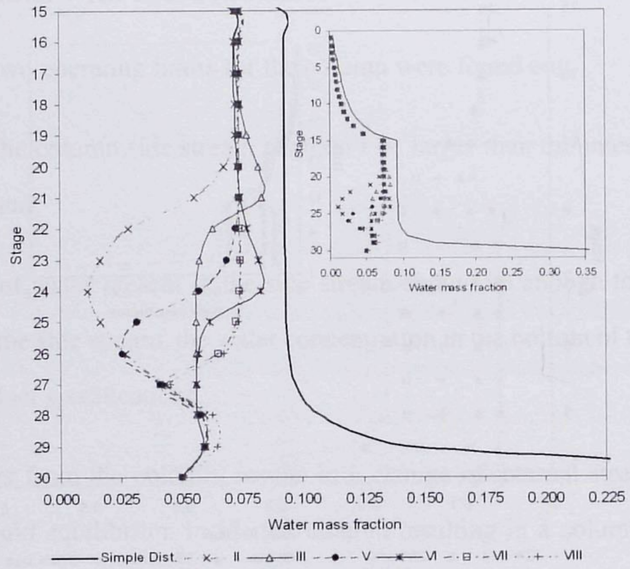


Figure 6.14: Change in column composition profile with different configurations

ing the side stream on stage n and the retentate stream on the stage below might give better results and smaller areas than in the case with side- and return streams in the same stage.

Simulations with return stream at the middle of stripping section

These configurations didn't show specific prblems as the previously described simulations. The water concentration in the side stream is larger, therefore the the flux is larger than for the previous case. However the required membrane areas are still large (1051 and 838 m^2 for configurations II and V respectively).

Simulations with return stream at the bottom of the column

The best results regarding least membrane area were obtained for the cases where the side stream flow is withdrawn from stage 21 or 24 and returning the retentate stream at the bottom (config-

urations III and VI). For these configurations membrane areas obtained were around 300 m^2 for different side stream flows.

Table 6.4 shows the results for the simulations discussed previously. Next section will show a detailed study of configurations III and VI.

Table 6.4: Simulation results with the lowest membrane area (2 MW)

Configuration	I	II	III	IV	V	VI	VII	VII
SS flow (kg/h)	–	6200	7070	–	7000	7050	10000	7000
$A_{membrane}$ (m^2)	–	1051	322	–	838	327	1191	1273

Simulations with different reboiler duties

Simulations were carried out varying side stream flow and reboiler heat duty. The results (membrane area) of the simulations at the same conditions are pretty similar for both configurations (the difference in area is around 5%).

For the same reboiler duty, membrane area is decreasing when side stream flow increases. The reason is that increasing side stream flow, more liquid stream is treated and the water content of the stream is less affected by depletion, which results in higher driving force.

The internal streams of the distillation column changes with reboiler heat duty. In order to compare the cases with different heat duty on the same basis, it is important to define a dimensionless number Φ (defined as the ratio of the side stream flow to the liquid flow of the stage above the side stream) that indicates the fraction of liquid withdrawn from the stage compared to the liquid available in the tray. Table 6.5 shows that for simulations with similar Φ number the area required increases when reboiler duty decreases. Figure 6.15 is a 3-D representation of how membrane area is affected with side stream flow and reboiler heat duty for configuration III. Detailed studies with real modules and reboiler heat duty of 2 and 1.6 MW are carried out in the

Table 6.5: Simulation results for ideal modules

Case	A	B	C	D	E	F	G	H
Reb. duty (MW)	2	2	2	1.6	1.6	1.6	1.2	1.2
Configuration III								
Φ (-)	0.60	0.86	0.94	0.62	0.87	0.96	0.90	0.94
Memb. area (m^2)	376	332	322	525	401	387	450	439
Configuration VI								
Φ (-)	0.60	0.87	0.94	0.62	0.87	0.96	0.94	0.99
Memb. area (m^2)	398	332	327	600	392	389	451	443

next section.

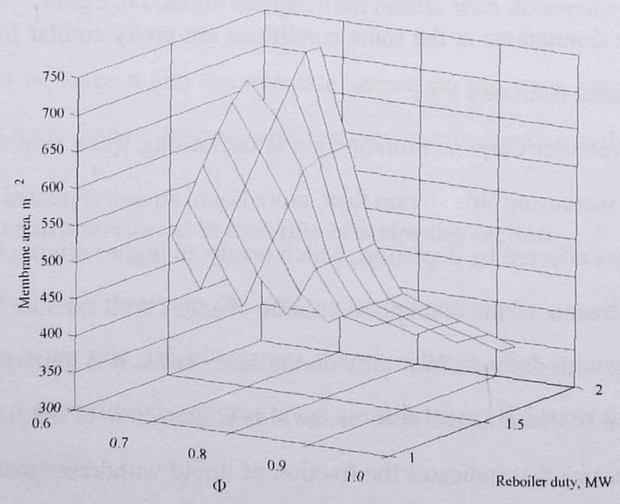


Figure 6.15: Membrane area as function of Φ ratio and reboiler duty for ideal modules

6.5.3 Simulations with real modules

The previous simulation results showed the performance of membrane modules with ideal conditions (pressure drop, concentration and temperature polarization neglected). In this section all those effects are accounted during calculations.

For the present simulations the temperature was not allowed to drop lower than 60 °C and several heaters were placed after certain number of membrane modules to increase temperature back to 63 °C, a uniform flux is ensured in this way.

Concentration polarization was minimized by having a fully turbulent stream in the retentate side (Re between 10,000 and 12,000). Unfortunately turbulence is coupled to pressure drop and the length of tubes helps to increase pressure drop even more. Intermediate pumps were used to have a maximum pressure inside the tubes of 1.1 bar.

Table 6.6 shows the results for real membrane modules and they include the extra utilities required to keep operation as close as possible to ideal conditions. Figure 6.16 presents the performance of a real module for configuration III.c. It shows the flux and water composition as function of installed area. It is clear that though there are some fluctuations in pressure and temperature, the flux is rather constant.

The best way to identify the best configuration for the hybrid process is to perform an economic evaliation taking into consideration the previous results. The description of the economic evaluation is given in the following section.

6.6 Economic evaluation

The evaluated processes are the separation section of the acetone production via catalytic dehydration of isopropanol (as described in [138]) and compared with the combined distillation / membrane process. The industrial scale separation task is defined as follows: a production of

Table 6.6: Simulation results for real modules

Case	a	b	c	d	e	f
Reboiler duty (MW)	2	2	2	1.6	1.6	1.6
Configuration III						
Φ (-)	0.60	0.75	0.87	0.60	0.75	0.91
$A_{membrane}$ (m^2)	340	336	340	365	364	343
Perm. cooling (MW)	0.20	0.22	0.22	0.21	0.21	0.21
Interstage heat. (MW)	0.23	0.24	0.25	0.23	0.23	0.24
Configuration VI						
Φ (-)	0.61	0.76	0.89	0.60	0.76	0.90
$A_{membrane}$ (m^2)	348	343	339	379	355	354
Perm. cooling (MW)	0.21	0.21	0.22	0.21	0.21	0.21
Interstage heat. (MW)	0.23	0.24	0.25	0.23	0.23	0.24

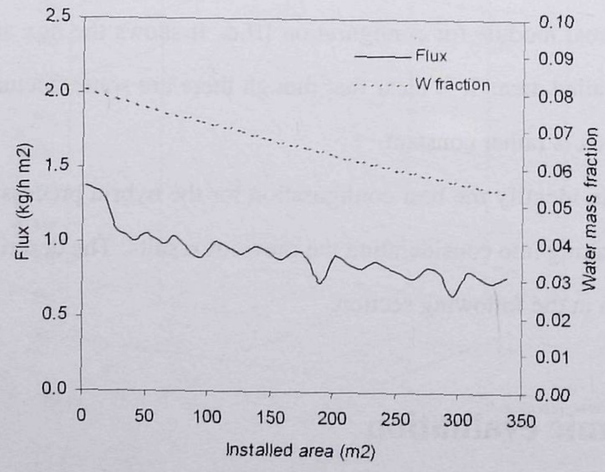


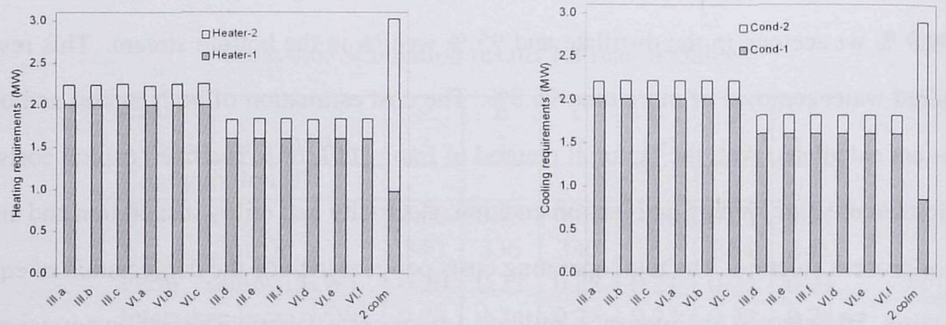
Figure 6.16: Membrane flux and water composition profile for configuration III.c

14,200 tonnes acetone per year with 8000 h of operation per year, with a minimum composition of 99.9 % wt acetone in the distillate and 95 % wt IPA in the bottom stream. This results in a required water removal of more than 96.8%. The cost estimation of both capital and operating costs are calculated with the factorial method of Lang [117, 66]. The fixed capital costs include equipment erection, piping and instrumentation, electricity and utility installation and any building or process stucture. The total operating costs per year include the depreciation of equipment (10 years, 5% interest), maintenance, utilities, labour costs, laboratory costs, supervision, manufacturing and production overheads, insurance, taxes and royalties. Table 6.7 presents the cost of the utilities used in the present evaluation. The price of the equipment was obtained from DACE price booklet [86]. An optimistic membrane lifetime of 5 years was considered in this study. Membrane installation cost was estimated as 50% of the membrane cost. The economic analysis of the hybrid membrane process is conducted for the cases in section 6.5.3.

Table 6.7: Data used for economic evaluation

	Unit	Price	Remarks
Low pressure steam	Euro/tonn	20	2 bar, T_{ini}=120 °C
Cooling water	Euro/m^3	0.05	ΔT_{max}=15 °C, T_{ini}=25 °C
Electricity	kWh	0.10	–
Membrane	Euro/m^2	2000	Installation not included

Figure 6.17 shows the utilities required for every option. In Figure 6.17(a) "Heater-1" is the column reboiler for the hybrid and conventional processes. "Heater-2" is the heat duty of the intermediate heat exchangers for the hybrid process, while for the conventional process is the reboiler heat duty of the second column. In Figure 6.17(b), "Cond-1" is the column condenser for the hybrid and conventional processes. "Cond-2" is the heat duty of the permeate condenser for the hybrid process, while for the conventional process is the condenser heat duty of the second column. It is clear that the conventional process make use of more heating and cooling



(a) Heating requirements (b) Cooling requirements

Figure 6.17: Utility requirements for the studied configurations and 2-column process

utilities than any of the studied options. This will have an impact on the annual costs.

Figure 6.18 shows the area required for every configuration. As the cases were already screened, we see that the difference is not so large among them (they are between 330 and 380 m^2), thus the difference in investment and annual cost is not large for the different options. The minimal required membrane area for the given separation task is found in the region of high heat duties and large side stream flows.

The investment costs (including installation) are depicted in Figure 6.19. The investment cost of the two-column process is almost the same to the hybrid process in the present study. On the other hand, it is evident that the major contribution to the investment cost of the hybrid process is the membrane. The extra heaters and permeate condensers are accounted under "Other".

Looking at the annual costs (Figure 6.20) some interesting results turn up. Comparing the membrane with the conventional process, all the studied options are cheaper, but the difference is not so big. The lower cost of the hybrid process is localized in the region of intermediate heat duties and large side stream flows. For "Column capital" is considered the 15% of the investment cost for columns and heat exchangers, whereas for "Memb.capital" 30% is considered. "Other"

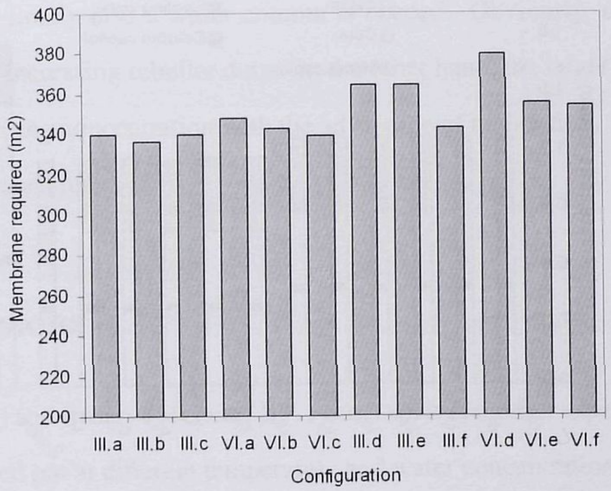


Figure 6.18: Membrane area required for the studied configurations

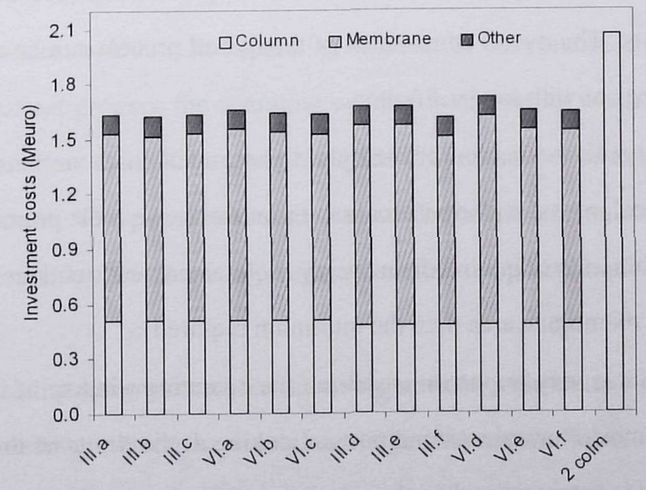


Figure 6.19: Investment cost for the studied configurations (including installation)

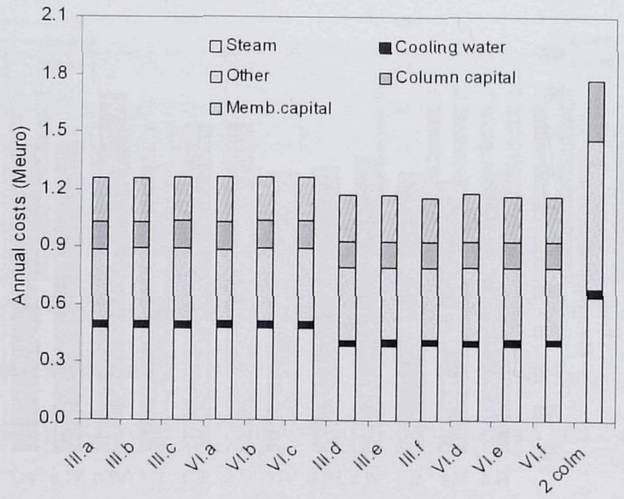


Figure 6.20: Annual costs calculated for the studied configurations

includes insurance, taxes and royalties, labor and project supervision costs, miscellaneous materials, lab costs and plant overheads. It is clear that membrane capital costs have a huge impact of the annual costs. The overal annual cost of the hybrid process can be more convenient with cheaper membranes or with longer lifetime.

From the economic evaluation of the hybrid process all cases are feasible to compete with the current (two-column) distillation process. From them, the most promising is configuration III.f due to a combination of intermediate energy requirement and small membrane area (approximately 5% more membrane area than the minimum required).

Summarizing, it is very important to delimit the operating window of the combined process to operate at the most convenient conditions. Looking at the limits of the current process the operating window is narrowing when the reboiler duty decreases. Knowing the amount of side stream that can be withdrawn from the column is important because less area is needed with a larger side stream according with the simulation results. Increasing reboiler heat duty means more reflux, making column internal streams larger, thus equipment should be bigger to handle larger capacity and finally also a wider column is needed. Obviously, the amount of utilities used increase when increasing reboiler duty. On the other hand, the larger the side stream is, the higher the water starting concentration with the advantage of higher flux. This brings the benefit of a smaller membrane area.

6.7 Conclusions

Binary (IPA / water) and ternary (acetone / IPA / water) pervaporation experiments at atmospheric pressure were carried out at different temperature and water concentration. Experiments showed that the flux increase with temperature and and water concentration while not suffering from the high IPA or acetone concentrations. This is a good indication for the industrial implementation of such membranes. From characterization experiments, model parameters were retrieved and used to simulate the performance of pervaporation modules coupled to a distillation column.

It is very important to delimit the operating window of the combined process. Looking at the limits of the current process, the operating window is narrowing when the reboiler duty decreases. This is important to know the amount of side stream that can be tapped from the column to feed the membrane. The parametric study shows the best characteristics for the combined process regarding reboiler heat duty, side stream flow and the position of the feed and retentate streams.

The most promising options found are the configurations with return stream at the bottom of the column, intermediate reboiler heat duty and large side stream flows. These configurations are convenient due to a combination of lower energy requirement and they use just a few percent more membrane area than the minimum required.

If the conditions of the hybrid process improve along with new membranes with high flux,

increased lifetime and lower membrane costs, hybrid processes will become a very attractive alternative for this or any other dewatering task.

Chapter 7

Experimental and module-scale comparison of pervaporation and vapor permeation

Pervaporation (PV) and vapor permeation (VP) through ceramic membranes are compared experimentally at lab-scale and with computer simulations. At saturation conditions up to 155 °C pure methanol fluxes through a tubular methylated silica membrane appeared to be equal for both pervaporation and vapor permeation. Also the separation of mixtures containing 18% wt methanol in the liquid feed (PV) and 21.1 to 24.8% wt in the vapor feed (VP) resulted in comparable methanol fluxes at equal driving force. From simulations it appeared that the choice for either pervaporation or vapor permeation as operation mode is on the one hand mainly imposed by hydrodynamics, resulting in different designs of module sequences. The choice for PV or VP as operation mode also depends on different operational aspects that may affect further separation units and this is different for each operation mode.

7.1 Introduction

The combination of distillation with membranes is an elegant method to increase overall efficiency and reduce energy consumption within processes containing azeotropic mixtures. For the bulk separation of hydrocarbon mixtures, either pervaporation (PV) or vapor permeation (VP) can be considered. The aim of this chapter is to compare pervaporation and vapor permeation at molecular and module level. Pure methanol pervaporation and vapor permeation will be compared up to 155 °C. Separation of pure methanol and mixtures of methanol in MTBE is compared for pervaporation and vapor permeation at above atmospheric conditions up to 140 °C using a methylated silica membrane. These experimental data are used to simulate module performance in order to determine the advantages and disadvantages of pervaporation and vapor permeation at module scale.

7.1.1 MTBE process

Separation is a very important step in the chemical production process, which makes use of different separation techniques like distillation, absorption and extraction among others. Membranes in industrial separation technology are rather new, however over the last three decades membrane separation has gained recognition as an important separation method and nowadays membrane processes are used in a wide range of applications. Until now pervaporation and vapor permeation have been used mainly for solvent dehydration, but recently reserachers are also using them every time more to organic / organic separation. A major drawback of polymeric membranes for pervaporation is their limited solvent and temperature stability. In this respect inorganic membranes are preferetially used, because thanks to their thermal and chemical stability that withstand better mixtures with organic components. Besides they show higher fluxes than their polymer counterparts. The large amount of literature concerning the separations of organic / organic mixtures [125, 22, 50, 43, 156, 88, 57, 79, 78, 120] show that there is a lot of interest to develop new methods to separate these mixtures cheaper more efficiently. The separation of methanol (MeOH) and methyl tert-butyl ether (MTBE) is a good example. MTBE has outstanding qualities as a high-octane fuel component. It is produced by the acid-catalysed reaction of methanol with isobutene [140]. In equimolar amounts 92% conversion at 60 °C can be achieved. An excess of methanol increases the conversion and also suppresses dimerisation and oligomerisation. Unfortunately this excess methanol remains in the MTBE product. The MTBE can't be fully recovered by distillation because methanol and MTBE form a minimum boiling azeotrope (51.6 °C) with composition 14 % wt methanol and 86 % wt MTBE at atmospheric pressure. Several papers show the advantage of combining pervaporation or vapor permeation with distillation for this process [50, 43, 44, 146], but no one has compared the combined processes with each other.

7.1.2 Comparison pervaporation / vapor permeation in literature

Will and Lichtenthaler [155] compared the two processes for binary alcohol / water systems as well as other binary and ternary aqueous systems and the 1-propanol / methanol system. At different ratios between the feed pressure and the saturated pressure, vapor permeation fluxes were by far smaller than pervaporation fluxes at equal feed concentration (in % wt). The small vapor permeation flux was attributed to different interactions between the solvent and the membrane in the vapor phase compared to the liquid phase. No comparison was presented at equal driving force or partial pressure difference over the membrane. Also the pure water fluxes cannot be interpreted as such, since only the pervaporation flux was modeled and during vapor permeation the vapor was not at dew or bubble point but slightly superheated. Selectivities found in this study were higher for vapor permeation.

Okamoto et al. [91] compared different types of polyimide membranes for the separation of ethanol / water mixtures. Differences between pervaporation and vapor permeation were found to be large for membranes having a higher total sorption in the liquid phase and small for poylimide membranes having a lower sorption.

Schehlmann et al. [114] focused on the influence of the feed density on the fluxes and they found for vapor permeation smaller fluxes and higher selectivities compared to pervaporation. These differences were attributed to differences in mass transfer kinetics in the vapor and liquid but this was not further studied.

Hamada et. al. [48] studied pervaporation and vapor permeation using three different polymeric membranes. It was concluded that differences between pervaporation and vapor permeation for the separation of water from 2-propanol could be attributed to the differences in solubility behavior of the components from the liquid respectively the vapor phase.

Uchityl and Petričkovič [104] compared pervaporation and vapor pervaporation of 1- and 2-propanol in a polyethylene membrane at 20 °C. Near saturated vapor conditions, sorption from vapor or liquid phase as well as vapor permeation and pervaporation fluxes appeared to be equal. Nevertheless, sorption from a liquid into a polymer was believed to be faster than sorption from a vapor, resulting in a slightly higher flux for pervaporation. Fialová et. al. [36] worked on the same system and with the same membrane under different experimental conditions (membrane thickness, feed concentration and temperature). She observed that the diffusion coefficients of 1-propanol were concentration independent and have an Arrhenius behavior for both pervaporation and vapor permeation. However pervaporation fluxes were higher than the vapor permeation ones and the difference between both fluxes became more considerable with increasing temperature. She concluded that this result could be explained by the the role of boundary layer during permeation.

Ribeiro et. al. [109] compared vapor permeation and pervaporation with a polydimethylsiloxane (PDMS) hollow-fibre module and diluted ethyl acetate aqueous solutions for an aroma recovery process. He expressed the fluxes as a function of the fugacities differences across the membrane for ethyl acetate. In both processes, the flux increased linearly with the ester fugacity in the feed stream. Moreover, for a given fugacity, no difference in fluxes was observed between the two membrane processes. This outcome is in perfect agreement with theoretical expectations. Since the difference between pervaporation and vapor permeation lies in the physical state of the feed stream, these processes must exhibit the same results when applied to a liquid solution and to the vapor at equilibrium with it. The equality of chemical potentials for each species in both phases constitutes the thermodynamical criterion of phase equilibrium, hence, the driving force for mass transfer (difference in chemical potentials of every component in the feed and permeate side) is equal in both processes.

Sommer and Melin [123] report on both pervaporation and vapor permeation using a tubular silica membrane. However no structural analysis of the difference between both processes was presented.

7.2 Model description

7.2.1 Driving force

The fugacity gradient is the driving force for both pervaporation and vapor permeation at molecular level. Thie way fugacity is approximated in liquid and vapor phase is different, bringing two different ways of calculating the driving force for pervaporation and vapor permeation.

The vapor fugacity in a real mixture is the effective partial pressure

$$f_i^v = \varphi_i^v \, y_i \, P \tag{7.1}$$

where the correction factor φ_i^v is the fugacity coefficient, P is the absolute pressure and y_i the molar fraction of component i. For a vapor at moderate pressures, φ_i^v is close to unity. Accordingly, for vapor permeation, the driving force can be expressed as the partial pressure difference

$$\Delta f_i^{VP} = \left\{(Py_i)_{feed} - (Py_i)_{permeate}\right\} \tag{7.2}$$

For pervaporation it is different, since the feed side is a liquid. In an ideal liquid solution, the liquid fugacity of each component in the mixture is directly proportional to the mol fraction of the component.

$$f_i^l = f_i^{o,l} x_i \tag{7.3}$$

The ideal solution assumes that all molecules in the liquid solution are identical in size and are randomly distributed. In general, non-ideality appears in mixtures of unlike molecules (either size, shape or intermolecular interactions). The activity coefficient, γ_i, represents the deviation of the mixture from ideality (as defined by the ideal solution):

$$f_i^l = f_i^{o,l}\, \gamma_i\, x_i \tag{7.4}$$

For a pure component $x_i = 1$ and $\gamma_i = 1$, so by this definition a pure component is ideal. The liquid phase reference fugacity $f_i^{o,l}$, can be calculated as

$$f_i^{o,l} = \varphi_i^v\, \Theta_i^l\, P_i^o \tag{7.5}$$

where φ_i^v is the fugacity coefficient of pure component i, P_i^o is the liquid vapor pressure of component i and Θ_i^l is the Poynting correction for pressure. At low and moderate pressures Θ_i^l

and φ_i^v are near unity, and can be ignored.

Combining equations 7.3 to 7.5 the liquid fugacity can be represented as

$$f_i^l = P_i^o x_i \gamma_i \tag{7.6}$$

and the driving force for pervaporation can be expressed as

$$\Delta f_i^{PV} = \left\{(P_i^o x_i \gamma_i)_{feed} - (Py_i)_{permeate}\right\} \tag{7.7}$$

When the fugacity difference is used as driving force, fluxes can be modeled using [25]

$$J_i = Q_i^o\, exp\left(\frac{-E_i}{RT}\right)\Delta f_i = Q_i\, \Delta f_i \tag{7.8}$$

For simulation of membrane transport at large scale, the following working expression is used [123]

$$J_i = Q_i\, \Delta f_i = Q_i^o\, exp\left\{\frac{-E_i}{R}\left(\frac{1}{T_0} - \frac{1}{T}\right)\right\}\Delta f_i \tag{7.9}$$

where $Q_{i,0}$ and E_i are derived from experimental data. The apparent activation energy (E_i) is a term that lumps and simplifies the adsorption and diffusion terms of the simplified Maxwell-Stefan equation (see Appendix 1).

The overall mass transfer resistance model is thoroughly described and discussed in Chapter 3 and will not be repeated in this section.

7.3 Experimental section

7.3.1 Set-up and procedure

The set-up used for conducting pervaporation and vapor permeation experiments at bubble point was purchased from Sulzer Chemtech. The maximum design operation pressure and temperature are respectively 16 barg and 200 °C. The pervaporation and vapor permeation operation modes of the set-up and the description of the experimental work are detailed in reference [25] and out of the scope of this work. Feed and permeate samples were analyzed using gas chromatograph (Chrompack CP9002).

7.3.2 Membranes and conditions

Two methylated silica membranes were supplied by the Energy research Center of the Netherlands (ECN). Both supported tubular membranes with an outer diameter of 14 mm, 2 mm thick and lengths of 12.9 and 13.6 cm, respectively. The mean pore diameter and thickness of each layer are depicted in Table 7.1. More information on the morphology of this membrane can be found in [25].

Table 7.1: Membrane tube characteristics

Layer	Material	Thickness	Pore size
Substrate	α-alumina	2 mm	3.4 μm
1	α-alumina	40 μm	0.16 μm
2	α-alumina	40 μm	0.16 μm
3	γ-alumina	1.75 μm	4.5 nm
4 (outside tube)	methylated silica	100 nm	n.a.

The conditions for the experimental series are presented in Table 7.2. Pure methanol pervaporation was done at saturation conditions at temperatures up to 155 °C with membrane M3

Table 7.2: Experimental conditions

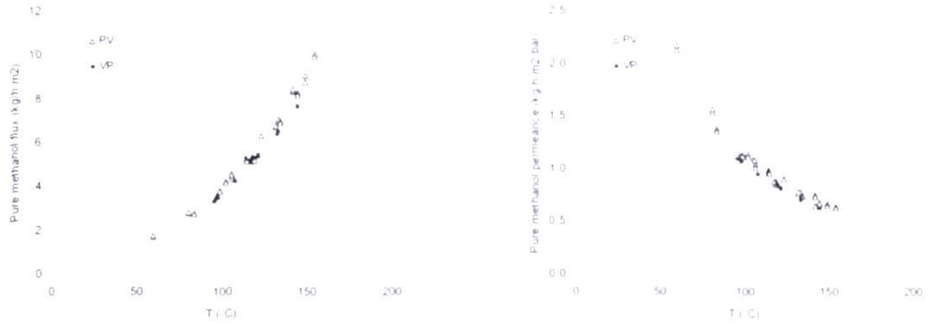
exper. series	memb. #	PV or VP	$MeOH_{feed}$ % wt	T range °C	P perm mbar
I	M3	PV	100	60-155	8-12
II	M3	VP	100	96-145	8
III	M3	PV	8.6-14.4	80-140	10
IV	M4	PV	17.7-18.4	80-139	9
V	M4	PV	17.2-18.0	79-138	108
VI	M4	VP	19.0-22.2	77-130	10

(series I) for comparison with vapor permeation at saturation conditions from 96 to 145 °C (series II). Separation of methanol from MTBE by pervaporation was carried out with both membranes. Membrane M3 was tested in series III at temperatures from 80 to 140 °C without the addition of make-up feed. As a result, during these tests the feed side concentration of methanol decreased from 14.4 at the begining to 8.6 % wt at the end of the experiment. Feed side concentration of methanol was kept constant at about 18 % wt during pervaporation with a permeate pressure of 9 mbar in series IV and 108 mbar in series V, with temperature varying between about 80 and 140 °C for both series. Separation of a mixture containing 19.0 to 22.0 % wt methanol was done by vapor permeation in series III and VI at temperatures between 77 and 130 °C with a permeate pressure of 10 mbar.

7.4 Results and discussion

7.4.1 PV and PV for pure methanol

Figure 7.1(a) presents the pure methanol fluxes for pervaporation and vapor permeation versus temperature. The fluxes for vapor permeation coincide with those for pervaporation, implying that pervaporation and vapor permeation at saturation conditions result in identical transport



(a) Methanol PV and VP fluxes (b) Pure methanol PV and VP permeances

Figure 7.1: Pure methanol experiments as function of temperature for pervaporation and vapor permeation

through the membrane. It is clear that pervaporation and vapor permeation fluxes are equal and therefore their respectives permeances and activation energies are the same.

Figure 7.1(b) shows the decrease in permeance with temperature. The sum of the adsorption enthalpy and diffusion energy appears in the permeance term (explained in detail in Appendix 1). The trend shown in Figure 7.1(b) implies that the decrease in methanol loading on the membrane surface is faster than the increase in diffusivity [8].

7.4.2 PV and VP for the mixture methanol / MTBE

The separation of methanol from MTBE by pervaporation is presented in Figure 7.2. Fluxes for MTBE were very low for all series, consequently membranes show very high selectivity.

The comparison pervaporation with vapor permeation can be seen in Figure 7.3 for different points of view. In Figure 7.3(a) the methanol and MTBE fluxes are presented versus temperature, while in Figure 7.3(b) methanol flux is presented versus their own driving force.

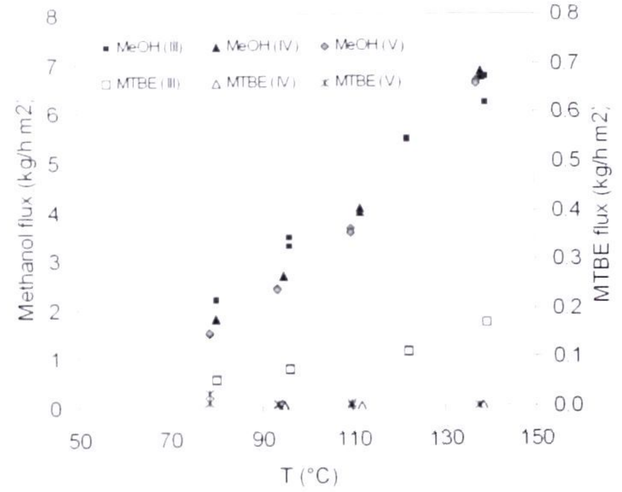
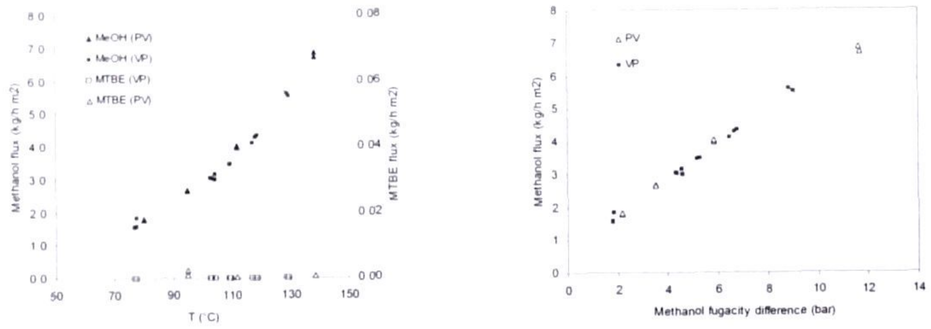


Figure 7.2: Pervaporation fluxes for methanol and MTBE as function of temperature for binary mixture (experimental series III, IV and V)



(a) Temperature (b) Fugacity difference

Figure 7.3: Pervaporation and vapor permeation fluxes for methanol and MTBE as function of temperature (a) or fugacity difference (b) for binary mixture using membrane M4

It is clear that the temperature and fugacity difference trends are practically the same for pervaporation and vapor permeation. Overall it is concluded that at saturation conditions, pervaporation and vapor permeation are equal transport processes.

7.5 Simulation study

7.5.1 Conditions and specifications

The simulation tool used throughout this thesis has been successfuly validated for PV and VP with the system methanol / MTBE in [95]. Model parameters for the present study were retrieved from experimental data series IV. The values of the parameters are shown in Table 7.3.

The debutanizer column from the Lyondell MTBE process is taken as the design case [25]. The feed for the pervaporation modules is a side stream from the debutanizer with 20 tons/h, 22.8 % wt methanol, 77.2 % wt MTBE, 8 bar pressure and temperature of 119.9 °C. The corresponding vapor in equilibrium with this liquid stream is the feed for the vapor permeation modules. The vapor feed stream remains the same (20 tons/h), but it contains 27.4 % wt methanol. All simulations were depleted until 10 % wt methanol with a permeate pressure of 100 mbar unless otherwise stated.

Table 7.3: Membrane parameters determined from experiments

Q^o_{MeOH} $kg/h \cdot m^2 \cdot bar$	$E^{app}_{act,\,MeOH}$ kJ/mol	Q^o_{MTBE} $kg/h \cdot m^2 \cdot bar$	$E^{app}_{act,\,MTBE}$ kJ/mol
0.89	-16.1	0.16	6.23

Both pervaporation and vapor permeation were simulated in a shell-and-tube configuration with concentric tubes (SMS module concept [146]). This module operates isothermally thanks to heating medium flowing in the shell side of the module. The outer tubes have an inside diameter

of 22 mm and the inner tubes have an outside diameter of 14 mm. Each module contains 24 double tubes of 1 meter length, with a total membrane area of 1.05 m^2 per module.

Concentration polarization was accounted during simulations, unless otherwise stated. In order to minimize transport limitation due to polarization, the membrane modules were adjusted by changing the number of parallel modules to have fully turbulent stream (Reynolds number between 10,000 and 12,000) averaged over the modules.

7.5.2 Simulation cases

The comparison of pervaporation and vapor permeation was perfomed taking into cosideration *equal* initial driving force. For case 2 *equal* methanol depletion was considered. The latter is very important to avoid misjudgements that VP requires more area than PV.

Table 7.4 gives a summary of the cases studied. They illustrate the effects of changes in depletion rate, operation mode and polarization resistance. Case 1 is considered as base case. The feed streams for PV and VP have the same chemical potential and the feed stream is depleted to 10 % wt methanol, taking polarization resistance into account. As previously mentioned, the liquid feed contains 22.8 % wt methanol (4560 kg/h), while the vapor feed contains 27.4 % wt methanol (5480 kg/h). When both streams leave the column they have the same driving force, but obviously there is more methanol to remove for VP before reaching the specifications (10 % wt methanol). Case 2 deals with this issue by simulating VP for the same methanol depletion as PV in Case 1. This will show if both processes remove the same amount of methanol using the same area. Case 3 performes the simulations with the conditions of Case 1 but neglecting polarization resistance.

Table 7.4: Description of simulation cases

case. #	operation mode	$MeOH_{final}$ % wt	polarization resistance
1	PV / VP	10	Yes
2	VP	14.5	Yes
3	PV / VP	10	No

7.5.3 Simulation results

Results of the simulations are presented in Table 7.5. In Case 1 the larger area required for vapor permeation than for pervaporation (approximately 40%) is due to the larger amount of methanol in the vapor feed.

Case 2 shows that PV and VP remove the same amount of methanol with the same membrane area. The difference in permeate stream is due to the different inital methanol concentration, this promotes larger flux for VP and as consequence a larger stream.

The effect of boundary layer resistance can be seen comparing Cases 1 and 3 for both pervaporation and vapor permeation. In order to arrive at the same Reynolds number, the module configuration is different for pervaporation and vapor permeation. For vapor permeation, more modules need to be installed in parallel than in series, thereby favoring a low absolute pressure drop over the system (here calculated at about 0.5 bar). The pressure drop in pervaporation was higher (2.9 bar), so installation of pumps in between the modules would be required, thereby both increasing capital and operating costs. Obviously the required areas are larger when polarization resistance was considered. For pervaporation the area increased 11.8% (from 636 to 711 m^2) while for vapor permeation the increase was 9.3% (from 931 to 1018 m^2). From these calculation it is clear that polarization resistance is similar for VP and VP at *the same* hydrodynamic conditions. It was observed that the boundary layer resistance is larger in pervaporation, which

Table 7.5: Simulation results

Case #	Operation mode	Area m^2	Permeate kg/h	$MeOH_{perm}$ % wt	Total flux kg/h m^2	Polarization resistance
1	PV	711	3355	89	4.7	10%
	VP	1018	4681	87	4.6	8%
2	VP	710	3510	89	4.9	8%
3	PV	636	3180	90	5.1	n.a.
	VP	931	4549	88	4.9	n.a.

is attributed to the slower diffusion in the liquid boundary layer compared to the vapor boundary layer Yet, these resistances are not large (10% for PV and 8% for VP) and can be concluded that providing fully turbulent conditions, the contribution of polarization to the total resistance is low.

Due to the fact that in vapor phase diffusivities are about three to four orders of magnitude larger than in liquid phase ($1.2 \cdot 10^{-6}$ vs $5.7 \cdot 10^{-9}$ m^2/s for this study) it is to be expected that concentration polarization in vapor permeation in general is smaller than in pervaporation. However, as the density in a vapor is about two orders of magnitude smaller than in a liquid (17 vs 660 kg/m^3 for this study), the increase in mass transport to the feed side boundary of the membrane caused by the larger diffusivities is partly compensated. The diffrence in vapor and liquid viscosity is not so large ($1.2 \cdot 10^{-5}$ vs $1.7 \cdot 10^{-4}$ Pa·s, respectively) and practically doesn't play a role for these calculations. Because the mass tranfer resistance in the membrane is expressed as function of the difference in equilibrium concentrations in the gas phase, all other mass transfer resistances have to be expressed on the same basis. According to Appendix 2, the overall mass transfer resistance for PV and VP can be represented by the following approximate relation:

$$\frac{1}{k_{ov}} \approx \frac{1}{k_{bl} \cdot \frac{\rho'_f}{\rho_v}} + \frac{1}{k_{mem}} \tag{7.10}$$

where ρ_f' is the molar density of the fluid at the feed side and $\rho_v'$is the molar density of the vapor at the feed side conditions $(P, T, x_i)_{feed}$. The calculated mass transfer coefficient is around 50 times higher for vapor than for liquid, but it compensates with the ratio of densities (around 34) to give similar numbers of mass transfer resistance. From Equation 7.10 it is also clear that if permeance is very small or large, the polarization contribution (for a given Re) to the overall mass transfer resistance will be the same for VP and PV. However, there is a region in which the difference can be around 10%, but then it reduces again as it is clearly shown in Figure 7.4. This figure is not only a mathematical result but also agrees with what it can happen in both processes, i.e., when the permeation rate is too low it is difficult to speak about polarization because permeation is so slow the concentration at the boundary layer hardly changes, therefore no polarization occurs. As the permeation rate increases the difference in bulk and boundary layer concentration increases as well to the point where the permeation of one of the components is so fast that the concentration of this component at the boundary layer is zero. In that case the contribution of polarization to mass transfer is almost 100%. Obviously permeances larger than 10 kg/h m^2 bar are not feasible and were just used in Figure 6 to have a clear picture of the behavior. To recap, we can say that the contribution of concentration polarization to the total mass transfer resistance is not dependant only on hydrodynamics, but also on membrane characteristics (i.e. permeance).

7.5.4 Operational aspects

Finally, it is important to mention the operational side of pervaporation and vapor permeation, which has some advantages and disadvantages for both that may be decesive for choosing one over the other.

Pervaporation is still preferred for engineers and researchers because handling liquids is eas-

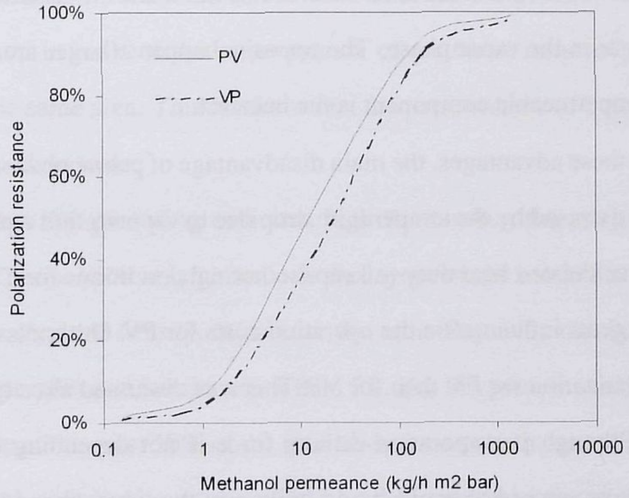


Figure 7.4: Increase of polarization resistance as function of methanol permeance for PV and VP

ier than vapors. This plays a role not only in for operation, but also on safety, since it is more difficult to detect vapors (for instance a leakage). Economically, most of the equipment and instrumentation for handling liquids are cheaper. To produce vapor (obviously) more energy is required than warming-up a liquid, however it requires less energy to keep a vapor at constant temperature. Increasing driving force for pervaporation is easier (and safer) than for vapor permeation, because on the one hand increasing temperature is easier than increasing pressure. On the other hand if the liquid has reached its boiling temperature at a certain pressure, it can be easily pumped to increase pressure and avoid vaporization, whereas VP driving force depends lineary on absolute pressure and therefore driving force can only be increased by compressors. If high pressures are applied, the cost of equipment will increase and safe design of high-pressure (and therefore high-temperature) modules should be applied as a consequence. If the most permeable component is also the most volatile, the area for vapor permeation is larger than for

pervaporation to achieve the same final concentration, since the fraction of the most volatile component is larger in the vapor phase. The opposite happens (larger area required for pervaporation) if the most permeable component is the heaviest.

Despite of all these advantages, the main disadvantage of pervaporation is the constant warming up of the liquid caused by the temperature drop due to vaporization enthalpy of the permeated components (the calculated heat duty to keep isothermal conditions for Case 1 is approximately 1 MW). This has great influence on the operation costs for PV. Other disadvantage is the higher concentration polarization for PV than for VP. This was discussed already at the end of the previous section. Although pervaporation driving force is not depending on pressure, feed side pressure has to be monitored to avoid liquid boiling in the tubes, then intermediate pumps and heaters should be placed where necessary to have operation at constant pressure and temperature.

7.6 Conclusions

Pervaporation and vapor permeation have been compared at lab-scale experimental basis for pure methanol and mixtures of methanol and MTBE at saturation conditions over a wide range of temperatures. From the pure methanol data it appeared that both processes are similar. The separation of the mixture methanol / MTBE confirmed the similarity. In fact, both processes are similar on the molecular scale. Model parameters were retrieved from experimental data to simulate pervaporation and vapor permeation at module-scale.

A simulation study was carried out to compare pervaporation (PV) and vapor permeation (VP) module performance with the same initial driving forces. In the simulations presented, vapor permeation required more area than pervaporation. The reason is because if the most permeable component is also the most volatile, the area for vapor permeation is larger than for pervaporation to achieve the same final concentration. Accordingly, the difference in area is due

to the amount of methanol that should be removed to reach the given specification. But if PV and VP are compared in basis of the same amount of methanol removed, it is clear that both processes require the same area. This confirms that the performance of both processes is similar on molecular and module scale.

It was also shown that providing sufficient high Re number, the main difference in pervaporation and vapor permeation at large scale is the layout of the module sequence, i.e. module configuration. As a result of density, to achieve the same Reynolds number, VP requires more modules placed in parallel and less in series than PV. For the present study the boundary layer resistance contribute at the most 10% of the total resistance in both cases (Re around 11,000). It was observed that the contribution of concentration polarization to the total mass transfer resistance is not dependant only on hydrodynamics, but also on membrane characteristics.

The many operational aspects discussed here showed the advantages and disadvantages of both operation modes. It is clear that the most suitable mode for a certain application will depend more on a series of specifications and conditions present at the plant, rather than an intrinsic advantage of either pervaporation or vapor permeation.

Appendix 1

From the Maxwell-Stefan equation to the engineering model

The purpose of every mathematical model described by theory is not only correlate properly the results obtained during experiments, but also to reliable predict the behavior of the property at different conditions than the experimental ones. Depending on the point of view, there are models established only on theoretical basis while some others rely on empirical obsevations. There is a thrid approach which takes elements from both approaches for the construction of a model. It is important to know that all of them may predict the desired property as close as possible within the conditions and constrains from which they were developed.

The following sections present different kinds of mathematical models used for the prediction of membrane mass transfer and show that the most compact and simplified approach (used during the present work) is just a specific case of the most general and theoretical approach, i.e., the Maxwell-Stefan equation.

The Maxwell-Stefan equation

The Maxwell-Stefan equation described by Krishna and Wesseling [64] can be written as

$$-\frac{c_i}{RT}\nabla_{T,p}\,\mu_i - \frac{c_i}{RT}\,V_i\,\nabla P_{abs} = \sum\nolimits_{j=1,j\neq i}^{n} \frac{\theta_j J_i - \theta_i J_j}{D_{ij}} + \frac{J_i}{D_i} \qquad \text{(A1-1)}$$

The second term with the absolute pressure gradient reflects the influence of the absolute

pressure on the driving force rather than the viscous flow contribution.

Replacing concentration c_i by the product of porosity ϵ, membranes's material density ρ^{silica} and the loading if component i $\theta_i q_i^{sat}$, the equation can be rewriten as

$$J_i = -\epsilon \rho^{silica} q_i^{sat} \theta_i D_i \frac{\nabla \mu_i}{RT} \tag{A1-2}$$

Simplification

Equation A1-2 can be simplified by assuming the chemical potential gradient to be constant over the layer thickness δ, giving

$$J_i = -\epsilon \rho^{silica} q_i^{sat} \theta_{i,\,avg} \frac{D_i}{\delta} \frac{\Delta \mu_i}{RT} \tag{A1-3}$$

where $\theta_{i,\,avg}$ is the average of the feed and permeate side degree of occupancy.

Equation A1-3 can be further simplified by eliminating the occupancy by asuming that the selective layer is fully saturated [78], i.e. $\theta_{i,\,avg}$=1

$$J_i = -\epsilon \rho^{silica} q_i^{sat} \frac{D_{i0}}{\delta} EXP\left(\frac{-E_{i,\,dif}}{RT}\right) \frac{\Delta \mu_i}{RT} \tag{A1-4}$$

All the material properties can be combined into one activated parameter F (which has the units of flux) to give

$$J_i = F_i \frac{\Delta \mu_i}{RT} \tag{A1-5}$$

or

$$J_i = F_{i,0} EXP\left(\frac{-E_i^{app}}{RT}\right) \frac{\Delta \mu_i}{RT} \tag{A1-6}$$

The activation energy for difusion is now an apparent one because the effect of the temperature on the adsortion is not separately considered. The benefit of this approach is that no material properties need to be known and the parameter F and E can be determined adjusting experimental data [154].

Simplified Model

Since $\Delta \mu_i / RT = ln\,(f_i^f / f_i^p)$, for small fugacity diferences over the selective layer the chemical potential difference can be approximated by the fugacity difference δf_i. It has been demonstrated by some authors [30, 59] that the assumption of linear adsorption (Henry regime) also allows expresing the driving force in terms of larger fugacity differences, hence

$$J_i = H_i \frac{D_i}{\delta} \Delta f_i \tag{A1-7}$$

and with

$$H_i \equiv \epsilon \rho^{silica} q_i^{sat} b_i = H_{i,0}\, EXP\left(\frac{-\Delta H_{i,\,ads}}{RT}\right) \tag{A1-8}$$

then

$$J_i \approx \frac{1}{\delta} H_{i,0}\, EXP\left(\frac{-\Delta H_{i,\,ads}}{RT}\right) D_{i,0}\, EXP\left(\frac{-E_i}{RT}\right) \Delta f_i \tag{A1-9}$$

or

$$J_i = \frac{1}{\delta} H_{i,0}\, D_{i,0}\, EXP\left(\frac{-(\Delta H_{i,\,ads} + E_i)}{RT}\right) \Delta f_i \tag{A1-10}$$

simplifying

$$J_i \equiv Q_{i,0}\, EXP\left(\frac{-E_{act,\,i}^{app}}{RT}\right) \Delta f_i \tag{A1-11}$$

or

$$J_i = Q_i \Delta f_i \tag{A1-12}$$

finally, assuming ideal gas the driving force can be expressed as

$$\Delta f_i = (P \cdot y_i)_{feed} - (P \cdot y_i)_{permeate} \tag{A1-13}$$

In equation A1-11 the apparent activation energy for permeance ($E^{app}_{act,\,i}$) is the sum of adsorption enthalphy and the activation energy for diffusion. This model also follows from the Maxwell-Stefan approach if the assumption of a loading independent diffusivity is released and is assumed to be proportional to the fraction of unnocupied sites as reported in [110]. In that case the Fickian-type equation A1-12 results as reported by Krishna [63].

Equation A1-11 was proposed by Wijmans [154] for polymer membranes and validated by Ten Elshof and Sommer for silica membranes [30, 123]. This equation is founded upon the following assumptions:

1. Adsorption is approximated by a Henry coeffient assuming low degree of occupancy.
2. The substitution of the chemical potential difference by partial pressure difference assumes a low product of the adsorption parameter b_i and the fugacity f_i.

For some conditions (very high pressures or temperatures) these assumptions are not true and therefore the model may show large deviations. Table A1-1 gives an overview of the above described models (from [25]).

Sumarizing, several authors have used partial pressure diference instead of the gradient in chemical potential as the driving force for membrane transport [154, 30, 123, 25, 11]. The main advantage of this modeling is the simplicity (using only two experimentally determined parameters) compared to the Maxwell-Stefan approach, that make use of detailed information of the material properties and the adsorption behavior in the material, specially difficult to find for commercial membranes.

Table A1-1: Simplification of Maxwell-Stefan equation

Model	Equation
Maxwell-Stefan (MS)	$J_i = -\epsilon\rho^{silica} q_i^{sat} \theta_i D_i \frac{\nabla\mu_i}{RT}$
Simple MS (average occupancy)	$J_i = -\epsilon\rho^{silica} q_i^{sat} \theta_{i,\,avg} \frac{D_i}{\delta} \frac{\Delta\mu_i}{RT}$
Simplified (saturated, θ_i=1)	$J_i = -\epsilon\rho^{silica} q_i^{sat} \frac{D_{i0}}{\delta} EXP\left(\frac{-E_{i,\,dif}}{RT}\right) \frac{\Delta\mu_i}{RT}$
"Simplified" model	$J_i = Q_{i,\,0}\, EXP\left(\frac{-E^{app}_{act,\,i}}{RT}\right) \Delta f_i$

Appendix 2

Modeling of mass transfer resistances for vapor permeation and pervaporation

For small to moderate driving forces the molar flux of a component through a membrane we can be described with the following equation:

$$J_i = Q_{i,m} \cdot (f_{i,R} - f_{i,P}) \tag{A2-1}$$

In this equation $f_{i,R}$ is the fugacity of the component at the membrane / retentate interface and $f_{i,P}$ the fugacity of the component at the membrane / permeate interface. In case that the vapor can be considered as an ideal gas the vapor fugacities can be replaced by partial pressures of the component in the vapor and the liquid fugacities are equal to the vapor pressures of the components in the liquid. We can therefore also write:

$$J_i = Q_{i,m} \cdot (p_{i,R} - p_{i,P}) \tag{A2-2}$$

where p is either partial pressure or vapor pressure. When we now substitute now the pressures for vapor concentrations we find:

$$J_i = QRT \cdot (c_{i,R} - c_{i,P}) = k_m \cdot (c_{i,R} - c_{i,P}) \tag{A2-3}$$

This equation is a useful tool for comparing the mass transfer resistance in the membrane with the mass transfer resistances of the adjoining boundary layers. When doing this we should keep in mind that the flux through the membrane is expressed as a product of a mass transfer coefficient, k_m, and a difference in vapor concentrations. The membrane resistance is then expressed by $\frac{1}{k_m}$. In fact the mass transfer through the membrane is modeled as diffusion through an apparent stagnant gas layer. As a consequence mass transfer through adjoining boundary layers has to be modeled in the same way.

Neglecting the mass transfer resistance in the permeate boundary layer we arrive then to the following equations for vapor permeation. The flux through the vapor boundary layer is defined as

$$J = k_{o-G} \cdot (c_G - c^*_{G-i-R}) \tag{A2-4}$$

$$\frac{c_G - c^*_{G-i-R}}{J} = \frac{1}{k_G} \tag{A2-5}$$

$$\frac{c^*_{G-i-R} - c^*_{G-i-P}}{J} = \frac{1}{k_m} \tag{A2-6}$$

$$\frac{c_G - c^*_{G-i-P}}{J} = \frac{1}{k_{o-G}} \tag{A2-7}$$

$$\frac{1}{k_{o-G}} = \frac{1}{k_G} + \frac{1}{k_m} \tag{A2-8}$$

where k_{o-G} is the overall, k_G is the boundary layer and k_m is the membrane mass transfer coefficient, respectively.

For pervaporation we find that the flux through the liquid boundary layer is defined as

$$J = k_L \cdot (c_L - c^*_{L-i-R}) = k_m \cdot (c^*_{G-i-R} - c^*_{G-i-P}) \tag{A2-9}$$

$$c^*_{G-i-R} = m \cdot c^*_{L-i-R} \tag{A2-10}$$

$$c_G = m \cdot c_L \tag{A2-11}$$

$$J = k_L \cdot \left(\frac{c_G}{m} - \frac{c^*_{G-i-R}}{m}\right) = k_m \cdot (c^*_{G-i-R} - c^*_{G-i-P}) \tag{A2-12}$$

$$\frac{c_G - c^*_{G-i-R}}{J} = \frac{m}{k_L} \tag{A2-13}$$

$$\frac{c^*_{G-i-R} - c^*_{G-i-P}}{J} = \frac{1}{k_m} \tag{A2-14}$$

$$\frac{c_G - c^*_{G-i-P}}{J} = \frac{1}{k_{o-G}} \tag{A2-15}$$

$$\frac{1}{k_{o-G}} = \frac{m}{k_L} + \frac{1}{k_m} \tag{A2-16}$$

Where k_{o-G} is the overall, k_L is the boundary layer, k_m is the membrane mass transfer coefficient, respectively, and m is defined as:

$$m = K \cdot \frac{\rho'_G}{\rho'_L} \tag{A2-17}$$

where K is the distribution coefficient between vapor and liquid on basis of mol fractions and $\rho_i^{'}$ represent the molar densities. For systems that are difficult to separate K is close to 1. In general vapor permeation and pervaporation are used for systems with low volatility difference. Therefore as a first approximation we are allowed to write:

$$\frac{1}{k_{o-G}} \approx \frac{1}{k_m} + \frac{1}{k_L \frac{\rho_L^{'}}{\rho_G^{'}}} \tag{A2-18}$$

Bibliography

[1] A.Kumar, S. Croteau, and O. Kutowy. Use of membranes for energy efficient concentration of dilute streams. *Applied Energy*, 64(1-4):107–115, 1999.

[2] P. Aptel, N. Challard, J. Cunny, and J. Neel. Application of the pervaporation process to separate azeotropic mixtures. *J. Memb. Sci.*, 1:271–287, 1976.

[3] P. Aptel, J. Cuny, J. Jozefonwicz, J. Morel, and J. Neel. Liquid transport through membranes by grafting of polar monomers onto poly(tetrafluoroethylene) films. *J. Appl. Polym. Sci.*, 16:1061–1076, 1972.

[4] M. Asaeda, M. Ishida, and Y. Tasaka. Pervaporation characteristics of silica-zirconia membranes for separation of aqueous organic solutions. *Sep. Sci. Technol.*, 40:239–254, 2005.

[5] M. Asaeda, J. Yang, and Y. Sakou. Porous silica-zirconia (50%) membranes for pervaporation of iso-propyl acohol (IPA)/water mixtures. *J. Chem. Eng. Jpn.*, 35(4):365–371, 2002.

[6] M. Asaeda, J. Yang, Y. Sakou, and K. Shimasaki. Stability and performance of porous silica-zirconia composite membranes for pervaporation of aqueous organic solutions. *J. Membr. Sci.*, 209:163, 2002.

[7] R.W. Baker and et.al. *Membrane separation systems: recent developments and future directions*. Noyes Publishing, Park Ridge, NJ, USA.

[8] W.J.W Bakker, L.J.P. van den Broeke, F. Kapteijn, and J.A. Moulijn. Temperature dependence on component permeation through a silicalite-1 membrane. *AIChE Journal*, 43:2203–2214, 1997.

[9] A.H. Ballweg, H.E.A. Bruschke, W.H. Schneider, and G.F. Tusel. Pervapoartion membranes. an economical method to replace conventional dehydration and rectification columns in ethanol destilleries. In *5th International symposium an alcohol fuel technology*, Auckland, NZ, May 1982.

[10] B. Basu and C. Visvanathan. Membrane permeation of a binary compound for co-current and cross flow modes. *Desalination*, 130:113–129, 2000.

[11] B. Bettens, S. Dekeyzer, B. van der Bruggen, J. Degreve, and C. Vandecasteele. Transport of pure components in pervaporation through a microporous silica membrane. *J. Phys. Chemistry B*, 109:5216–5222, 2005.

[12] K.W. Boddeker and G. Bengtson. Phenolanreicherung durch pervaporation. *Erdoel und Kohle*, 40:439, 1987.

[13] H.E.A. Bruschke. Verwendung einer mehrschichtigen membran zur trennung von fluessigkeitsgemischen nach dem pervaporationsverfahren. European Patent EP096339, 1982.

[14] H.E.A. Bruschke, W.H. Schneider, and G.F. Tusel. Pervaporation membrane for the separation of water and oxygen-containing simple organic solvents. In *European Workshop on Pervaporation*, Nancy, France, September 1982.

[15] H.E.A. Bruschke, W.H. Schneider, and G.F. Tusel. Verfahren zur reduktion des alkoholgehaltes alkolischer getranke. European Patent EP0332738, 1994.

[16] J. Campaniello, C.W.R. Engelen, W.G. Haije, P.P.A.C. Pex, and J.F. Vente. Long term pervaporation performance of microporous methylated silica membranes. *Chem. Commun.*, pages 833–834, 2004.

[17] J. Caro, M. Noack, P. Koelsch, and R. Schaefer. Zeolite membranes - state of their development and perspective - review article. *Micropor. Mesopor. Mat.*, 38:3–24, 2000.

[18] C. Casado, A Urtiaga, D. Gorri, and I. Ortiz. Pervaporative dehydration of organic mixtures using a commercial silica memebrane: Determination of kinetic parameters. *Sep. Purif. Technol.*, 42:39–45, 2005.

[19] Y. Cen and R.N. Lichtenthaler. *Vapor Permeation in Membrane Separations. Technology Principles and Applications*. Elsevier Science, 1995.

[20] S. Chen and et.al. Pervaporation separation of water / ethanol mixture by sulfonated polysulfone membrane. *J. Memb. Sci.*, 183:29–36, 2001.

[21] S. Chen and et.al. Pervaporation separation of water / ethanol mixture through lithiated polysulfone membrane. *J. Memb. Sci.*, 193:59–63, 2001.

[22] W.J. Chen and C.R. Martin. Highly methanol-selective membranes for the pervaporation separation of methyl-tert-butyl ether / methanol mixtures. *J. Membr. Sci.*, 107:101–108, 1995.

[23] F.P. Cuperus and et.al. Dehydration using ceramic silica pervaporation membranes: The influence of hydrodynamic conditions. *Sep. Purif. Technol.*, 27:225–229, 2002.

[24] A. Dafinov, R. Garcia-Valls, and J. Font. Modifications of ceramic membranes by alcohol adsorption. *J. Membr. Sci.*, 196:69, 2002.

[25] F.T. de Bruijn. *Pervaporation and vapor permeation of methanol and MTBE through a microporous methylated silica membrane*. PhD thesis, TU Delft, December 2006.

[26] F.T. de Bruijn, J. Gross, Z. Olujic, P.J. Jansens, and F. Kapteijn. On the driving force of methanol pervaporation through a microporous methylated silica membrane. *Ind. Eng. Chem. Res.*, page submited for publication, 2006.

[27] F.T. de Bruijn, L. Sun, Z. Olujic, P.J. Jansens, and F. Kapteijn. Influence of the support layer on the flux limitation in pervaporation. *J. Membr. Sci.*, 223:141–156, 2003.

[28] Les Usines de Melle. British Patent 1097819, January 1968.

[29] R. Dessau. Dehydrogenation of alcohols over non-acidic metal-zeolite catalysts. Patent US5103066, July 1992.

[30] J.E. Ten Elshof, C.R. Abadal, J. Sekulic, S.R. Chowdhury, and D.H.A. Blank. Transport mechanisms of water and organic solvents through mocroporous silica in the pervaporation of binary liquids. *Micro. Meso. Materials*, 65:197–208, 2003.

[31] H. Eustache and G. Histi. Separation of aqueous organic mixtures by pervaporation and analysis by mass spectrometry or a coupled gas chromatograph-mass spectrometer. *J. Membr. Sci.*, 8:105, 1981.

[32] J. Fahey. Field of dreamers. *Forbes*, June 2006, June 2006.

[33] Fakhri. *Hybrid distillation / vapor permeation systems for solvent dehydration*. PhD thesis, TU Delft, September 1999.

[34] S.C. Fan, C.L.Li, Y.C. Wang, and et.al. Application of aromatic polyamide membranes for pervaporation and vapor permeation. *Desalination*, 148:43–48, 2002.

[35] X. Feng and R.Y.M. Huang. Liquid separation by membrane pervaporation: a review. *Ind. Eng. Chem. Res.*, 36:1048–1066, 1997.

[36] K. Fialova, R. Petrickovic, M. Sharma, and P. Uchytil. Steady state sorption measurement and the transport mechanism in polymeric membrane during vapor permeation. *J. Membr. Sci.*, 275:166–174, 2006.

[37] L.J. Filar. Patent US2744143, September 1953.

[38] A. Font, J.C. Asensi, F. Ruiz, and V. Gomis. Application of isooctane to the dehydration of ethanol. design of a column sequence to obtain absolute ethanol by heterogeneous azeotropic distillation. *Ind. Eng. Chem. Res.*, 42:140–144, 2003.

[39] J. Fontalvo-Alzate. *Design and performance of two-phase flow pervaporation and hybrid distillation process*. PhD thesis, TU Eindhoven, March 2006.

[40] W.F. Furter and R.A. Cook. Salt effect in distillation: a literature review. *Int. J. Heat Mass Transfer*, 10:23–36, 1967.

[41] T. Gallego-Lizon, Y. S. Ho, and L. Freitas dos Santos. Comparative study of commercially available polymeric and microporous silica membranes for the dehydration of IPA/water mixtures by pervaporation/vapor permeation. *Desalination*, 149:3–8, 2002.

[42] J. Gmehling and U. Onken. *Vapor-liquid equilibrium data collection. Aqueous - organic systems*, volume I of *Part 1*. DECHEMA chemistry data series, Frankfurt/Main, 1977.

[43] B. Gonzalez and I. Ortiz. Modelling and simulation of a hybrid process pervaporation-distillationfor the separation of azeotropic mixtures of alcohol-ether. *J. Chem. Technol. Biot.*, 77:29–42, 2001.

[44] B. Gonzalez and I. Uribe. Mathematical modeling of the pervaporative separation of methanol-methylterbutyl ether mixtures. *Ind. Eng. Chem. Res.*, 40:427–435, 2001.

[45] D. Grewell, S. Khanal, H. van Leeuwen, and M. Krapfl. Ultrasonic boosts release rates of corn sugars for ethanol production. electronic reference from Iowa State University News Service, June 2006.

[46] J. Guan and X. Hu. Simulation and analysis of pressure swing adsorption: ethanol drying process by the electrical analogue. *Sep. Purif. Technol.*, 31:31–35, 2003.

[47] V. Gupta. Purification of acetone. Patent US5567853, October 1996.

[48] T. Hamada, M. Taya, and S. Tone. Pervaporation and vapor permeation behavior of water and 2-propanol in water-selective membranes. *J. Chem. Eng. Jpn.*, 30:600–608, 1997.

[49] W.S. Ho and K. Sirkar. *Membrane Handbook*. Van Nostrand, NY, USA, 1992.

[50] U. Hommerich and R. Rautembach. Design and optimization of combined pervaporation / distillation process for the production of MTBE. *J. Membr. Sci.*, 146:53–64, 1998.

[51] C. Hsu and et.al. Pervaporation separation of a water - ethanol mixture by psf-peg membrane. *J. Appl. Polym. Sci.*, 87:2158–2164, 2003.

[52] J. Huang and et.al. Dehydration of water-alcohol mixtures by pervaporation and vapor permeation through surface resintering expanded poly(tetrafluoroethylene) membranes. *European Polym. J.*, 38:179–186, 2002.

[53] M. Hung and et.al. Pervaporation separation of a water / ethanol mixture by a sodium sulfonate polysulfone membrane. *J. Appl. Polym. Sci.*, 90:3374–3383, 2003.

[54] A.E. Jansen, W.F. Versteeg, B. van Engelenburg, J.H. Hanemaaijer, and B.P. ter Meulen. Methods to improve flux during alcohol/water azeotrope separation by vapor permeation. *J. Membr. Sci.*, 68:229–239, 1992.

[55] L. Jiang, L.T. Biegler, and V.G. Fox. Design and optimization of pressure swing adsorption systems with parallel implementation. *Comp. Chem. Eng.*, 29:393–399, 2005.

[56] J.L.Humphrey and A.F. Seibert. Separation technologies - an opportunity for energy savings. *Chem. Eng. Prog.*, 88(3):32–41, 1992.

[57] A. Jonquieres, R. Clement, P. Lochon, J. Neel, M. Dresch, and B. Chretien. Industrial state-of-the-art of pervaporation and vapor permeation in the western countries. *J. Membr. Sci.*, 206:87–117, 2002.

[58] P. Kanti and et.al. Dehydration of ethanol through blend membranes of chitosan and sodium alginate by pervaporation. *Sep. Purif. Technology*, 40:259–266, 2004.

[59] F. Kapteijn, J.M. Moulijn, W. Zhu, and T.Q. Gardner. *Zeolite membranes: modeling and application*. Structured catalysts and reactors. CRC Taylor and Francis, 2nd edition edition, 2006.

[60] Kirk and Othmer. *Enciclopedia of chemical technology*, volume 1. Wiley-Interscience, USA, 3rd edition, 1978.

[61] P. Kreis and A. Gorak. Process analysis of hybrid separation processes - combination of distillation and pervaporation. *Chem. Eng. Res. Design*, 84(A6):1–6, June 2003.

[62] P.M.R. Kreis. *Prozesanalyse hybrider Trennverfahren*. PhD thesis, Universitaet Dortmund, June 2004.

[63] R. Krishna. A unified approach to the modeling of intraparticle diffusion in adsorption processes. *Gas Separation and Purif.*, 7(2):91–104, 1993.

[64] R. Krishna and J.A. Wesselingh. The maxwell-stefan approach to mass transfer. *Chem. Eng. Sci.*, 52(6):861–911, 1997.

[65] J. Kuhn. Heat and mass transfer in a pervaporation membrane. Master thesis, TU Eindhoven, May 2004.

[66] H.J. Lang. Simplified approach to preliminary cost estimates. *Chem. Eng. (NY)*, 55:112, 1948.

[67] K.W. Lawson and D.R. Lloyd. Membrane distillaion 1. module design and performance evaluation using vacuum membrane distillation. *J. Membr. Sci.*, 120:111–121, 1996.

[68] E.L. Ligero and T.M.K. Ravagnani. Dehydration of ethanol with salt extractive distillation - a comparative analysis between processes with salt recovery. *Chem. Eng. Process.*, 42:543–552, 2003.

[69] B. Lim and et.al. Morphology of crosslinked poly(butyl methacrylate-co-methyl methacrylate) porous membrane. *J. Membr. Sci.*, 209:293–307, 2002.

[70] F. Lipnizki, R.W. Field, and P.K. Tne. Pervaporation-based hybrid processes: a review of process design, applications and economics. *J. Membr. Sci.*, 153:183–210, 1999.

[71] F. Liu and X. Liu. Separations of acetone-butanol-ethanol (abe) from dilute aqueous solutions by pervaporation. *Sep. Purif. Technol.*, 42:273–282, 2005.

[72] S.X. Liu, M. Pen, and L.M. Vane. Cfd simulation of effect of baffle on mass transfer in a slit-type pervaporation module. *J. Membr. Sci.*, 265(1-2):124–136, 2005.

[73] S.X. Liu, M. Peng, and L. Vane. Cfd modeling of pervaporative mass transfer in the baoundary layer. *Chem. Eng. Sci.*, 59:5853–5857, 2004.

[74] H. K. Lonsdale. The growth of membrane technology - review. *J. Membr. Sci.*, 10:81–181, 1982.

[75] M.L. Maloncy, J.C. Jansen, and T. Marschmeyer. Technical and economical evaluation of a zeolite membrane based heptane hydroisomerization process. *Chem. Eng. J.*, 106:187–195, 2005.

[76] J. Marriott and E. Sorensen. A general approach to modelling membrane modules. *Chem. Eng. Sci.*, 58:4975–4990, 2003.

[77] J. Marriott and E. Sorensen. The optimal design of membrane systems. *Chem. Eng. Sci.*, 58:4991–5004, 2003.

[78] S. Marx. *Application of pervaporation to the separation of methanol from tertiary amyl methyl ether*. PhD thesis, University of Potchefstroom, South Africa, 2002.

[79] S. Marx, P. van der Gryp, H. Neomagus, R. Everson, and K. Keizer. Pervaporation separation of methanol from methanol/tert-amylmethyl ether mixtures with a commercial membrane. *J. Membr. Sci.*, 209:353–362, 2002.

[80] M. Matsukata, M. Takada, and et.al. Cfd analysis of flow in tubular zeolite membrane modules. In *AIChE Annual Meeting, Conference Proceedings*, NY, USA, November 2005. AIChE.

[81] E. Maus and H.E.A. Bruschke. Separation of methanol from methylesters by vapor permeation: Experiences of industrial applications. *Desalination*, 148:315–319, 2002.

[82] G.W. Meindersma and A.B. de Haan. Economical feasibility of zeolite membranes for industrial scale separations of aromatic hydrocarbons. *Desalination*, 149:29–34, 2002.

[83] Y. Morigami, M. Kondo, J. Abe, H. Kita, and K. Okamoto. The first large-scale pervaporation plant using tubular-type module with zeolite naa membrane. *Sep. Purif. Technology*, 25:251–260, 2001.

[84] Y. Morigami, M. Kondo, J. Abe, H. Kita, and K. Okamoto. The first large-scale pervaporation plant using tubular-type module with zeolite NaA membrane. *Sep. Purif. Technology*, 25(1-3):251–260, 2001.

[85] M. Mulder. *Basic Principles of Membrane Technology*. Kluwer Academic Publishers, 2nd ed. edition, 2003.

[86] Bureau NAP/DACE. *DACE-prijzenboekje*. Dutch Association of Cost Engineers, 22nd edition, May 2002.

[87] A. Navajas and et.al. Preparation of mordenite membranes for pervaporation of water - ethanol mixtures. *Desalination*, 148:25–29, 2002.

[88] M. Niang and G. Luo. A triacetate cellulose membrane for the separation of methyl tert-butyl ether/methanol mixtures by pervaporation. *Sep. Purif. Technology*, 24:427–435, 2001.

[89] M. Nomura, T. Yamaguchi, and S. Nakao. Ethanol / water transport through silicalite membranes. *J. Membr. Sci.*, 144:161–171, 1998.

[90] S.P. Nunes and K.V. Peinemann. *Membrane Technology in the Chemical Industry*. Wiley-VCH, 2001.

[91] K. Okamoto, N. Tanihara, and et.al. Vapor permeation and pervaporation separation of water-ethanol mixtures through polymide membranes. *J. Membr. Sci.*, 68:53–63, 1992.

[92] E. Okumus and et.al. Effect of fabrication and process parameters on the morphology and performance of a pan-based zeolite-filled pervaporation membrane. *J. Membr. Sci.*, 223:23–38, 2003.

[93] A.H. Olzinger. *Chem. Eng. (NY)*, 82:50–53, June 1975.

[94] P.A.Kober. Pervaporation, perstillation and percrystallization. *J. Amer. Chem. Soc.*, 39:9444, 1917.

[95] P. Perez, F.T. de Bruijn, Z. Olujic, and P.J. Jansens. Experimental comparison of vapor permeation and pervaporation with (methylated-) silica membranes and validation of a design tool for scale-up. In *Proceedings of the International Conference on Porous Ceramic Materials*, Bruges, Belgium, October 2005.

[96] P. Perez, Z. Olujic, J. de Graauw, and P.J. Jansens. Modeling and simulation of inorganic shell and tube membranes for vapor permeation. *Chem. Eng. Proc.*, 45:973–979, 2006.

[97] P. Perez, Z. Olujic, and P. Jansens. A design tool for shell and tube ceramic vapor permeation membrane modules. In et al. K.V. Peninemann, editor, *Euromembrane 2004 Book of Abstracts*, page 70, 28 Septamber - 1st October 2004, Hamburg, Germany 2004.

[98] P. Perez, Z. Olujic, and P.J. Jansens. A design tool for shell and tube vapor permeation modules. In *Proceedings of the 8th International Conference on Inorganic Membranes*, Cincinnati, USA, July 2004.

[99] P. Perez, Z. Olujic, and P.J. Jansens. Modeling shell and tube modules with silica membranes for vapor permeation. In *Proceedings of the 5th Iberoamerican Conference on Membrane Science and Technology*, Valencia, Spain, July 2005.

[100] P. Perez, Z. Olujic, P.J Jansens, M. Nienoord, and R. Creusen. A ceramic membrane based distillation/vapor permeation process for ethanol dehydration. In VDI and Dechema, editors, *Proceedings of the 9th Aachen Membrane Colloquium*, Aachen, Germany, March 2003.

[101] R.H. Perry and D.W. Green. *Perry's Chemical Engineers' Handbook*. Mac Graw-Hill, 7th ed. edition, 1997.

[102] T.A. Peters, J. Fontalvo, M.A.G. Vorstman, N.E. Benes, R.A. van Dam, Z.A.E.P. Vroon, E.L.J. van Soest-Vercammen, and J.T.F. Keurentjes. Hollow fibre microporous silica membranes for gas separation and pervaporation - synthesis, performance and stability. *J. Membr. Sci.*, 248:73–80, 2005.

[103] T. Pettersen, A. Argo, R.D. Noble, and C.A. Koval. Design of combined membrane and distillation processes. *Sep. Technology*, 6:175–187, 1996.

[104] P.Uchytil and R. Petrickovic. Vapor permeation and pervaporation of propan-1-ol and propan-2-ol in polyethylene membrane. *J. Membr. Sci.*, 209:67–79, 2002.

[105] M. Rafik and et.al. Plasma modified poly(vinyl alcohol) membranes for the dehydration of ethanol. *Polym. International*, 52:1222–1229, 2003.

[106] R. Rautenbach and R. Albrecht. *Membrane Processes*. John Wiley and Sons, 1989.

[107] R. Rautenbach and U. Meyer-Blumenroth. Module and process design for vapor permeation. *Desalination*, 77:295–322, 1990.

[108] S. Ray and S.K. Ray. Dehydration of acetic acid, alcohols and acetone by pervaporation using acrylonitrile-maleic anhydride copolymer membrane. *Sep. Sci. Technol.*, 40:1583–1596, 2005.

[109] C.P. Ribeiro, P.L.C. Lage, and C.P. Borges. A combined gas-stripping vapour permeation process for aroma recovery. *J. Membr. Sci.*, 238:9–19, 2004.

[110] L. Riekert. Rates of sorption and diffusion of hydrocarbons in zeolites. *AIChE Journal*, 17:446–454, 1971.

[111] R.M. Rioux and M.A. Vannice. Hydrogenation/dehydrogenation reactions: isopropanol dehydrogenation over copper catalysts. *J. Catalysis*, 216:362–376, 2003.

[112] U. Sander and H. Janssen. Industrial applications of vapor permeation. *J. Membr. Sci.*, 61:113–129, 1991.

[113] U. Sander and P. Soukup. Design and operation of a pervaporation plant for ethanol dehydration. *J. Membr. Sci.*, 36:463–475, 1988.

[114] M.S. Schehlmann, E. Wiedemann, and R.N. Lichtenthaler. Pervaporation and vapor permeation at the azeotropic point or in the vicinity of the lle boundary phases of organic / aqueous mixtures. *J. Membr. Sci.*, 107:277–282, 1995.

[115] M. Seiler. Power ethanol. Separator's Digest p20-22, ACHEMA 2003.

[116] J. Sekulic and et.al. Microporous silica and doped silica membrane for alcohol dehydration by pervaporation. *Desalination*, 148:19–23, 2002.

[117] R.K. Sinnott. *Coulson and Richardson's Chemical Engineering*, volume 6 (Chemical Engineering Design). Butterworth / Heinemann, Oxford, UK, 1999.

[118] S. Sircar. Pressure swing adsorption. *Ind. Eng. Chem. Res.*, 41:1389, 2002.

[119] K.K. Sirkar. Membrane separation technologies: current developments. *Chem. Eng. Comm.*, 1997:145–184, 157.

[120] B. Smitha, D. Suhanya, S. Sridhar, and M. Ramakrishna. Separation of organic-organic mixtures by pervaporation - review. *J. Membr. Sci.*, 241:1–21, 2004.

[121] S. Sommer. *Pervaporation and vapor permeation with microporous inorganic membranes*. PhD thesis, RWTH Aachen, December 2002.

[122] S. Sommer, B. Klinkhammer, and T. Melin. Integrated system design for dewatering of solvents with microporous silica membranes. *Desalination*, 149:15–21, 2002.

[123] S. Sommer and T. Melin. Influence of operation parameters on the separation of mixtures by pervaporation and vapour permeation with inorganic membranes. part 1: Dehydration of solvents. *Chem. Eng. Sci.*, 60:4509–4523, 2005.

[124] M. Staudacher, M. Harasek, T. Brinkmann, W. Hilgendorff, and A. Friedl. Cfd-simulation of mass transfer effects in gas and vapour permeation modules. *Desalination*, 146:237–241, 2002.

[125] W. Stephan, R.D. Noble, and C.A. Koval. Design methodology for a membrane / distillation column hybrid process. *J. Membr. Sci.*, 99:259–272, 1995.

[126] H. Strathmann. Membrane separation processes - review. *J. Membr. Sci.*, 9:121–189, 1981.

[127] H.J. te Hennepe, M.H.V. Mulder, C.A. Smolders, and D. Bargemann. Pervaporation process and membrane. Patent US4025562, 1990.

[128] the EET-Kiemproject KIEM98102. The technical and economic feasibility study of the hybrid process for ethanol dehydration. Technical Report TNO-rapport-R 2000/427, EET office, 2001.

[129] the EET project office. *Dehydration of organic solvens with distillation and vapor permeation*. Project proposal EETK 20046, 2001.

[130] the European Parliament. Richtlijn 2003/30/eg van het europees parlement en de raad ter bevordering van het gebruik van biobrandstoffen of andere hernieuwbare brandstoffen in het vervoer. Publicatieblad van de Europese Unie, May 2003.

[131] to Allied Chemical. British Patent 999441, July 1965.

[132] to Allied Chemical. British Patent 1257595, December 1971.

[133] to Shell Chemical. British Patent 938854, October 1953.

[134] to Standard Oil Development. British Patent 665376, January 1952.

[135] A. Toutianoush and et.al. Pervaporation separation of alcohol / water mixtures using self-assembled polyelectrolyte multiplayer membranes of high charge density. *Mat. Sci. Eng. C*, 22:459–463, 2002.

[136] A. Trianto, W.L. Qiao, and T. Kokugan. Isopropyl alcohol dehydrogenation on modified porous membrane reactor. *J. Chem. Eng. Jpn.*, 34(8):1065–1068, 2001.

[137] M. Tsuyumoto, A. Teramoto, and P. Meares. Dehydration of ethanol on a pilot scale, using a new type of hollow-fiber membrane. *J. Membr. Sci.*, 133:83–94, 1997.

[138] R. Turton and et.al. *Analysis, Synthesis and Design of Chemical Processes*. Prentice Hall, New Yersey, USA, 1998.

[139] R.K. Tyagi, A.E. Fouda, and T. Matsuura. A pervaporation model: Membrane design. *Chem. Eng. Sci.*, 50(19):3105–3114, 1995.

[140] Ullman. *Encyclopedia of Chemical Technology*. electronic edition, 2004.

[141] T. Uragami and et.al. Permeation and separation under high temperature and high pressure for ethanol / water vapors through cross-linked quaternized chitosan composite membranes. *Desalination*, 147:449–454, 2002.

[142] A. Urtiaga, C. Casado, and I. Ortiz. Symposium proceedings on membranes, preparation, properties and applications. page 257. Materials Research Society, 2003.

[143] L. van der Ent. Succesverhaal rond damppermeatie. *NPT Processtechnologie*, pages 25–28, Sept-Oct 1999.

[144] G.J.S. van der Gulik, J.G. Wijers, and J.T.F. Keurentjes. Measurement of 2d-temperature distributions in a pervaporation membrane module using ultrasonic computer tomography and comparison with fluid dynamics calculations. *J.Membr.Sci.*, 204:111–124, 2002.

[145] R. van Grinsven. Ethanol dehydration with hybrid distillation/vapor-permeation. Master thesis, TU Delft, August 2002.

[146] H.M. van Veen. Inorganic membranes for pervaporation. proof of concept. Public report, ECN, June 2004.

[147] H.M. van Veen, Y.C. van Delft, C.W.R. Engelen, and P.P.A. Pex. Dewatering of organics by pervaporation with silica membranes. *Sep. Purif. Technology*, 22-23:361–366, 2001.

[148] L.M. Vane and F.R. Alvarez. Vibrating pervaporation modules: Effect of module design on performance. *J. Membr. Sci.*, 255:213–224, 2005.

[149] A.W. Verkerk, P. van Male, M.A.G. Vorstman, and J.T.F. Keurentjes. *J. Membr. Sci.*, page 227, 2001.

[150] B.J. Voslamber. Modeling and simulation on hybrid distillation / vapour permeation process. Master's thesis, TU Delft, February 1996.

[151] Wang and et.al. Pervaporation properties of novel alginate composite membranes for dehydration of organic solvents. *J. Membr. Sci.*, 193:85–95, 2001.

[152] web Earth Policy Institute. Ethanol's potential: Looking beyond corn. electronic reference (http://www.earth-policy.org/Updates/2005/Update49.htm), visited in July 2006.

[153] J.G. Wijmans, A.L. Athayde, R. Daniels, J.H. Ly, H.D. Kamaruddin, and I. Pinnau. The role of boundary layers in the removal of volatile organic compounds from water by pervaporation. *J. Membr. Sci.*, 109:135–146, 1996.

[154] J.G. Wijmans and R.W. Baker. A simnple predictive treatment of the permeation process in pervaporation. *J. Membr. Sci.*, 79:101–113, 1993.

[155] B. Will and R.N. Lichtenthaler. Comparison of the separation of mixtures by vapor permeation and by pervaporation using pva composite membranes. 1. binary alcohol-water systems. *J. Membr. Sci.*, 68:119–125, 1992.

[156] N. Wynn. Reactions and separations. pervaporation comes of age. *CEP magazine*, 97(10):66–72, 2001.

[157] D. Zhongwei, L. Liying, and M. Runyu. Study on the effect of flow maldistribution on the performance of the hollow fibres modules used in membrane distillation. *J. Membr. Sci.*, 215:11–23, 2003.

List of Symbols

C	constants used in the Sherwood equation	
$\mathbb{D}$	diffusivity coefficient	$(m^2 \cdot s^{-1})$
E	activation energy	$(J \cdot mol^{-1})$
F	activated transport parameter	$(mol \cdot m^{-2} \cdot s^{-1})$
H	Henry coefficient	$(mol \cdot m^{-1})$
ΔH	enthalpy of adsorption	$(J \cdot mol^{-1})$
J	molar flux	$(mol \cdot h^{-1} \cdot m^{-2})$
K	Distribution coefficient	(–)
L	feed side molar flow	$(mol \cdot s^{-1})$
MW	molecular weight	(–)
N_t	number of membrane tubes	(–)
P	absolute pressure	(Pa)
P^o	vapor pressure	(Pa)
Q	membrane permeance	$(mol \cdot m^{-2}\ s^{-1}\ Pa^{-1})$
R	gas constant	$(J \cdot K^{-1}\ mol^{-1})$
Re	Reynolds number	(–)
Sc	Schmidt number	(–)
Sh	Sherwood number	(–)

T	temperature	(K)
V	permeate side molar flow	$(mol \cdot s^{-1})$
c	molar concentration	$(mol \cdot m^{-3})$
d	tube diameter	(m)
f	Fanning friction factor	$(-)$
k	mass transfer coefficient	$(m \cdot s^{-1})$
l	length of the module	(m)
m	coefficient relating mass and liquid concentrations	
f	fugacity	(Pa)
k	mass transfer coefficient	$(m \cdot s^{-1})$
p	partial pressure	(Pa)
q	loading	$(mol \cdot kg^{-1})$
u	stream linear velocity	$(m \cdot s^{-1})$
x	feed side mol fraction	$(-)$
y	permeate side mol fraction	$(-)$

Greek

α	selectivity	$(-)$
α_i	perm-selectivity = $\frac{Q_{water}}{Q_{ethanol}}$	$(-)$
γ	activity coefficient	$(-)$
δ	thickness of support layer	(m)
Θ	Poynting correction factor for liquid	$(-)$
ϵ	layer porosity	$(-)$

μ	chemical potential	$(J \cdot mol^{-1})$
θ	occupancy	$(-)$
φ	fugacity coefficient	$(-)$
Φ	Side Stream liquid flow / Liquid flow tray above SS	
ρ'	molar density	$(mol \cdot m^{-3})$
ρ	density	$(kg \cdot m^{-3})$

Sub- and superscripts

$_A$	most permeable component
$_{act}$	ref. to apparent act. energy
$_B$	less permeable component
$_h$	hydraulic diameter
$_{bl}$	boundary layer
$_{feed}$	feed side
$_G$	in gas phase
$_{G-i-R}$	gas at the interface (retentate side)
$_{G-i-P}$	gas at the interface (permeate side)
$_i$	component i
$_{Kn}$	Knudsen diffusivity
$_L$	in liquid phase
$_{L-i-R}$	liquid at the interface (retentate side)
$_m$	membrane
$_{ov}$	overall coefficient

$o-G$	overall gas coefficient
p	mean pore diameter of the support layer
$perm$	permeate side
ref	reference framework
sl	support layer
ads	adsorption
dif	diffusion
avg	average
sat	saturation
app	ref. to apparent act. energy
l	ref. to liquid
o	property measured at a certain reference temperature
v	ref. to vapor
$*$	in vapor - liquid equilibrium

Acknowledgements

This is the final chapter of a story that started in January 2002. Here I would like to thank all the persons that directly or indirectly contributed to the development of this thesis. Since I don't want to miss any name of all the persons that I share my time with, I won't mention the famous list with all the names of the people in the groups. Merci de votre compréhension.

First of all thanks to my promotors Prof. Peter Jansens and Prof. Andrzej Górak and to my co-promotor Dr. Žarko Olujić. Peter, thanks for all the confidence and freedom you gave me during these years. We did not have so many meetings as you used to have with other PhD's, but for sure the once we had were very productive. Prof. Dr.-Ing. Andrzej Górak, thank you for the kind invitation to work at the Chair of Fluid Separation Processes. It was a great experience for me to work and live in Dortmund. I met a lot of nice people there and had a lot of experiences that I will always remember. Žarko, thanks for your understanding and your day-to-day coaching. Thanks for your patience and for your calm words towards my nasty e-mails. After reading your answers most of the time I was very embarrassed for sending such exaggerated messages. Thanks for showing me that behind a good engineer there is always a great person. Special thanks to Prof. de Graauw that came always so enthusiastic to my room to see my progress and discuss my latest results. The only words that I can say are: Thank you Jan, your contribution has been invaluable for this thesis. Your passion for science is an example for all of us. I enjoyed every moment that we worked together, especially when you related me

all those work experiences you had. Thanks also to Prof. Koos Jansen, Prof. Mathias Wesseling and Harry Kooijman for your remarks and discussions to improve my thesis.

Finally I would like to thank (without any special order) to my colleagues from API for their support and understanding during my (our) PhD, to all the people in the Chair of Fluid Separation Processes (TVT) at Dortmund University, to my colleagues from (the former) OCK and TOCK groups at Delft ChemTech, to the people from the University of México and to all my friends and acquaintances. Without your company / friendship I wouldn't have made it to the end.

Paris, December 2006

List of publications

Journal publications

P. Pérez, Ž. Olujić, J. de Graauw, P.J. Jansens, *Modeling and simulation of inorganic shell and tube membranes for vapor permeation*, **Chemical Engineering and Processing, 45 (2006) p.973–979.**

Ž. Olujić, P. Pérez, F.T. de Bruijn, J. de Graauw, P.J. Jansens, *Augmenting distillation by membranes: Developments and prospects*, **Chemical and Biochemical Engineering Quarterly, 20 (2006) p.301–318.**

Contribution to conferences

P. Perez, Z. Olujic, P.J. Jansens, M. Nienoord, R. Creusen, *A ceramic membrane based distillation / vapor permeation process for ethanol dehydration*, **Proceedings of the 9th Aachen Membrane Colloquium**, Aachen, Germany, 2003.

P. Perez, Z. Olujic, P.J. Jansens, *A design tool for shell and tube vapor permeation modules*, **Proceedings of the 8th International Conference on Inorganic Membranes**, Cincinnati, USA, 2004.

P. Perez, Z. Olujic, P.J. Jansens, *A design tool for shell and tube ceramic vapor permeation membrane modules*, **Proceedings of Euromembranes 2004**, Hamburg, Germany, 2004.

P. Perez, Z. Olujic, P.J. Jansens, *Modeling shell and tube modules with silica membranes for vapor permeation*, **Proceedings of the 5th Iberoamerican Conference on Membrane Science and Technology**, Valencia, Spain, 2005.

D. Teleman, P. Perez, S. Lauterbach, P. Kreis, A. Gorak, *Applications of pervaporation for dehydration of organic mixtures*, **Marie Curie Actions, Making Europe more attractive for researchers**, Pisa / Livorno, Italy, 2005.

P. Perez, F.T. de Bruijn, Z. Olujic, F. Kapteijn, P.J. Jansens, *Experimental comparison of vapor permeation and pervaporation with (methylated-) silica membranes and validation of a design tool for scale-up*, **Proceedings of the International Conference on Porous Ceramic Materials**, Bruges, Belgium, 2005.

Curriculum Vitae

Paulo Pérez

Date of birth	4th of May 1974	
Education		
1992–1997	University of Mexico (UNAM)	
	Faculty of Chemistry	Chemical Engineer
1999–2001	Delft University of Technology	
	Delft Ingenious Design	Postgraduate Designer
2002–2006	Delft University of Technology	
	Laboratory for Process Equipment	PhD Researcher
Relevant Training		
VI-XII / 2005	University of Dortmund	
	Chair of Fluid Separation Processes	Marie Curie Fellow
Professional Experience		
1998	Mexican Petroleum Institute	
	Basic Engineering Department	Process Engineer
IX / 2006-	General Electric Plastics	
	LNP - Fosses	Process Engineer